003

ENTERED

RECEIVED MAY 16 2016

Los Alamos NATIONAL LABORATORY EST 1943

Environmental Protection & Compliance Division
Environmental Compliance Programs (EPC-CP)
PO Box 1663, K490
Los Alamos, New Mexico 87545
(505) 667-0666

Environmental Management
Los Alamos Field Office, A316
3747 West Jemez Road
Los Alamos, New Mexico, 87544
(505) 665-5325

Date: MAY 12 2016
Symbol: EPC-DO-16-118
LA-UR: 16-22806
Locates Action No.: NA

Ms. Michelle Hunter, Chief
Ground Water Quality Bureau
New Mexico Environment Department
Harold Runnels Building, Room N2261
1190 St. Francis Drive
P.O. Box 26110
Santa Fe, NM 87502

Dear Ms. Hunter:

Subject: Additional Information for Discharge Permit Application DP-1835

In April 2015 the U.S. Department of Energy and Los Alamos National Security, LLC (DOE/LANS) submitted a discharge permit application (DP-1835) to inject treated groundwater into multiple Class V Underground Injection Control (UIC) wells at Los Alamos National Laboratory (ENV-DO-15-0085). At the recommendation of the New Mexico Environment Department (NMED), DOE/LANS are submitting additional information to support the above-referenced permit application. Specifically, the NMED requested information on the predicted geochemistry associated with introduction of treated groundwater into the aquifer using injection wells, and additional hydrologic information associated with use of the injection wells. The following three enclosures are being submitted to provide the requested information:

Enclosure 1: Geochemical Analysis of Potential Impacts of Injecting Treated Water into Injection Wells in Mortandad Canyon.

- The geochemical code PHREEQC was used to evaluate the potential impacts of injecting treated groundwater into new injection wells in and near Mortandad Canyon.

Enclosure 2: Interim Measures Work Plan for Chromium Plume Control (EP2015-0089).

- On October 15, 2015, the NMED Hazardous Waste Bureau approved with modifications the Interim Measures Work Plan for Chromium Plume Control. Specifically, Appendix A provides detailed hydrologic analysis of the overall interim measure, including use of the injection wells.

Enclosure 3: Injection Wells Hydrology Fact Sheet.

- DOE/LANS have prepared a fact sheet and conceptualized figure of the injection wells to answer frequently asked questions.

Please contact Robert S. Beers by telephone at (505) 667-7969 or by email at bbeers@lanl.gov if you have questions regarding this information.

Sincerely,

John P. McCann
Acting Division Leader
Environmental Protection & Compliance Division
Los Alamos National Security, LLC

Sincerely,

David S. Rhodes, Director
Office of Quality and Regulatory Compliance
Environmental Management
Los Alamos Field Office

JPM:DSR:MTS:RSB/lm

Enclosures:

1) Geochemical Analysis of Potential Impacts of Injecting Treated Water into Injection Wells in Mortandad Canyon
2) Interim Measures Work Plan for Chromium Plume Control (EP2015-0089)
3) Injection Wells Hydrology Fact Sheet

Cy: James Hogan, NMED/SWQB, Santa Fe, NM, (E-File)
John E. Kieling, NMED/HWB, Santa Fe, NM, (E-File)
Steven M. Yanicak, NMED/DOE/OB, (E-File)
David S. Rhodes, EM-SG, (E-File)
Jody M. Pugh, NA-LA, (E-File)
Cheryl L. Rodriguez, EM-LA, (E-File)
Paul B. Underwood, EM-LA, (E-File)
Kirsten M. Laskey, EM-LA, (E-File)
Jordan Arnswald, NA-LA, (E-File)
Craig S. Leasure, PADOPS, (E-File)
William Mairson, PADOPS, (E-File_
Michael T. Brandt, ADESH, (E-File)
Raeanna Sharp-Geiger, ADESH, (E-File)
John P. McCann, EPC-DO, (E-File)
Randall Mark Erickson, ADEM, (E-File)
Enrique Torres, ADEM, (E-File)
Bruce Robinson, ADEM-PO, (E-File)
Stephani F. Swickley, ADEM-PO, (E-File)

Cy (continued):
Danny Katzman, ADEM-PO, (E-File)
Michael T. Saladen, EPC-CP, (E-File)
Robert S. Beers, EPC-CP, (E-File)
Saundra Martinez, OIO-DO, (E-File)
lasomailbox@nnsa.doe.gov, (E-File)
emla.docs@em.doe.gov, (E-File)
locatesteam@lanl.gov, (E-File)
epc-correspondence@lanl.gov, (E-File)
epccat@lanl.gov, (E-File)

COPY

Los Alamos
NATIONAL LABORATORY
EST 1943

GROUND WATER
MAY 13 2016
BUREAU

Environmental Protection & Compliance Division
Environmental Compliance Programs (EPC-CP)
PO Box 1663, K490
Los Alamos, New Mexico 87545
(505) 667-0666

Environmental Management
Los Alamos Field Office, A316
3747 West Jemez Road
Los Alamos, New Mexico, 87544
(505) 665-5325

Date: MAY 12 2016
Symbol: EPC-DO-16-118
LA-UR: 16-22806
Locates Action No.: NA

Ms. Michelle Hunter, Chief
Ground Water Quality Bureau
New Mexico Environment Department
Harold Runnels Building, Room N2261
1190 St. Francis Drive
P.O. Box 26110
Santa Fe, NM 87502

Dear Ms. Hunter:

Subject: **Additional Information for Discharge Permit Application DP-1835**

In April 2015 the U.S. Department of Energy and Los Alamos National Security, LLC (DOE/LANS) submitted a discharge permit application (DP-1835) to inject treated groundwater into multiple Class V Underground Injection Control (UIC) wells at Los Alamos National Laboratory (ENV-DO-15-0085). At the recommendation of the New Mexico Environment Department (NMED), DOE/LANS are submitting additional information to support the above-referenced permit application. Specifically, the NMED requested information on the predicted geochemistry associated with introduction of treated groundwater into the aquifer using injection wells, and additional hydrologic information associated with use of the injection wells. The following three enclosures are being submitted to provide the requested information:

Enclosure 1: Geochemical Analysis of Potential Impacts of Injecting Treated Water into Injection Wells in Mortandad Canyon.

- The geochemical code PHREEQC was used to evaluate the potential impacts of injecting treated groundwater into new injection wells in and near Mortandad Canyon.

Enclosure 2: Interim Measures Work Plan for Chromium Plume Control (EP2015-0089).

- On October 15, 2015, the NMED Hazardous Waste Bureau approved with modifications the Interim Measures Work Plan for Chromium Plume Control. Specifically, Appendix A provides detailed hydrologic analysis of the overall interim measure, including use of the injection wells.

ENCLOSURE 1

Geochemical Analysis of Potential Impacts of Injecting Treated Water into Injection Wells in Mortandad Canyon

EPC-DO-16-118

LA-UR-16-22806

Date: MAY 1 2 2016

Geochemical Analysis of Potential Impacts of Injecting Treated Water into Injection Wells in Mortandad Canyon

Executive Summary

The geochemical code PHREEQC was use to evaluate the potential impacts of injecting treated water into new injection wells in and near Mortandad Canyon as part of interim measures for remediation of hexavalent chromium contamination in the regional aquifer beneath the canyon. The impacts evaluated were limited to changes in dissolved species water chemistry caused by the anion exchange treatment process used to remove chromium, with the primary potential issue being the precipitation of mineral phases that could plug pore spaces in the near-well aquifer sediments or the filter packs of the injection wells. Treated water chemistry data from pumping tests conducted in 2013 were used to determine a range of potential injection water chemistries resulting from the treatment process, and groundwater from monitoring well R-42 was used as the baseline contaminated aquifer water because it has the highest concentrations of major cations and anions and thus represents a worst case in terms of potential precipitation of mineral phases.

The geochemical calculations indicate that the primary potential issue from treatment is an elevation of pH during the treatment process, which apparently occurred unexpectedly, and infrequently during 2013. If persistent elevated pH is present, it could potentially cause calcite precipitation, with a worst-case estimate of about 16 mg of calcite precipitated per kg of water, if the pH were to rise from an aquifer value of about 7.8 to 8.6 (approximately the highest treated water pH observed in 2013). Several other non-reactive mineral (silicate) phases are also predicted to precipitate at elevated pH conditions, but these would be unlikely to form because of slow precipitation kinetics at ambient temperatures. Also, these phases are not known to occur in regional aquifer sediments. pH excursions as low as 6.5 were also observed in treated water in 2013, but pH decreases result in higher solubilities of calcite and most other amphoteric phases that might precipitate, so these pHs are not a concern. Also, no pH change taking place during treatment, which was the most common observation in treated water in 2013, resulted in no mineral phases predicted to increase in saturation relative to untreated groundwater. Amorphous silica is very close to saturation in regional aquifer waters, and it is probably the next most likely mineral to precipitate after calcite, but its solubility is insensitive to pH over the range measured in 2013, so it would not be expected to precipitate as a result of the treatment process alone.

The potential impacts of suspended solids in treated waters (including debris accumulated during any storage of water) or biofouling resulting from inadvertent concentration increases in organic nutrients/biostimulants were not considered in this analysis because these will depend on process conditions that are not yet established and also on abnormal process conditions. However, previous data for suspended solids and total organic carbon (TOC) concentrations in treated waters indicate that levels of these constituents are no higher than in aquifer waters, so concerns from these constituents should be minimal if process upsets or abnormal conditions causing increases in their concentrations are avoided. Complexation of metal cations with dissolved organic carbon (DOC) is unlikely based on the low TOC-DOC concentrations measured in both groundwater and treated water. Therefore, facilitated transport of metals is not anticipated to occur during injection.

Introduction

The interim measure for Cr(VI) in the regional aquifer beneath Mortandad Canyon involves the removal of Cr(VI) from pumped aquifer water using commercial anion exchange resins. The resins selectively remove chromate/dichromate, but they also remove other anions, including NO_3^-, $SO_4^{=}$, and, to some extent, HCO_3^-. These anions are exchanged with Cl^- from the resin, so the treated water has higher concentrations of Cl^- and lower concentrations of the other anions relative to the influent water. As the resins mature, increasing amounts of the other anions 'bleed' through the resin and decreasing amounts of Cl^- are released. The resins are changed/regenerated before any chromate bleeds through. Available data indicate that concentrations of cations and uncharged species (e.g., SiO_2/H_4SiO_4) are not altered by the anion exchange process.

Treated water so far has been dispositioned by land application, but the long-term plan is to inject the treated water into injection wells that are being installed along the downgradient plume edge. The purpose of this report is to provide an evaluation of the potential for the injection of this water to result in clogging or permeability reduction in the aquifer very near the injection wells that could significantly reduce injection well efficiency.

Methods

The geochemical code PHREEQC (Parkhurst and Appelo, 2013) was used to calculate the saturation indices[1] of all the minerals present in the Lawrence Livermore National Laboratory (LLNL) geochemical database (Johnson, 2010) using as inputs R-42 water chemistry and 3 different potential water chemistries that approximately bound the treated water chemistries measured during pump testing of R-42 and R-28 in 2013. The LLNL database has the most complete compilation of mineral phase equilibrium constants and aqueous speciation of any database available for PHREEQC. However, calculations were also done using the minteq.v4 and wateq4f databases to ensure that no mineral phases were excluded and to address potential uncertainties associated with database inconsistencies. No additional mineral phases and no significant inconsistencies were identified using the other databases, so the results from the calculations with these other databases are not discussed further here.

Figure 1 shows anion concentration data as a function of pH in water that was treated from monitoring wells R-42 and R-28 during pump tests in 2013. Although the data show a considerable amount of scatter, it is apparent that Cl^- concentrations tended to be higher and the concentrations of other anions tended to be lower at lower pHs, which is believed to be representative of effluent from fresher anion exchange resin. The R-42 anion concentrations and

[1] The saturation index for a given mineral phase is the log of the activity product of the solution species that form the phase divided by the equilibrium constant (solubility product) for the phase – when the index is greater than zero, the phase is supersaturated or oversaturated and predicted to precipitate; when it is less than zero, the phase is undersaturated and it should not precipitate.

the anion concentrations of the 3 different representative treated waters used in the PHREEQC calculations are shown superimposed on this plot (large filled-in symbols). The three different treated water chemistries were selected to be representative of low, intermediate (unchanged)

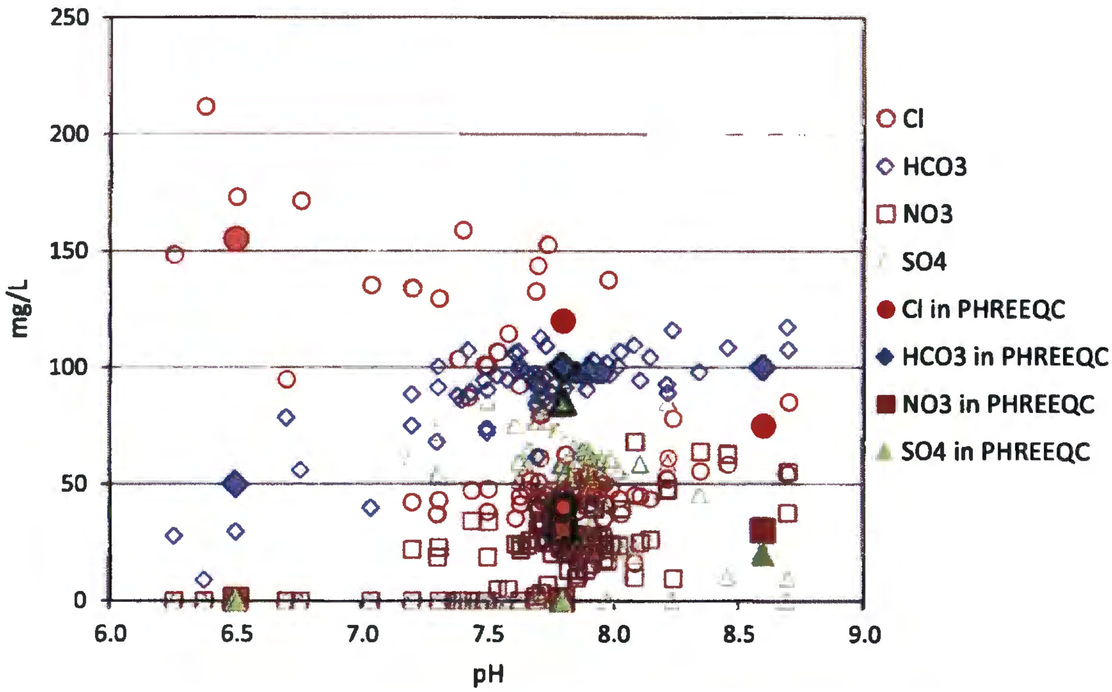

Figure 1. Anion concentrations measured in treated waters from 2013 as a function of pH (open symbols). Large filled symbols are treated water anion concentrations assumed in PHREEQC calculations at pHs of 6.5, 7.8 (aquifer pH) and 8.6. Large filled symbols with black outlines are anion concentrations in untreated R-42 water assumed in PHREEQC calculations. Note that the HCO_3^- concentration in treated water at pH 7.8 is identical to the HCO_3^- concentration in untreated R-42 water (symbols coincide).

and high pH waters, respectively. Table 1 lists the concentrations of all constituents, including cations and uncharged species, used in the PHREEQC calculations for each of the waters. Note that many of the minor cation or metal constituents were included at the high end of their reported concentration ranges or at their detection limits so as to increase the probability of mineral phases precipitating. All waters were assumed to contain 7 mg/L dissolved O_2, with the Eh of the buffered by the O^0/O^{-2} (H_2O) redox couple.

Eighty-five mineral phases were calculated by PHREEQC to be supersaturated in untreated R-42 water when the LLNL database was used. This result is clearly unrealistic and reflects the lack of consideration of kinetic limitations when using a geochemical code that only calculates thermodynamic equilibria. Many of the supersaturated phases will not form under ambient temperatures and pressures, and often when one phase precipitates, it reduces the concentrations of some solution species to the point where the precipitation of other phases is precluded. The number of supersaturated mineral phases decreased relative to R-42 water in all the treated water chemistries except for the water with a pH of 8.6, which had 92 saturated phases, or seven more than in untreated R-42 water.

Table 1. Constituent concentrations in untreated R-42 water and in treated water at the 3 pHs assumed in PHREEQC calculations. All concentrations are in mg/L unless otherwise stated.

Element/Ion	R-42, pH 7.8	Treated, pH 6.5	Treated, pH 7.8	Treated pH 8.6
Al	0.01	0.01	0.01	0.01
As	0.0015	0.0015	0.0015	0.0015
Ba	0.08	0.08	0.08	0.08
B	0.03	0.03	0.03	0.03
Br	0.02	0.02	0.02	0.02
Ca	53	53	53	53
HCO_3^-	100	50	100	100
Cl	40	155	120	75
Cr(VI)	1	0.001	0.001	0.001
F	0.2	0.2	0.2	0.2
Fe (total)	0.012	0.012	0.012	0.012
K	2.3	2.3	2.3	2.3
Li	0.035	0.035	0.035	0.035
Mg	15	15	15	15
Mo	0.002	0.002	0.002	0.002
Na	17	17	17	17
Ni	0.02	0.02	0.02	0.02
NO_3^- as N	6.8	0.4	0.4	6.8
O_2	7	7	7	7
Se	0.0015	0.0015	0.0015	0.0015
SiO_2	77	77	77	77
Sr	0.2	0.2	0.2	0.2
$SO_4^=$	85	0.1	0.1	20
U(VI)	0.001	0.001	0.001	0.001
V	0.02	0.02	0.02	0.02
Zn	0.01	0.01	0.01	0.01

Note that many cation/metal concentrations are set equal to their highest measured values or their detection limits to maximize the potential for mineral phase precipitation.

The first step in eliminating supersaturated mineral phases from further consideration was to identify any phase that did not show an increase in saturation index in any of the 3 treated water chemistries relative to R-42 water. The rationale was that anything that did not increase in saturation index after treatment would be unlikely to precipitate, even if the phase was already calculated to be supersaturated in R-42 water. This eliminated all but 35 mineral phases from further consideration. Of the remaining minerals, 24 were more saturated in the pH 8.6 water than in untreated R-42 water, and 11 were more saturated in the pH 6.5 water. No phases were more saturated in the treated water at a pH of 7.8 because without a pH change the replacement of NO_3^-, $SO_4^=$, and HCO_3^- with Cl^- tends to increase the solubility of most cations (chloride phases tend to have higher solubilities than sulfate and carbonate phases, with a few exceptions, such as silver).

Of the 35 remaining supersaturated phases, four carbonate minerals that precipitated in the pH 8.6 treated water ($MgCO_3$, $SrCO_3$ and two $CaCO_3$ phases) were eliminated on the basis that another carbonate phase, calcite, would precipitate before any of these other four phases because it consistently had a higher saturation index and is a reactive mineral, and also the precipitation of calcite would drop the saturation indices of the other phases below zero (i.e., undersaturated). Note that the carbonate phases other than calcite were undersaturated in the original R-42 water, whereas calcite was slightly supersaturated in R-42 water.

At this stage, untreated R-42 water simulations were run in PHREEQC with each of the remaining 31 mineral phases separately/individually forced to precipitate by setting their saturation indices to zero (i.e., exactly saturated). PHREEQC will calculate the moles of each phase precipitated (or dissolved) per kg of water to reach saturation from either an over- or under-saturated initial condition. This process was repeated for treated water at a pH of 8.6 using the 20 remaining mineral phases that increased in saturation relative to R-42 water, and also in treated water at a pH of 6.5 with the 11 mineral phases that increased in saturation relative to R-42 water. The moles of each mineral phase precipitated per kg of R-42 water were then subtracted from the moles of that mineral phase precipitated in either the higher or lower pH treated waters, and the differences were taken to be the maximum number of moles of precipitate per kg of water that could form as a result of the treatment process. In taking this approach, it was implicitly assumed that any pre-existing supersaturation in R-42 water would not result in precipitation, so only the increases over R-42 saturation levels were considered to cause precipitation. The molar quantities precipitated were then converted to mass quantities (mg solid phase per kg of water) by multiplying the molar concentrations by the formula weight of the minerals times 1000 (mg/g). The forced precipitation of each individual mineral phase in separate PHREEQC simulations placed a conservative upper bound on the masses of mineral phases precipitated because in reality as one mineral phase precipitates it will decrease the concentrations of solution species that may contribute to the precipitation of other mineral phases.

After all these calculations, the final step in the process was to eliminate any mineral phases for which less than 1 mg/L or mg/kg H_2O was predicted to precipitate. The rationale for this elimination criterion was that the lowest measured suspended solids concentration in treated water samples reported in 2014 was slightly more than 1 mg/L, so if mineral precipitation was predicted to be less than 1 mg/L it would effectively be accounted for in the expected suspended solids loading (which was no higher than in untreated aquifer waters). The application of this criterion eliminated all of the minerals that were predicted to precipitate in treated water at a pH of 6.5, and it also eliminated all but 8 of the minerals predicted to precipitate in treated water at a pH of 8.6. Most of the eliminated minerals were phases that were limited as to how much mass could precipitate because of the very low concentrations in R-42 water of one or more of the elements in their mineral structures (most often Al, Ba, Zn, or Ni). In these cases, even if all of the minor element(s) assumed to be present in R-42 water was consumed in precipitation reactions, the amount of precipitate that could form was exceedingly small.

Results and Conclusions

Table 2 lists the 8 minerals that were predicted to precipitate in the treated water at a pH of 8.6, and it also lists the masses of each precipitate calculated to form per kg of treated water. The minerals are listed in order of predicted mass precipitated. Calcite tops the list at about 16 mg per kg of water, or approximately 16 mg per liter of water. Although significant masses of other minerals are also predicted to precipitate (some comparable to calcite), these minerals are of much less practical concern than calcite because they are unlikely to form at the ambient

Table 2. Mineral phases predicted to precipitate in masses exceeding 1 mg/kg of water in treated water at a pH of 8.6 (listed in order of predicted mass precipitated).

Mineral Phase	mg precipitated per kg H_2O
Calcite ($CaCO_3$)	16.4
Dolomite ($CaMg(CO_3)_2$)	14.3
Sepiolite ($Mg_4Si_6O_{15}(OH)_2{:}6H_2O$)	13.9
Talc ($Mg_3Si_4O_{10}(OH)$)	10.6
Tremolite ($Ca_2Mg_5Si_8O_{22}(OH)_2$)	10.6
Anthophyllite ($Mg_7Si_8O_{22}(OH)_2$)	10.2
Diopside ($CaMgSi_2O_6$)	10.1
Antigorite ($Mg_{48}Si_{34}O_{85}(OH)_{62}$)	8.6

Note: Next highest mineral mass precipitated per kg of water was 0.015 mg/kg, and the highest mineral mass precipitated per kg of water at pH 6.5 was 0.016 mg/kg.

temperatures and pressures of the treatment process. The other minerals all tend to form under higher temperature and pressure conditions or over much longer time scales than calcite. The fact that these other minerals are not observed in measurable quantities in aquifer sediments despite being predicted to be supersaturated at ambient aquifer pH values suggests that they can remain supersaturated for very long times at the temperature and pressure conditions prevailing in the aquifer. The silicate minerals listed in Table 2 are non-reactive and their precipitation/dissolution does not control solute chemistry in the regional aquifer.

The reason for the calcite precipitation at elevated pH is that the solution equilibrium between bicarbonate (HCO_3^-) and carbonate ($CO_3^=$) shifts to a greater fraction of carbonate as pH increases, and thus the saturation index of calcite increases at higher pH for the same total concentration of HCO_3^- plus $CO_3^=$. In addition, the partial pressure of carbon dioxide gas in groundwater decreases within increasing pH, resulting in a lower solubility of calcite. Even if the treatment process removes some of the HCO_3^- and replaces it with Cl^-, an increase in pH can still result in a greater concentration of $CO_3^=$ in treated water despite the overall decrease in concentration of HCO_3^- plus $CO_3^=$. Thus, pH increases of treated water are probably the biggest potential geochemical issue for maintaining good injection rates of treated water into injection wells. It should be noted that permeability decreases due to calcite precipitation can be reversed relatively easily by injecting mildly acidic solutions, for example HCl, to dissolve the freshly precipitated calcite.

Although amorphous silica (SiO_2) does not appear in Table 2 because its saturation index was not predicted to increase in any of the treated waters relative to R-42 water, it is probably the second most likely phase to precipitate in treated water. It is very close to saturation in regional aquifer waters, and slight amounts of evaporation or decreases in temperature could result in some precipitation.

The potential impacts of suspended solids loading in treated waters (including debris accumulated during any tank or pond storage of water) or biofouling resulting from inadvertent introduction of organic nutrients/biostimulants were not considered in this analysis because these will depend on process conditions that are not expected to occur. Previous data for suspended solids and total organic carbon concentrations in treated waters indicate that levels of these constituents are not elevated relative to aquifer waters, so concerns from these constituents should be minimal if process upsets or abnormal conditions causing significant increases in the concentrations of these constituents are avoided.

References

Johnson, J., 2010. llnl.dat 4023 2010-02-09. Data from 'thermo.com.V8.R6.230' prepared by Jim Johnson at Lawrence Livermore National Laboratory, in Geochemist's Workbench format. Converted to PHREEQC format by Greg Anderson with help from David Parkhurst.

Parkhurst, D. L. and Appelo, C. A. J., 2013. PHREEQC (Version 3.0.4) - A computer program for speciation, batch speciation, one-dimensional transport, and inverse geochemical calculations, U.S. Geological Survey Techniques and Methods, Book 6, Chapter A43, p. 497, http://pubs.usgs.gov/tm/06/a43/.

ENCLOSURE 2

Interim Measures Work Plan for Chromium Plume Control
(EP2015-0089)

EPC-DO-16-118

LA-UR-16-22806

Date: May 12, 2016

LA-UR-15-23126
May 2015
EP2015-0089

Interim Measures Work Plan for Chromium Plume Control

Los Alamos
NATIONAL LABORATORY
EST 1943

Prepared by the Environmental Programs Directorate

EP2015-0089

Interim Measures Work Plan for Chromium Plume Control

May 2015

Responsible project manager

Stephani Swickley	[signature]	Project Manager	Environmental Remediation Program	5/19/15
Printed Name	Signature	Title	Organization	Date

Responsible LANS representative:

Randall Erickson	[signature]	Acting Associate Director	Environmental Programs	5/19/15
Printed Name	Signature	Title	Organization	Date

Responsible DOE representative:

Christine Gelles	[signature] for	Acting Manager	DOE-EM-LA	5/21/15
Printed Name	Signature	Title	Organization	Date

CONTENTS

Figures

Appendix

1.0 INTRODUCTION

This interim measures (IM) work plan (IMWP) for plume control describes proposed activities to control chromium plume migration in groundwater at the Los Alamos National Laboratory (LANL or the Laboratory) boundary. The Laboratory proposes to conduct the IM in accordance with Section VII.B.1 of the March 1, 2005, Compliance Order on Consent (the Consent Order). The IM is proposed to control chromium migration in groundwater while long-term corrective action remedies are being evaluated. The work proposed in this IMWP follows from the "Interim Measures Work Plan for the Evaluation of Chromium Mass Removal," submitted to the New Mexico Environment Department (NMED) in April 2013 (LANL 2013, 241096). That work plan was prepared in response to requirements in a letter from NMED dated January 25, 2013 (NMED 2013, 521862), which directed that the work plan assess the potential for active long-term removal of chromium from the regional aquifer by pumping with a pilot extraction test well. This plan describes the installation and operation of extraction and injection wells to control plume migration.

Investigations and conceptual models related to chromium contamination are summarized in a number of reports, including the "Investigation Report for Sandia Canyon" (LANL 2009, 107453) and the "Phase II Investigation Report for Sandia Canyon" (LANL 2012, 228624). Additional information presented in the "Summary Report for the 2013 Chromium Groundwater Aquifer Tests at R-42, R-28, and SCI-2" (LANL 2014, 255110) and other previously unreported testing results at the new chromium extraction well CrEX-1 inform the technical recommendations in this work plan. Figure 1.0-1 shows the current extent of the chromium plume defined by the 50-ppb New Mexico groundwater standard. Figure 1.0-1 also includes time-series plots for wells R-45 and R-50, located at the downgradient portion of the plume. Chromium concentrations at these downgradient plume-edge wells show interannual variability in chromium concentrations, but the overall trend shows a distinct overall increasing trend in chromium concentrations. These increasing trends are the reason the Laboratory is proposing the plume-control actions presented in this IMWP.

2.0 OBJECTIVES

The principle objective of the IM presented in this work plan is to achieve and maintain the 50-ppb downgradient chromium plume edge within the Laboratory boundary. The activities conducted under this work plan are being proposed to expedite control of plume migration.

The measures implemented under this work plan to achieve this objective have the metric of reduction of chromium concentrations at R-50 to the 50-ppb New Mexico groundwater standard or less over a period of approximately 3 yr. The method used to achieve this objective is to pump at an existing extraction well (CrEX-1) and to inject treated water into new injection wells located primarily along the downgradient portion of the plume. A secondary objective of hydraulically controlling plume migration in the eastern downgradient portion of the plume near well R-45 is expected to be met through injection in two wells located near R-45, as discussed in sections 3.1 and 3.2 of this plan. The pumping conducted for hydraulic control will also incidentally reduce the mass of chromium within the regional aquifer, but mass removal is not specifically an objective of this IM. Another objective is to obtain additional information of the aquifer properties (i.e., aquifer heterogeneity, hydraulic connections between pumping and observation wells) in the plume area by monitoring responses to pumping conducted for plume control.

3.0 APPROACH

To rapidly reduce off-site chromium transport in the regional aquifer, a pump and treat (P&T) and injection approach is proposed to achieve hydraulic control of off-site plume migration. Plume control would be implemented using a method of hydraulic capture that utilizes existing extraction well CrEX-1 and a configuration of injection wells to control migration of chromium contaminated groundwater (Figure 3.0-1). The time frame to achieve the 50-ppb New Mexico groundwater standard within the Laboratory boundary along the southern portion of the plume is modeled at less than 3 yr. Once achieved, it is anticipated that intermittent versus continual pumping will occur to maintain hydraulic control of the plume. This P&T and injection effort may be implemented intermittently but is intended to be of limited duration until a final remedy is proposed and approved by NMED. Updates to the estimations of plume response will be ongoing as data from pumping and injection are obtained.

Groundwater plumes are generally mitigated using one or a combination of three categorical approaches: monitored natural attenuation (MNA), P&T, or in situ strategies. MNA requires documentation that natural processes are occurring within the aquifer to reduce concentrations or toxicity of target contaminants. P&T can be conducted with the specific objective of achieving optimal removal of target contaminants from groundwater or to hydraulically control plume migration. In situ approaches generally involve the use of amendments directly within the aquifer either to favorably alter the geochemistry of the contaminants or to enhance naturally occurring biological processes that can favorably alter groundwater contaminants, in either case rendering them immobile or nontoxic.

All of the above-mentioned approaches other than hydraulic control, as proposed in this IMWP for plume control, would be expected to produce a much slower response at the advancing plume edge or have not yet been fully evaluated for technical feasibility in the groundwater setting beneath Mortandad Canyon. Groundwater modeling indicates that pumping to remove chromium within the plume centroid does not appreciably affect the concentration of chromium at the southern plume edge until after 10 yr or more, and thus does not meet the primary objective of this IMWP. Groundwater modeling of various scenarios shows that a combination of pumping and injection along the downgradient plume edge has a rapid effect on stabilizing the plume edge (as defined by the 50-ppb New Mexico groundwater standard) well within the Laboratory boundary in less than 3 yr of operation (Appendix A).

Disposition options, other than injection of treated groundwater via injection wells, were considered, including land application and piping and discharge of treated groundwater via an existing outfall that would release water into the same pathway that the chromium source initially followed. Relatively small volumes of treated groundwater may be land-applied in accordance with approved permits, largely for local dust suppression in the project area, but limitations on the amount of water that can be land-applied because of field logistics of distributing sufficient water on a continual basis would not result in sufficient extraction rates. Dispositioning treated water via a pipeline and existing outfall does not provide the significant benefit of rapid hydraulic control that injection wells provide and, therefore, does not support the objectives of this IMWP. However, the pipeline and outfall option for treated groundwater will likely be evaluated as a potential component of a final remedial solution to the plume.

Other, more complex approaches, including MNA and in situ strategies that may eventually be applied to address the chromium plume, are being evaluated under a separate work plan for plume-center characterization. A final evaluation of technologies, including ranking and cost benefit, will be provided in a corrective measures evaluation report for NMED.

3.1 Hydraulic Capture

The goal of hydraulic capture is to create and maintain a capture zone that will arrest plume migration. An initial area of capture was determined from the 7-wk pumping period conducted at CrEX-1 in fall 2014. Appendix A presents the pressure-response data obtained from surrounding monitoring wells and provides an initial estimate of the capture zone. However, to optimize hydraulic capture of chromium-contaminated groundwater moving within the aquifer, existing extraction well CrEX-1 will operate continuously. This is consistent with the initial purpose of CrEX-1 "to evaluate further the capture zone" and "to evaluate the potential to control chromium migration towards the Laboratory boundary via hydraulic control" (LANL 2014, 254824). An initial period of pumping at CrEX-1 (a minimum of 5–6 mo) at approximately 80–100 gallons per minute (gpm) will help further establish and determine the extent, orientation, and shape of the capture zone established by pumping. The shape of the capture zone is expected to be impacted by aquifer heterogeneity. Analysis of pressure-response data from surrounding monitoring wells and piezometers will help with spatial characterization of aquifer heterogeneity and spatial propagation of the zones of hydraulic influence and hydraulic capture. All monitoring wells within the Interim Facility-Wide Groundwater Monitoring Plan's (IFGMP's) Chromium Investigation monitoring group and newly installed regional aquifer piezometers installed in corehole borings will have dedicated transducers for continuous monitoring of pressure response associated with pumping at CrEX-1 (and Los Alamos County water-supply wells).

If extended pumping at CrEX-1 and use of injection wells does not establish a capture zone sufficient to arrest plume migration, installation, and operation of an additional extraction well will be considered. The location of an additional extraction would be determined from newly obtained data. Modeled estimations of the shape of the capture zone over 1-, 3-, and 5-yr pumping durations in CrEX-1 are presented in Appendix A (Figures A-6.0-1a, b, and c).

Pumped and treated water will be land-applied in accordance with an approved discharge permit pending issuance from the NMED Groundwater Quality Bureau because no other option is currently available for its disposition. The land-application permit will limit the period of application to months when the ground is not frozen to avoid runoff of applied water. After injection wells are installed and permitted (as discussed in section 3.2), reinjection will be the primary method of disposition and will allow for continuous pumping throughout the year, unconstrained by limitations of land application. The treatment and water management approach is described in section 3.5.

3.2 Injection Wells

Existing modeling analyses described in Appendix A suggest that the hydraulic capture of the contaminated groundwater at CrEX-1 will be substantially aided by siting the injection wells at the downgradient plume edge (Figure 3.0-1). Six injection wells are proposed to support plume control and provide operational flexibility during maintenance downtime. The priority injection well locations are those situated along the Laboratory boundary west and east of R-50 because of their specific role in helping to control chromium plume migration to the south (off-site). The next priority wells are those at the plume edge west of R-45 to help address what appears to be the advancement of the plume in that area, as manifested by the increasing chromium concentration at well R-45. The next priority well is the one situated at the plume edge west of R-44 to ensure the plume does not advance to the southeast in the R-44 area. A sixth injection well is currently planned in the centroid near R-42. This location was selected as a potential injection well location not only to provide an additional disposition location but also to test how injection of treated water may enhance diffusive processes between fine-grained, low-permeability zone that may contain higher concentrations of chromium and coarse-grained, high-porosity and permeability zones that have lower chromium concentrations because of dilution from high ambient groundwater flow or because of removal by pumping.

A typical injection well design is shown in Figure 3.2-1. Injection wells will be completed with screens in the upper portion of the regional aquifer. Data from existing monitoring wells and from the recent corehole drilling campaign indicate that contamination is dominantly within the upper 50 ft of the aquifer, so injection-well screens will be targeted for that interval. Specific hydraulic performance will vary between injection wells depending on the geology encountered, but the basic assumption is that injection wells will be able to accept injection rates comparable with the rates of extraction. Because of terrain constraints and the large number of cultural sites in the project area, angled drilling may be used to achieve target locations in the aquifer. Angled drilling would utilize existing monitoring well pads. Preliminary estimates indicate that the largest angle that will be drilled is approximately 23 degrees from vertical at chromium injection well CrIN-5.

3.3 Interim Measure Performance

Modeling results indicate the plume responds quickly to pumping at CrEX-1 and injection in the two injection wells west and east of R-50. The modeling analysis assumes that injection of treated water is distributed across the two injection wells at a rate equivalent to pumping at CrEX-1. Pumping at CrEx-1 in fall 2014 indicated the maximum sustainable pumping rate is approximately 80–100 gpm.

Figure 3.3-1 shows projections of the plume over 1-yr, 3-yr, and 5-yr time frames. The operational approach used for the model assumes that CrEX-1 is pumping at 80 gpm and injection is occurring at approximately 40 gpm in each of the wells west and east of R-50. The model indicates the plume edge will be well within the Laboratory boundary by the second year of full operation. Currently, existing downgradient portions of the plume not captured by pumping at CrEX-1 will continue to migrate but at concentrations increasingly below the 50-ppb New Mexico groundwater standard. Injection wells along the eastern portion of the plume, especially near R-45, are also expected to limit plume expansion to the east (Figure A-8.0-3 in Appendix A). Some uncertainty exists in the potential influence of injection on groundwater flow direction in that portion of the plume, but dilution of plume concentrations in that area as a result of injection would likely also result in decreases in chromium concentrations along that potential flow path. There are some uncertainties specifically with respect to how quickly the plume will respond to pumping because the model and the projections shown in Figure 3.3-1 do not yet represent the role that dual porosity may play with respect to the distribution of chromium within the aquifer. Seven weeks of pumping in CrEX-1 in fall 2014 showed steady concentrations of chromium, possibly indicating that chromium is primarily within coarse, permeable strata in this portion of the plume. Additional pumping at CrEX-1 will improve the understanding of whether dual porosity plays a role in the distribution of chromium in the aquifer in the CrEX-1 area.

Once downgradient plume control is achieved, it is anticipated that operations will become intermittent for operational efficiency but in a manner that still maintains plume control. It is anticipated that hydraulic control measures will continue until a final remedy is approved and implementation is underway.

3.4 Performance Monitoring

Existing monitoring wells within the Chromium Investigation monitoring group under the IFGMP (Figure 1.0-1) will continue to be sampled in accordance with the current approved IFGMP (LANL 2014, 256728). However, key wells for monitoring performance of the IM are R-50, screens 1 and 2; R-44, screens 1 and 2; and R-45, screens 1 and 2. These wells are situated along the downgradient edge of the plume and, therefore, are well suited for monitoring performance of the hydraulic containment strategy.

Although somewhat variable, the overall trend in chromium concentrations in R-45 and R-50 over the past few years has been increasing within the upper screens. The chromium concentration in these wells is expected to decline in response to the pumping and injection approach described here. Well R-44 is currently showing low and stable chromium concentrations that should remain the same or decline in response to pumping and injection. Figure A-8.0-4 in Appendix A shows estimations of the trend of chromium concentrations at R-50, screen 1, and R-45, screen 1, in response to pumping and injection. New piezometers installed in coreholes drilled in 2014 and 2015 within the plume area will be used along with existing monitoring wells to continuously monitor pressure responses associated with pumping and injection and may also be monitored periodically for changes in water quality.

3.5 Groundwater Treatment and Disposition

The treatment system will consist of extraction well CrEX-1 (and a possible additional extraction well), a treatment system, a spray irrigation system for potential land application, and ultimately up to six injection wells. Once fully operational, the system will run continuously with pumped groundwater being treated at the surface and delivered to injection wells via piping. The treatment unit is likely to be sited at the CrEX-1 location to minimize the distance that contaminated groundwater is conveyed before pumping begins. Two treatment trains, each consisting of two ion-exchange vessels, will operate in series to treat groundwater extracted from CrEX-1. The first vessel removes up to 99% of the chromium (and nitrate), and the second vessel is used for redundancy and polishing. A third treatment train is held in reserve as a spare. Water quality in the treatment stream will be monitored in accordance with an NMED-approved discharge permit to ensure that water land-applied or dispositioned via reinjection will meet the criteria set forth in the permit(s). When the injection wells are operational, a computer-control system will be in place to monitor and control flow rates, pressures, water levels, and injection rates into the wells to ensure the systems are operating as designed. Flow rate of injected water will be monitored, and pressure at each injection well will be maintained at a design level. Water levels in all injection wells will be monitored by a control system with system shutdown mechanisms in places. Each injection well will also be equipped with a submersible pump to allow each well to be periodically back-flushed for maintenance. The approved discharge permit will include contingencies for failures in any part of the treatment and discharge system.

4.0 SCHEDULE

Implementation of the IMWP scope currently depends on the Laboratory's receiving approval from NMED for the land application of treated water pumped from CrEX-1. It is currently anticipated that a discharge permit will be in place for land application sometime in June 2015 to allow the Laboratory to begin pumping at CrEX-1. Under that scenario, pumping could be conducted continuously from approximately July to approximately November 2015, at which time pumping and land application will terminate because the permit will not allow land application on frozen ground. Additional restrictions on initial operations at CrEX-1 are the limits established for allowed days of pumping under the existing New Mexico Office of the State Engineer (OSE) permit. Eighty-seven days of pumping remain on the existing OSE permit. Additionally, existing National Environmental Policy Act (NEPA) coverage provides for an additional 13 million gallons of pumping. Extending operation of CrEX-1 past these limits requires completion of the Environmental Assessment process under the NEPA, an OSE permit for change in point of diversion, and a discharge permit for land application of treated water. The process involved for all of these permits is underway.

Drilling and construction of injection wells is expected to begin in fall 2015. The goal is to have the pumping, treatment, and injection infrastructure in place for operation in 2016; however, operation of the injection wells depends upon receiving the discharge permit for injection wells, the application for which was submitted April 2015. Once the system is fully operational, pumping and injection will operate continuously while monitoring is conducted by the Laboratory to determine whether hydraulic capture meets the objective of achieving and maintaining the plume edge within the Laboratory boundary.

If the goal is met, an updated extraction and injection operational program to maintain hydraulic control will be implemented. The updated strategy will consider opportunities to minimize groundwater extraction while still controlling the migration of chromium.

5.0 MANAGEMENT OF INVESTIGATION-DERIVED WASTE

Investigation-derived waste will be managed in accordance with EP-DIR-SOP-10021, Characterization and Management of Environmental Programs Waste. This standard operating procedure incorporates the requirements of applicable U.S. Environmental Protection Agency and NMED regulations, U.S. Department of Energy orders, and Laboratory requirements. The primary waste streams include development water, drill cuttings, drilling fluid, decontamination fluids, and contact waste.

6.0 REFERENCES

The following list includes all documents cited in this plan. Parenthetical information following each reference provides the author(s), publication date, and ER ID or ESH ID. This information is also included in text citations. ER IDs were assigned by the Environmental Programs Directorate's Records Processing Facility (IDs through 599999), and ESH IDs are assigned by the Environment, Safety, and Health (ESH) Directorate (IDs 600000 and above). IDs are used to locate documents in the Laboratory's Electronic Document Management System and, where applicable, in the master reference set.

Copies of the master reference set are maintained at the NMED Hazardous Waste Bureau and the ESH Directorate. The set was developed to ensure that the administrative authority has all material needed to review this document, and it is updated with every document submitted to the administrative authority. Documents previously submitted to the administrative authority are not included.

LANL (Los Alamos National Laboratory), October 2009. "Investigation Report for Sandia Canyon," Los Alamos National Laboratory document LA-UR-09-6450, Los Alamos, New Mexico. (LANL 2009, 107453)

LANL (Los Alamos National Laboratory), September 2012. "Phase II Investigation Report for Sandia Canyon," Los Alamos National Laboratory document LA-UR-12-24593, Los Alamos, New Mexico. (LANL 2012, 228624)

LANL (Los Alamos National Laboratory), April 2013. "Interim Measures Work Plan for the Evaluation of Chromium Mass Removal," Los Alamos National Laboratory document LA-UR-13-22534, Los Alamos, New Mexico. (LANL 2013, 241096)

LANL (Los Alamos National Laboratory), March 2014. "Summary Report for the 2013 Chromium Groundwater Aquifer Tests at R-42, R-28, and SCI-2," Los Alamos National Laboratory document LA-UR-14-21642, Los Alamos, New Mexico. (LANL 2014, 255110)

LANL (Los Alamos National Laboratory), March 2014. "Drilling Work Plan for Groundwater Extraction Well CrEX-1," Los Alamos National Laboratory document LA-UR-14-21478, Los Alamos, New Mexico. (LANL 2014, 254824)

LANL (Los Alamos National Laboratory), May 2014. "Interim Facility-Wide Groundwater Monitoring Plan for the 2015 Monitoring Year, October 2014–September 2015," Los Alamos National Laboratory document LA-UR-14-23327, Los Alamos, New Mexico. (LANL 2014, 256728)

NMED (New Mexico Environment Department), January 25, 2013. "Response, Proposal to Submit Interim Measures Work Plan for Chromium Contamination in Groundwater," New Mexico Environment Department letter to P. Maggiore (DOE-LASO) and J.D. Mousseau (LANL) from J.E. Kieling (NMED-HWB), Santa Fe, New Mexico. (NMED 2013, 521862)

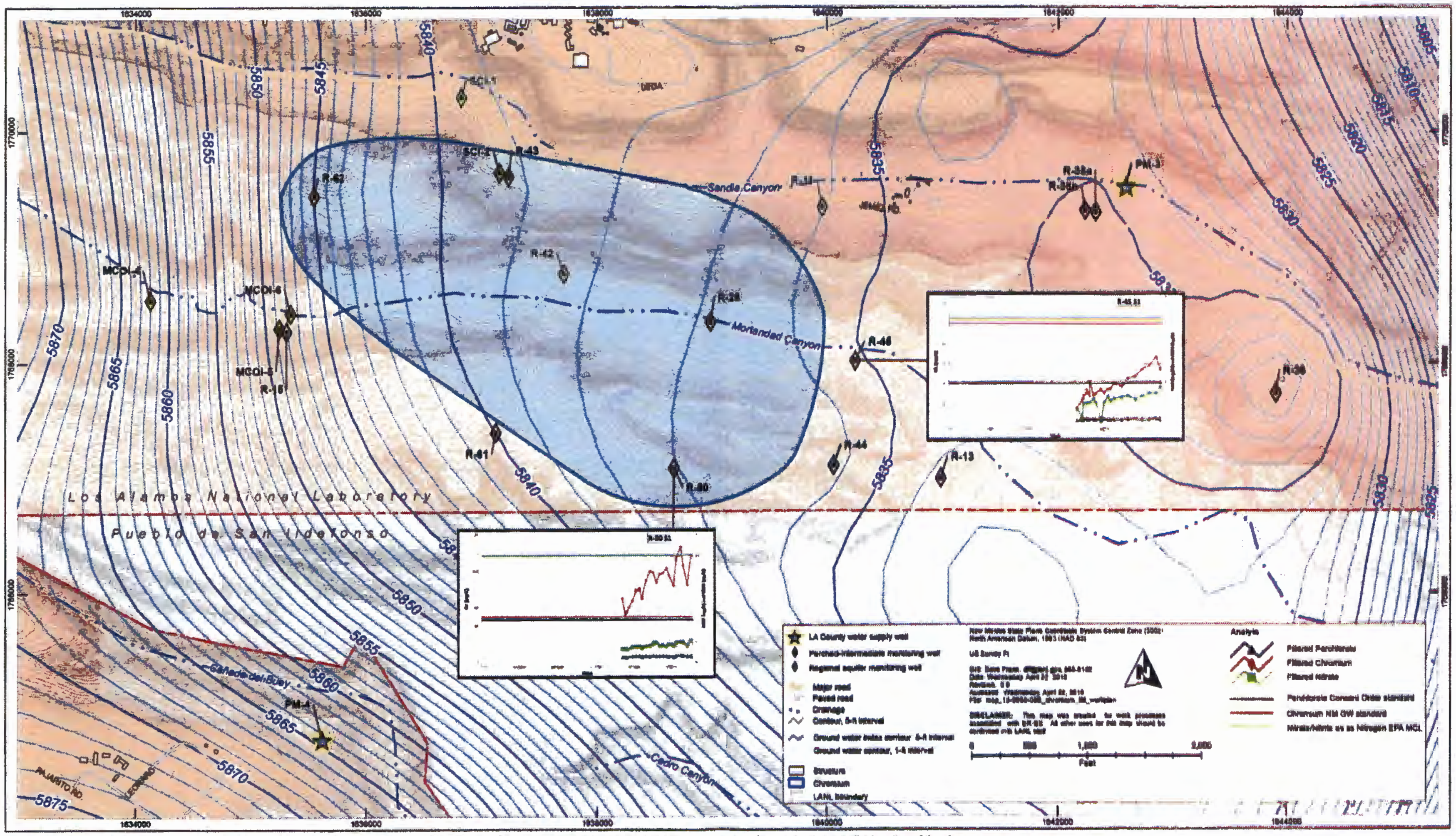

Notes: Shaded area represents the approximate plume edge at the 50-ppb level for chromium. The two time-series plots show increasing chromium concentrations at the downgradient portion of the plume.

Figure 1.0-1 Extent of chromium contamination in groundwater

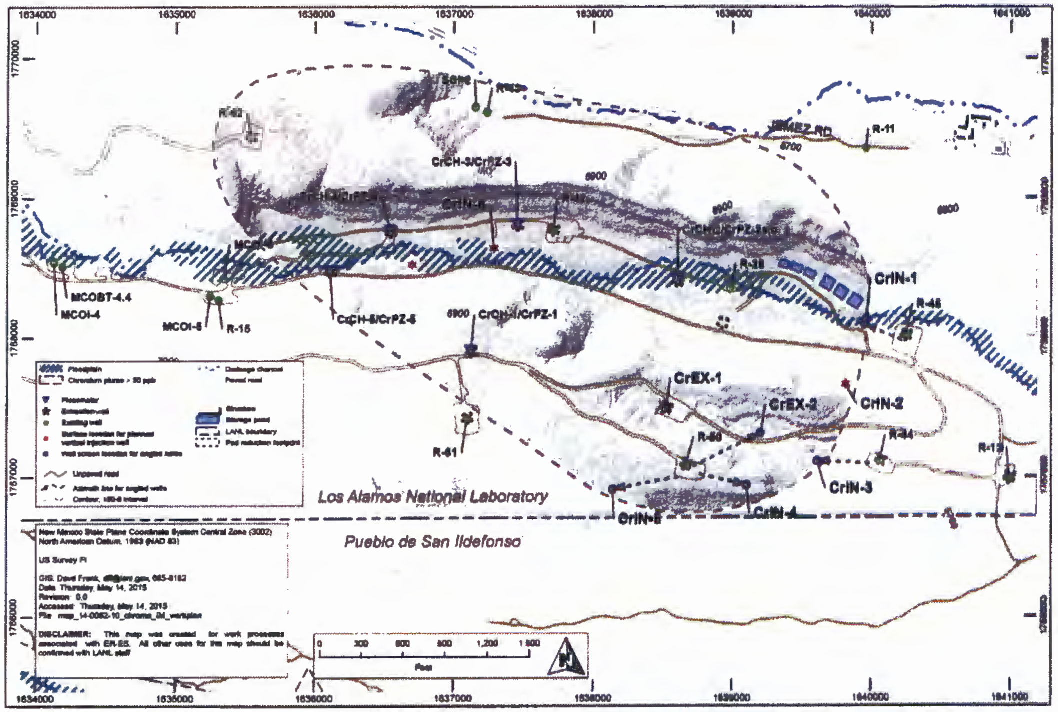

Figure 3.0-1 Location of the existing extraction well for hydraulic control and proposed locations for injection wells

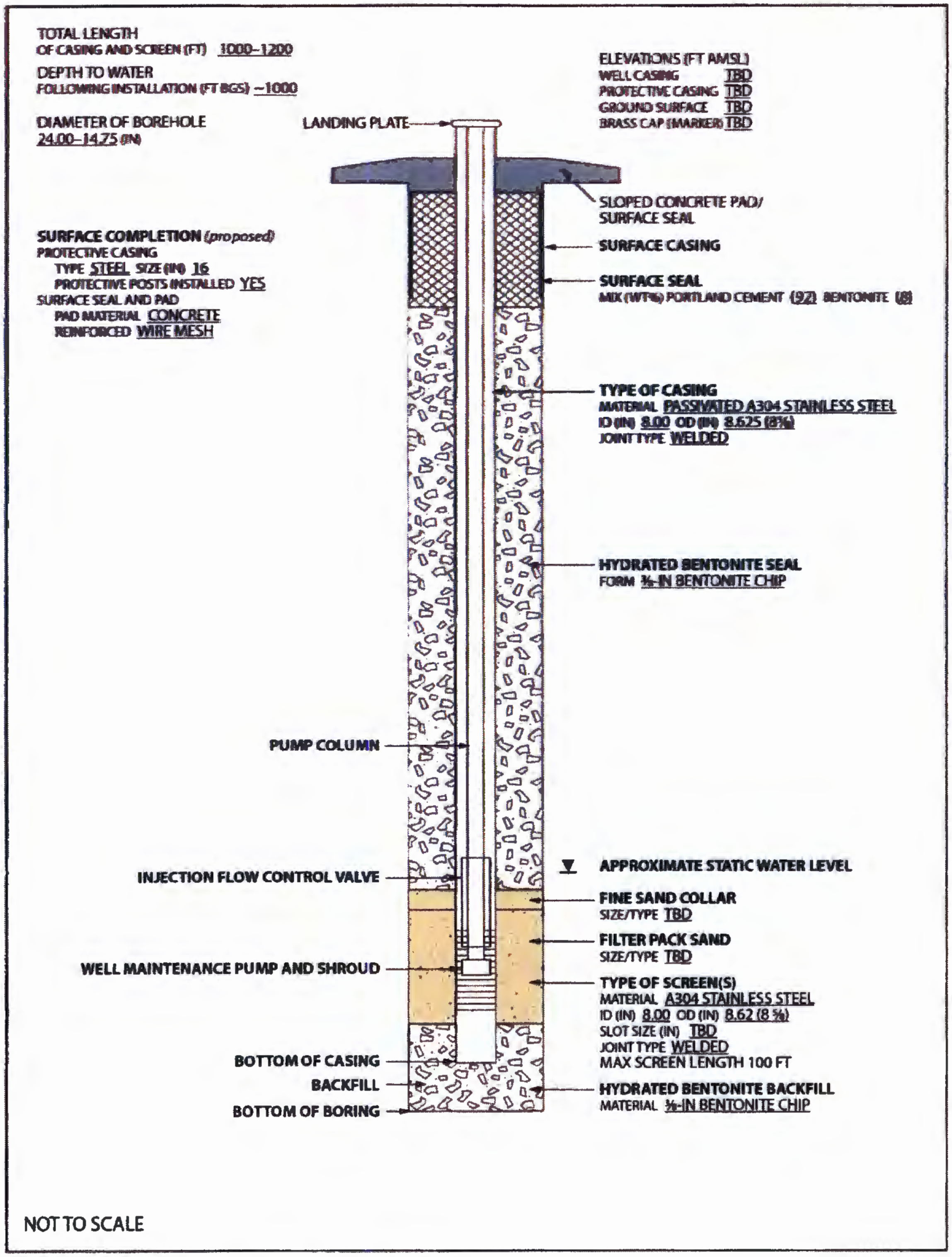

Figure 3.2-1 Generalized injection well design

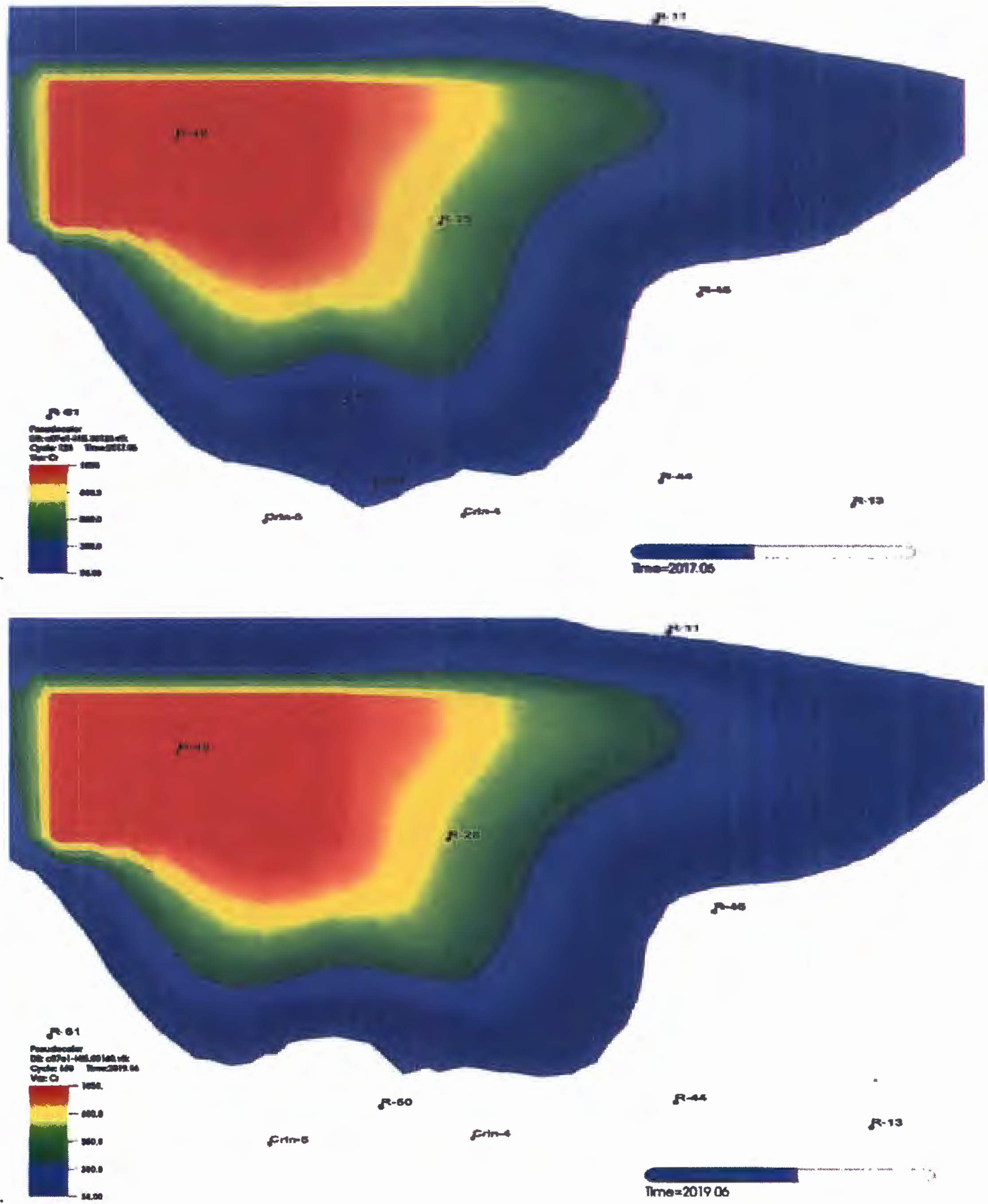

a.

b.

Note: The modeled scenarios assume pumping at CrEX-1 at 80 gpm and injection in CrIN-1 and CrIN-2 at 40 gpm each.

Figure 3.3-1 Snapshot estimations of the extent of chromium at the 50-ppb level for (a) 1-yr, (b) 3-yr, and (c) 5-yr time frames after initiation of pumping and injection

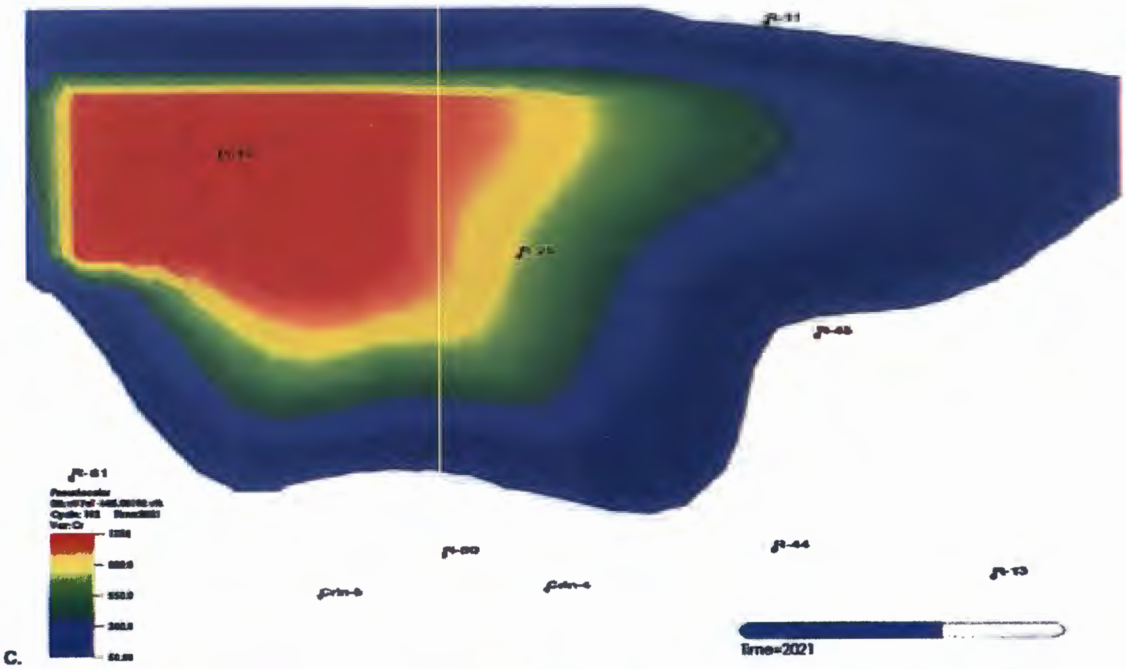

c.

Note: The modeled scenarios assume pumping at CrEX-1 at 80 gpm and injection in CrIN-1 and CrIN-2 at 40 gpm each.

Figure 3.3-1 (continued) Snapshot estimations of the extent of chromium at the 50-ppb level for (a) 1-yr, (b) 3-yr, and (c) 5-yr time frames after initiation of pumping and injection

Appendix A

Modeling Analyses

A-1.0 INTRODUCTION

This appendix provides a detailed analysis of the hydraulic pressure data collected during the pumping test conducted at regional chromium extraction well CrEX-1 by Los Alamos National Laboratory (LANL or the Laboratory). Preliminary analyses were presented in the "Completion Report for Chromium Extraction Well 1" (hereafter, the CrEX-1 Completion Report) (LANL 2015, 600170). The appendix also provides a modeling analysis of potential capture zones (CZs) and plume responses under different pumping regimes and injection scenarios.

A-2.0 HYDROGEOLOGY

CrEX-1 was installed initially to test the concept of hydraulic capture of chromium-contaminated groundwater to arrest plume migration at the southern downgradient edge of the plume. The CrEX-1 borehole was drilled using fluid-assisted dual-rotary drilling methods and mud-rotary methods. Drilling fluid additives included potable water, a foaming agent and benonite-based drilling mud. The CrEX-1 screened intervals consist of a 50.0-ft screen from 990 to 1040 ft below ground surface (bgs) and a 20-ft-long screen from 1070 ft to 1090 ft bgs that is isolated from the upper screen with a packer. A 30-ft section of blank casing separates the two screens. CrEX-1 is completed in the Puye Formation ([Tpf] 809 ft to 1054 ft bgs); mixed Miocene deposits ([Tjpf and Tcar] 1054 ft to 1070 bgs); and Miocene pumiceous sediments ([Tjfp] 1070 ft to 1155 ft bgs). Since only the upper 50-ft screen was pumped, the aquifer test provides information about the properties of Puye Formation. Aquifer testing indicated CrEX-1 will perform effectively and will be capable of sustained pumping at approximately 80–100 gallons per minute (gpm) (LANL 2015, 600170).

On October 3, 2014, following well installation, well development, installation of the packer between the upper and lower screens, and aquifer testing, the depth to water was 997.2 ft bgs. The upper screen of CrEX-1 straddles the regional water table. This allows for effective interrogation of the upper most portion of the regional aquifer next to the regional water table where the highest contaminant concentrations are expected. As a result, the effective screen length is about 43 ft (from the water table to the bottom of the upper screen which is at 1040 ft bgs).

The pumping of CrEX-1 produces a maximum drawdown of about 6.2 m (~20 ft) within the pumped upper screen at a pumping rate of approximately 80 gpm. However, the well-specific capacity does not decline with the increase of the pumping rate (and the respective increase of the pumping drawdown; see below). This suggests that borehole skin effects cause a portion of the drawdown; as a result, the drawdown in the aquifer near the well is expected to be much lower than the one observed within the pumped borehole. Nevertheless, the pumping causes a decline in the regional water table, and it is expected that residual vadose-zone groundwater flow from the capillary fringe may impact the drawdowns observed in CrEx-1. Therefore, unconfined (phreatic) groundwater flow is occurring near the pumped well. However, the observed drawdowns are still small compared with the aquifer thickness (>100 ft), and therefore it is acceptable to use analytical solutions and numerical models that interpret the flow as confined.

Based upon the depth to water of 997.2 ft bgs measured at CrEX-1 on October 3, 2014, after installation, initial development and aquifer testing, the water-level elevation was approximately 5834.73 ft above mean sea level ([amsl] the top of well casing is at elevation 6831.91 ft and the water level in the well is 997.2 bgs).

A-3.0 CrEX-1 PUMPING TEST DATA

CrEX-1 was tested from October 1 to 4, 2014. Testing consisted of a five-step pumping test on October 1, and a 24-h constant-rate pumping test that was begun on October 3. The pumping rates during the five-step test and the 24-h pumping test were relatively steady. The water level declines and rebounds very fast in response to pumping. The initial recovery of water levels to elevations higher than the equilibrated static level during rebound when pumping stops could indicate groundwater recharge from the vadose zone, but there may be other explanations such as elastic deformations in the porous media. The water level also recovers relatively fast to the prepumping conditions after pumping stops, suggesting the aquifer at CrEX-1 has relatively high hydraulic conductivity and that borehole skin effects may be impacting the observed drawdowns within the pumping well. The aquifer testing was performed in the upper screen only. A 50-horsepower, 6-in.-diameter Grundfos submersible pump was used to perform the aquifer tests.

Five short-duration pumping intervals (steps) without recovery in between were conducted on October 1. The primary objective of the short-duration step tests was to assess the hydraulic behavior of the system and properly determine the optimal pumping rate for the 24-h test. The step tests demonstrated that the specific capacity of the well does not seem to depend on the pumping rate, which suggests the well is fully developed. During the step tests, the specific capacity varied between 100 and 120 m^2/d (5.5 and 6.6 gpm/ft). The pumping at the highest rate produced about 5 m (~16 ft) drawdown within the screen. However, the well-specific capacity does not decline with the increase of the pumping rate (LANL 2015, 600170, Appendix D). This suggests that borehole skin effects cause a portion of the drawdown. Nevertheless, the pumping causes a decline in the regional water table. Therefore, unconfined (phreatic) groundwater flow is occurring near the pumped well.

A 24-h aquifer test was completed on October 3. The test was conducted at a pumping rate of 517.6 m^3/d (94.9 gpm). The 24-h aquifer test analyses suggested a formation transmissivity on the order of 490 m^2/d (40,000 gallons per day/ft). This transmissivity value is very similar to the estimate obtained by a recent analysis of R-28 aquifer test conducted in 2014 (LANL 2014, 255110).

The saturated thickness corresponding to the transmissivity value is not known in order to estimate hydraulic conductivity. The saturated thickness is impacted by the pumping because the pumping causes a decline in the regional water table. If it is assumed the saturated thickness is the length of the initial saturated screened interval (~43 ft before the pumping started) minus a half the observed drawdown (~10 ft), the estimated average hydraulic conductivity is about 49 m/d or 161 ft/d. However, this estimate is uncertain. Still, the value of hydraulic conductivity is consistent with the estimate obtained for R-28 (~120 ft/d).

The CrEX-1 transmissivity and hydraulic conductivity estimate suggests the extraction well is within a highly permeable zone of the regional aquifer. This can be very beneficial in terms of the CrEX-1 primary objective of hydraulic capture. Appendix D of the CrEX-1 Completion Report presents the complete results and analysis of the CrEX-1 aquifer test.

After the completion of the 24-h-pumping test, CrEX-1 was continuously pumped from October 5 to November 26, 2014. The 52-d pumping was conducted at an average pumping rate of about 81 gpm. On December 1, the pumping resumed for another 11 d at a similar rate. During the last 2 d of pumping, higher pumping rates were attempted, but it appeared that at rates greater than 100 gpm too much drawdown occurred in the well to sustain rates greater than 100 gpm.

The extended pumping at CrEX-1 provided additional data for analyses of aquifer properties. More importantly, the extended pumping allowed for detection of pressure declines at the nearby observation wells.

A-4.0 ANALYSIS OF CrEX-1 PUMPING TEST DATA

The water-level data for the CrEX-1 pumping test were analyzed using the method described in (Vesselinov and Harp 2011, 227709) to estimate the drawdowns that can be attributed to each nearby monitoring well. The analyses account for the pumping effects caused not only by CrEX-1 but also the municipal water supply pumping at PM-4, PM-2, O-4, etc. The analyses utilize two open-source codes developed at the Laboratory: WELLS (http://wells.lanl.gov) and MADS (http://mads.lanl.gov). WELLS is applied to simulate the drawdowns caused by the pumping at CrEX-1 and the water supply wells. MADS is applied to (1) deconstruct pumping drawdowns caused by different pumping wells and (2) estimate aquifer properties by matching the simulated and observed hydraulic heads at the observation wells.

Figures A-4.0-1 through A-4.0-19 present the results of this analysis. Each figure shows the model-based deconstruction of the water-level transients observed in each monitoring well during the 2014 CrEX-1 pumping period. In each figure, the upper plot shows the observed and simulated water levels at the monitoring well, and the lower plot shows the attribution of the drawdown to each of the wells pumped during the observation period: O-4, PM-2, PM-3, PM-4, PM-5, CrEX-1, R-42, and R-28. The analyses require long data records. The longer the record, the more accurate are the deconstructed pressure estimates. Table A-4.0-1 lists the estimated CrEX-1 drawdowns at the end of the CrEX-1 pumping tests.

Uncertainties associated with estimates of aquifer properties based on the CrEX-1 pumping data are because of the small magnitude of the drawdowns measured in some of the observation wells. The presented estimates in Table A-4.0-1 are preliminary. Additional data collected during upcoming 2015 CrEX-1 pumping test will help to substantially reduce the uncertainties and better characterize aquifer properties.

Based on the results shown in Figures A-4.0-1 through A-4.0-19, the following important observations can be made about the aquifer behavior during the 2014 CrEX-1 pumping test.

The CrEX-1 induced drawdown is uncertain at CrPZ-1 (CrCH-1 on Figure A-4.0-1). The collected pressure record was very short. However, it can be concluded that changes in the pumping rates in CrEX-1 in December 2014 may have caused pressure transients at CrPZ-1; although this conclusion is expected, more data are needed to better understand the CrPZ-1 hydraulic response to CrEX-1 pumping.

R-1 transients are well reproduced by the model but the model-estimated CrEX-1 drawdown is questionable and small, if present (Figure A-4.0-2). R-11 and R-13 transients are also well reproduced by the model (Figures A-4.0-3 and A-4.0-4); the CrEX-1 drawdown in these wells is small but potentially well defined by the existing data and applied model.

There are some potential problems with the late 2014 water-level data collected at R-15 (Figure A-4.0-5); the steady flat pressure decline observed in late 2014 contradicts the previous model analyses. Therefore, the data are not sufficient to define the CrEX-1 drawdown in this monitoring well.

R-33 screen 1 and R-35b transients are well reproduced by the model, but the CrEX-1 drawdown contribution is questionable and small, if present (Figures A-4.0-6 and A-4.0-7). The pressure data collected in R-33 screen 2 is difficult to analyze because of the strong pressure transients caused by the municipal water-supply pumping, and thus the data and modeling results are not included here.

Data gaps and uncertainties are associated with the R-42 pressure record that make the analyses difficult and the CrEX-1 drawdown estimate is uncertain (Figure A-4.0-8).

R-43 screen 1 and screen 2 transients are well reproduced by the model, but the model-predicted CrEX-1 drawdown is uncertain and small, if present (Figures A-4.0-9 and A-4.0-10).

Figures A-4.0-11 through A-4.0-18 show the drawdowns in a series of two-screen wells near CrEX-1: R-44, R-45, R-50, and R-61. The results for these wells show that pressure transients are very well reproduced by the model.

R-50 screens show the largest drawdowns observed by any of the monitoring wells (Figures A-4.0-15 and A-4.0-16). There are important discrepancies between the observed and model simulated pressure transients during the CrEX-1 pumping test related to R-50. The model reproduces relatively well the pressure transient including the limited recovery record after the pumping termination (Figures A-4.0-15 and A-4.0-16). However, the model overpredicts the pressure decline at the beginning of the CrEX-1 pumping test. It is expected that this be caused by phreatic effects. The applied model does not account for vadose zone and water table hydraulic impacts during the CrEX-1 pumping test and this is the possible reason for the discrepancy. This observation is important because it provides insights about the aquifer properties in the area between CrEX-1 and R-50. Additional pressure data collected during 2015 CrEX-1 pumping conducted for the interim measure will help to better understand site hydraulic conditions.

Figure A-4.0-19 shows the pressure transients in R-62. Data gaps and uncertainties are associated with R-62 pressure record that make the analyses difficult and the estimates unclear.

It is important to note that substantial data gaps and uncertainties are also associated with R-28 pressure records in 2014 (the data are not presented here), making a complete analysis related to the CrEX-1 pumping test difficult. More data are needed to understand the R-28 hydraulic response to CrEX-1 pumping.

As discussed earlier, the aquifer is expected to be heterogeneous. The estimated transmissivity and storativity values in Table A-4.0-1 seem to confirm this expectation. The estimated values in the table represent effective aquifer properties between the pumping (CrEX-1) and observation wells. The analyses are based on an analytical model (Theis) that assumes uniformity in aquifer properties and confined conditions. These assumptions are not expected to be valid so the estimated transmissivity and storativity values should be analyzed with care. Nevertheless, the relatively large variability in the estimated transmissivity and storativity values suggest pronounced aquifer heterogeneity.

A-5.0 ANALYTICAL ANALYSIS OF CrEX-1 CAPTURE ZONE

Table A-4.0-1 shows the pumping-related drawdowns at the end of the 2014 CrEX-1 pumping period. Here, the zone of influence (the ZOI or the cone of depression) is identified as the area within which measurable pumping drawdown greater than 0.01 m can be detected. Theoretically, very small (immeasurable) drawdowns will be manifested throughout the regional aquifer. However, practically speaking, the ZOI is defined as the zone where drawdown greater than 0.01 m can be detected. The CrEX-1 ZOI appears to be extensive (Table A-4.0-1). The only nearby well that was not apparently influenced by CrEX-1 pumping is R-36.

The ZOI during aquifer pumping is different than the CZ, which represents the portion of the aquifer that is affected by the pumping well in such a way that all the groundwater within the CZ will be pumped out by the well. In the case of a uniform isotropic aquifer, the shape of ZOI and CZ will be similar: it will be a circle centered at the pumping well. The radius of the circle will depend on the pumping time. Typically, the ZOI is larger than the CZ.

However, in the case of ambient flow, the shape of the CZ will have an elongated form with a predominantly upstream spatial extent. A schematic representation of the CZ shape is presented in Figure A-5.0-1. The CZ estimate typically assumes only an advective steady-state groundwater flow. However, because of groundwater dispersion, some of the groundwater within the CZ will escape capture while some of the groundwater outside the CZ will be captured. Because of transients in the groundwater pressures and flow velocities from induced pumping at CrEX-1, the CZ will grow around the pumping well until a quasi-steady-state flow regime is established around the pumping well.

Under the quasi-steady-state, the pressures still decline from pumping; however, the hydraulic gradients equilibrate to the final steady-state values. The zone of quasi-steady-state flow regime (ZQSS) grows in time around the pumping well, and the rate of propagation depends on the aquifer properties and the pumping rate. Both the ZOI and the ZQSS are expected to have a similar shape (circular in the case of a uniform aquifer). The CZ shape depends on the ambient flow properties (Figure A-5.0-1) that is, the magnitude of the ambient groundwater flow. The CZ extent upgradient grows in time and depends on both the pumping duration and rate, and on the ambient groundwater flow properties. The CZ extent downgradient reaches an inflection point after a given period of pumping and cannot be increased further.

In general, the CZs of pumping wells have a three-dimensional shape characterized by three-dimensional structure and properties of the regional groundwater flow during the aquifer test. As a result, the CZ depends on various hydrogeologic factors:

- pumping rate and duration;
- shape of the regional water table;
- aquifer thickness;
- spatial and temporal distribution in aquifer flow velocities controlled predominantly by heterogeneity and anisotropy in aquifer properties (permeability, storativity, etc.);
- spatial and temporal variability in aquifer recharge controlled predominantly by heterogeneity and anisotropy in vadose zone properties and spatial and temporal distribution of infiltration along the nearby canyons; and
- influence of water-supply pumping at nearby municipal water-supply wells (PM-3, PM-5, PM-4 and PM-2); the water-supply pumping causes small changes in the water levels measured at monitoring wells. As a result, it is expected that the water-supply pumping does not significantly affect the shape of the CrEX-1 CZ.

It is important to emphasize that the magnitude of aquifer recharge can be an important factor affecting the size of the estimated CrEX-1 CZ. In general, the magnitude of aquifer recharge on the Pajarito Plateau is relatively small (less than 1 mm/yr), and recharge at this scale is not expected to significantly influence the shape of the CZ of pumping wells. In this case, for modeling purposes, the regional water table can be approximated as a no-flow boundary. However, higher recharge rates in the plume area resulting from localized recharge along Sandia and Mortandad Canyons can significantly influence the shape of the CZ.

A-5.1 CrEX-1 Capture Zone Estimate Based on the Pumping Rate Only

The CZ at CrEX-1 can be estimated based on the volume of water pumped. This approach allows for better approximation of the CZ size at early times when the pumping period is relatively short (for example, less than 100 to 300 days).

In this case, the CZ is assumed to have a cylindrical shape with a constant vertical height *H* (depending on the well screen length) and time-varying horizontal radius *R*. To account for the three-dimensional component of groundwater flow near the well screen, the vertical height *H* is assumed to be approximately 1.5 times the screen length; for example, *H* is ~15 m (50 ft) for CrEX-1. In this case, the three-dimensional aspect of the groundwater flow increases the CZ thickness only below the screen, not above the screen because at the top the CZ is bounded by the regional water table. The cylinder radius can be computed using the following formula:

$$R = \sqrt{\frac{Q_P t}{\pi \phi_S H}}$$

where Q_p is the pumping rate, *t* is pumping duration, ϕ_S is the water storage porosity. If the total water-filled porosity is assumed to be 0.3, the CZ after 52 d of pumping has a radius of 32 m (~110 ft) around the well. However, this CZ estimate does not account for ambient groundwater flow in the aquifer.

A-5.2 CrEX-1 Capture Zone Estimate Based on Ambient Aquifer Flow

The CZ can also be estimated based on the width of groundwater flow within which the ambient groundwater flux is equal to the pumping rate (Figure A-5.0-1). In this case, the CZ grows upgradient until reaching a width within which the ambient groundwater flow rate is equal to the pumping rate (Figure A-5.0-1). This approach allows for a better approximation of the CZ size at late times when the pumping period is relatively long, allowing establishment of a quasi-steady state flow regime near the pumping well. This approach is best applied for long-duration pumping periods, greater than 100 to 300 days. This is a function of the aquifer properties. In this case, the width of the CZ perpendicular to the groundwater flow direction becomes a constant in time once the flow reaches a quasi-steady state.

Assuming uniform confined groundwater flow conditions, the flow rate Q through a vertical section in the regional aquifer with a horizontal width *W* can be computed as:

$$Q = ITW$$

The width *W* can be computed as:

$$W = \frac{Q_P}{IT}$$

The ambient groundwater flow in the aquifer near CrEX-1 has hydraulic gradient of about 0.001. For pumping rate of 81 gpm and transmissivity of 40,000 gpd/ft, the width of CZ upgradient from CrEX-1 is about 900 m (~3000 ft) perpendicular to the groundwater flow direction. The CZ width adjacent to CrEX-1, W_w (Figure A-5.0-1) is exactly half of the upgradient width *W*, or about 450 m (~1500 ft). These are initial model estimates because there are uncertainties in the ambient hydraulic gradient and the large-scale aquifer transmissivity that define the ambient groundwater flux. For example, if the hydraulic gradient is an order of magnitude higher (0.01, i.e., ambient groundwater flux is an order of magnitude higher), the width of CZ upgradient from CrEX-1 will be approximately 90 m (~300 ft). The data collected during fieldwork in 2015 (pumping and tracer tests) will provide additional information to constrain this uncertainty. It is also important to emphasize that these estimates are based on assumptions for uniform and homogenous groundwater flow; aquifer heterogeneity will further impact the shape and site of the CZs.

The maximum length of capture in the downgradient direction, L_0, from the pumping well (Figure A-5.0-1) can be expressed as follows:

$$L_0 = \frac{Q_p}{2\pi TI}$$

For a pumping rate of 81 gpm, the length of CrEX-1 CZ in the downgradient direction, L_0, is about 143 m (~580 ft). If the hydraulic gradient is an order of magnitude higher (0.01), the width of CZ upgradient from CrEX-1 is only about 14 m (~45 ft).

Once the equilibrium between the pumping and ambient flow rates has been established, the pumped well will capture the groundwater flowing toward the well in the CZ. The length *L* of the CZ upgradient of CrEX-1 (Figure A-5.0-1) depends on the groundwater flow pore velocity and the pumping duration.

It is important to emphasize that the dimension of the CZ computed above is for long-term pumping periods. For example, if the CrEX-1 pumping was turned on for an extended period of more than 300 d, the presented CZ estimates will be valid estimates (assuming that the aquifer is uniform). However, the CrEX-1 aquifer test data also demonstrate that the aquifer is also highly heterogeneous. As a result, the shape of the steady-state CZ will likely have a much more complicated shape and will likely have dimensions less than those estimated above.

The CrEX-1 CZ during the 2014 pumping period (because of the relatively short duration of the tests) is expected to be more consistent with the estimates based on the pumped volume. Therefore, the CrEX-1 CZ during the 2014 pumping period is estimated to have radius of about 32 m (110 ft) around the pumping well.

A-6.0 NUMERICAL MODEL ANALYSIS OF CrEX-1 PUMPING

A numerical model of groundwater flow and contaminant transport in the regional aquifer beneath the Sandia and Mortandad Canyons area is developed to inform and enhance the understanding of the fate and transport of chromium in the environment. This section describes the current state of the development of the numerical model and discusses the current modeling results. This is a work in progress and a continuation of the model analyses presented in the 2008 "Fate and Transport Investigations Update for Chromium Contamination from Sandia Canyon" (LANL 2008, 102996) and the 2012 "Phase II Investigation Report for Sandia Canyon" (LANL 2012, 228624).

Flow numerical simulations are applied to predict the groundwater flow in the regional aquifer in the chromium plume area. Groundwater flow and contaminant transport in the unsaturated zone are not part of the current modeling effort.

A three-dimensional unsaturated zone model is contained in Appendix J of the 2008 "Fate and Transport Investigations Update for Chromium Contamination from Sandia Canyon" (LANL 2008, 102996). The vadose-zone model analyses demonstrated the potential three-dimensional channeling and lateral diversion (along hydrostratigraphic contacts) of water infiltrating beneath Sandia Canyon before it reaches the regional aquifer. Further developments of the three-dimensional unsaturated zone model are ongoing as well.

The current goal is to generate a model calibrated against existing water-level observations during the 2014 CrEX-1 pumping period. The model will also be calibrated to reproduce the pumping effects caused by municipal water supply–well pumping near the plume area. Additionally, the model will be calibrated to the cross-well pumping effects caused by pumping at R-42 and R-28 during short- and longer-term pumping tests previously conducted in these wells.

However, the model currently does not represent (1) the ambient groundwater flow at the site, (2) the long-term water-level changes in the regional aquifer, and (3) the long-term chromium concentration transients observed in the site monitoring wells. In the future, these components will be added to the calibration process as well. The model is also representing the aquifer as confined. More complex model analyses accounting for the impacts of the phreatic and the vadose zones on the regional aquifer flow will be developed in the future as well. The model also currently simulates the flow medium as a single continuum and does not represent potential dual porosity within the aquifer materials. Updated modeling analyses will incorporate dual porosity effects for the regional aquifer, which may also exhibit substantial spatial variability especially as it affects storage of chromium.

The model is calibrated against existing water-level drawdowns observed at regional wells R-1, R-33 (2 screens), R-15, R-62, R-43 (2 screens), R-42, R-28, R-61 (2 screens), R-50 (2 screens), R-45 (2 screens), R-44 (2 screens), R-11, R-13, R-35b, R-36, and R-34; 16 wells and 22 screens in total. The model simulates the pumping effects caused by CrEX-1, R-42, R-28, PM-1, PM-2, PM-3, PM-4, PM-5, and O-4.

The model is calibrated using an automated calibration process employing the Levenberg-Marquardt optimization algorithm as implemented in the code MADS (http://mads.lanl.gov). The objective function subject to minimization is defined as

$$\Phi = [\mathbf{c} - f(\mathbf{b})]^T \mathbf{W} [\mathbf{c} - f(\mathbf{b})]$$

where **c** is a vector [N×1] of optimization targets, b is a vector [M×1] of model parameters, **W** is a diagonal weight matrix [N×M], and *f* is the model. While Φ is minimized, the algorithm searches for the maximum-likelihood parameter set **b** that provides the best fit between simulated $f(\mathbf{b})$ and measured **c** quantities. The vector of optimization targets includes estimated drawdowns in the monitoring wells. **W** represents the relative weight of each optimization target defined subjectively based on the magnitude of the calibration data. The vector **b** includes various model parameters considered in the inverse analysis.

The model development included a series of inverse analyses with different complexity. The final model has on the order of 84 unknown model parameters (outlined in the next section) and about 182,070 calibration targets.

The model domain and the computational grid are shown in Figure A-6.0-1. The figure represents the three-dimensional model domain, computational grid, and locations of the monitoring well screens included in the model. The computational grid is structured with local grid refinements near the existing wells. Vertically, the grid has higher resolution close to the top of the model and grid spacing increases with depth. The lateral spacing is approximately 50 × 50 m (~160 × 160 ft). The vertical spacing varies from about 1 m to 15 m. The grid includes about 540,000 nodes and about 3,053,000 elements. The colors in Figure A-6.0-1 represent the different geologic units. The top of the model is constrained by the regional water table. The grid is designed to provide sufficient computational accuracy and efficiency for the performed model analyses. The model domain extends approximately 20 km west-east, approximately 16.5 km north-south, and approximately 1075 m vertically. All the model boundaries are defined as no-flow boundaries. Initial boundary condition is a constant head (zero drawdown) throughout the model domain. The regional aquifer is simulated as confined while, in reality, the aquifer is phreatic (unconfined). Model simulations representing the regional water table as a material boundary are feasible but much more computationally intensive. Given the small magnitude of the water-level fluctuations, the current modeling approach is justified.

The computer code LaGriT (http://lagrit.lanl.gov) was used to create the computational grids. The flow and transport simulations were performed with the Finite Element Heat and Mass Transfer code ([FEHM] http://fehm.lanl.gov) (Zyvoloski et al. 1996, 054421; Zyvoloski et al. 1997, 070147). FEHM was developed by researchers at the Laboratory and is capable of simulating three-dimensional, time-dependent, multiphase, non-isothermal flow, and multicomponent reactive groundwater transport through porous and fractured media. FEHM has been used in a wide variety of applications. The software is mature, has users throughout the world, and has been certified through the Yucca Mountain Project Software Quality Assurance Program. FEHM is available to the public and operates under various operating systems (Windows, MAC OS X, Linux, etc.).

The simulations are performed assuming unknown aquifer properties. The grid does not include distinct stratigraphic boundaries although they are known to be present within the model domain. Previous analyses of water-level responses to water-supply pumping and during the CrEX-1, R-28, and R-42 pump tests indicate aquifer materials are heterogeneous potentially at scales less than the size of the individual units and no distinct contrasts exist between different units. Therefore, aquifer permeability is simulated using geostatistical modeling and the pilot-points method. The pilot points are fixed locations where aquifer permeability and storativity are adjusted during the calibration process. The permeability and storativity at the pilot points are applied to compute aquifer permeability and storativity within the model domain using kriging. The values at the pilot points are adjusted during model calibration to represent heterogeneous fields that produce groundwater flow consistent with the observed calibration data. The analyses presented below employed 28 pilot points located within and around the area containing the chromium plume. The applied set of pilot points cannot be expected to characterize small-scale aquifer heterogeneity; it is expected only to define potential large-scale structures that control groundwater flow and contaminant transport. No prior information from pumping tests at the monitoring wells is applied to define or constrain the aquifer permeability at the pilot points. The three-dimensional kriging is performed using the code GSTAT (http://www.gstat.org) to compute permeability values for each node in the model domain representing aquifer heterogeneity.

The modeling results representing a comparison between the calibration targets and obtained model drawdowns predictions are shown in Figures A-6.0-2 through A-6.0-17. In general, the model predicts with good fidelity the observed drawdowns. Some of the drawdowns during CrEX-1 pumping are matched very well, especially at the wells located relatively close to CrEX-1. For example, the calibration targets for R-11, R-13, R-44 screen 1, R-45 screen 1, R-50 screen 1, R-50 screen 2, drawdowns are well represented by the model. The matches between observations and model predictions for the other monitoring well screens need more work.

The inverse analysis specifically targeted the characterization of the mid- and late-time drawdowns in R-50 screens 1 and 2 (Figures A-6.0-15 and A-6.0-16) and these portions of the drawdown curves are well predicted by the numerical model. As discussed in section 4 above, the early-time drawdowns in R-50 (Figures A-4.0-15 and A-4.0-16) are not well represented because of a potential impact of conditions that are not embodied in the current numerical model; the 2015 CrEX-1 pumping record will help to better resolve this conceptual uncertainty. Since the hydraulic communication between R-50 and CrEX-1 is important for predictions related to the impact of CrEX-1 pumping on the R-50 chromium concentrations, the capability of the current model to represent a large portion of the observed drawdown curves in R-50 is of great importance.

It is essential to note that the results modeled are based on relatively limited existing data and will be significantly enhanced during the upcoming pumping and monitoring period.

The estimated hydraulic conductivity (lateral and vertical) is shown in Figure A-6.0-18. The inverse model analysis accounts for R-28 and CrEX-1 pumping records. The inverse model analysis also takes into account the pressure changes observed during municipal water-supply pumping in the nearby groundwater production wells. The obtained estimates of the aquifer properties represent a three-dimensional tomographic image of the aquifer hydraulic conductivity. The figure demonstrates the pronounced aquifer heterogeneity, which is an estimate, based only on the pumping drawdowns observed in the monitoring wells. It is expected the solution is nonunique and that numerical models with alternative conceptualization and model parameters can be obtained that are also consistent with the available data. Therefore, the obtained modeling results should not be considered to be the only possible solution of the analyzed problem. It is also important to note that these results are preliminary and will benefit from additional data collected for the interim measure. Additional modeling work is being performed to address these uncertainties and their impact on the selection of potential remediation scenarios.

A-7.0 NUMERICAL MODEL ANALYSIS OF CrEX-1 CAPTURE ZONE

The estimated hydraulic conductivity field discussed in section A-6.0 (Figure A-6.0-18) is applied to estimate the CrEX-1 CZ. To do so, the hydraulic conductivity field is applied in the 2012 numerical model. The 2012 model is used because it has been already calibrated to the hydraulic heads in the aquifer in the plume area (LANL 2012, 228624). The current model presented in section A-5.0 has not yet been calibrated to the hydraulic heads. The current model has been calibrated only against the drawdowns caused by site pumping tests and municipal water-supply pumping. The mapping of the new estimates of the hydraulic conductivity field on the 2012 model definitely impacts the accuracy in the model predicted hydraulic gradients. This is done only to get preliminary estimate of the potential shape of the CrEX-1 CZ and the effect of aquifer heterogeneity on model predictions. This is a preliminary analysis. An updated model currently being calibrated against hydraulic heads observed to date in the monitoring wells in the plume area combined with additional model updates based on future data will give much more representative results.

Preliminary model predictions of the CrEX-1 CZ after 1, 3, and 5 yr of pumping are presented in Figure A-7.0-1. The model predictions represent the groundwater flow paths assuming only advective flow. However, dispersion processes occurring in the groundwater flow within porous media will impact the CZ estimates. The predictions are based on the heterogeneities presented in Figure A-6.0-18.

The CrEX-1 modeled CZs are shown in Figure A-7.0-1. The model predicts that the CZ extends to the west-northwest of the well. This result suggests that long-term CrEX-1 pumping may have beneficial impact on the plume concentrations. However, because of aquifer heterogeneity, including a zone of relatively low permeability in the R-42 area (Figure A-6.0-18), the long-term CrEX-1 pumping would not be expected to significantly affect chromium concentrations in the centroid of the chromium plume.

Preliminary model predictions in Figure A-7.0-1 represent the groundwater flow paths, assuming only advective flow. However, dispersion processes are expected to occur in groundwater flow within porous media, and these processes will impact the shape of the CZs. As a result of the dispersion, some of the contaminant mass outside the model predicted CZ is expected to be captured as well. However, the dispersion may also cause some of contaminant mass within the modeled CZ to escape capture by CrEX-1. The CrEX-1 CZ will be also impacted by transients in the regional groundwater flow. Additional pumping and injection of groundwater near CrEX-1 will impact the shape of the CrEX-1 CZ as well.

These modeling results are preliminary and will be updated as more data are available from the pumping and monitoring of pressure responses. The preliminary results demonstrate the potential complexity in the aquifer properties and the associated difficulties to estimate the CrEX-1 CZs. The ongoing modeling analyses and the upcoming additional data collection activities in 2015 are expected to reduce these uncertainties.

A-8.0 NUMERICAL MODEL ANALYSIS OF PLUME RESPONSE TO THE INTERIM MEASURES

In this section, the 2012 model is applied to estimate the impact of the proposed interim measures activities on the chromium concentrations and plume configuration in the regional aquifer. The 2012 model is the preferred model for this analysis because it has been successfully calibrated to (1) the hydraulic heads and (2) the chromium concentrations in the aquifer in the plume area. However, the 2012 model is not calibrated to represent the drawdowns observed during the recent R-28 and CrEX-1 pumping periods. The 2012 model is also not calibrated to represent the 2014 tracer test data. Future modeling analyses will use the model update discussed in section 5 that will include all these calibration data sets.

A model prediction of the chromium concentrations in 2016 and 2021 without active pumping is shown in Figure A-8.0-1. The model predictions are based on the 2012 model (LANL 2012, 228624). These results are presented for a comparison with the modeling results presented below for the case of active groundwater pumping and injection.

Model predictions of the impact of various interim measures scenarios on the chromium concentrations are presented in Figure A-8.0-2 and A-8.0-3. The plots are showing model predictions in 2016, 2017, 2019, and 2021 (after 0, 1, 3 and 5 yr of pumping/injection, respectively).

In the first case (Figure A-8.0-2), CrEX-1 is pumping for 5 yr at 80 gpm (2016–2021), CrIN-4 and CrIN-5 are injecting at 40 gpm each for 5 yr (2016–2021). CrIN-4 and CrIN-5 are located east and west of R-50, respectively. The model predicts that pumping of CrEX-1 as well as the injection at CrIN-4 and CrIN-5 provide a very beneficial impact on the contaminant plume, substantially decreasing the contaminant concentrations at the downgradient plume edge in the area around R-50.

In the second case (Figure A-8.0-3), CrEX-1 is pumping for 5 yr at 80 gpm (2016–2021), CrIN-1 and CrIN-2 are injecting at 40 gpm each for 5 yr (2016–2021). CrIN-1 and CrIN-2 are located in the area near R-45. Note that in this case, the model predicts that pumping at CrEX-1 and injection near R-45 does not have as beneficial an impact on the contaminant plume near the Laboratory boundary as in the previous case with groundwater injection at CrIN-4 and CrIN-5. However, the model predicts that injection of groundwater in CrIN-1 and CrIN-2 has a beneficial impact on the contaminant concentrations in the R-45 area.

These model scenarios are also illustrated by the concentration curves for R-45 screen 1 and R-50 screen 1 presented in Figure A-8.0-4. The figure presents model predictions for the chromium concentration in these two well screens under different scenarios. The scenarios are (1) no action; (2) CrEX-1 pumping only (at 80 gpm for 5 yr); (3) CrEX-1 pumping and CrIN-4/CrIN-5 injecting (pumping regime as defined above); and (4) CrEX-1 pumping and CrIN-1/CrIN-2 injecting (pumping regime as defined above). R-45 concentrations are substantially impacted only by the CrIN-1/CrIN-2 injection (scenario 4 above). R-50 concentrations are impacted in all pumping/injection scenarios but the most favorable impact occurs when CrIN-4/CrIN-5 are injecting (scenario 4 above).

9.0 REFERENCES

The following list includes all documents cited in this appendix. Parenthetical information following each reference provides the author(s), publication date, and ER ID or ESH ID. This information is also included in text citations. ER IDs were assigned by the Environmental Programs Directorate's Records Processing Facility (IDs through 599999), and ESH IDs are assigned by the Environment, Safety, and Health (ESH) Directorate (IDs 600000 and above). IDs are used to locate documents in the Laboratory's Electronic Document Management System and, where applicable, in the master reference set.

Copies of the master reference set are maintained at the New Mexico Environment Department Hazardous Waste Bureau and the ESH Directorate. The set was developed to ensure that the administrative authority has all material needed to review this document, and it is updated with every document submitted to the administrative authority. Documents previously submitted to the administrative authority are not included.

LANL (Los Alamos National Laboratory), July 2008. "Fate and Transport Investigations Update for Chromium Contamination from Sandia Canyon," Los Alamos National Laboratory document LA-UR-08-4702, Los Alamos, New Mexico. (LANL 2008, 102996)

LANL (Los Alamos National Laboratory), September 2012. "Phase II Investigation Report for Sandia Canyon," Los Alamos National Laboratory document LA-UR-12-24593, Los Alamos, New Mexico. (LANL 2012, 228624)

LANL (Los Alamos National Laboratory), March 2014. "Summary Report for the 2013 Chromium Groundwater Aquifer Tests at R-42, R-28, and SCI-2," Los Alamos National Laboratory document LA-UR-14-21642, Los Alamos, New Mexico. (LANL 2014, 255110)

LANL (Los Alamos National Laboratory), January 2015. "Completion Report for Groundwater Extraction Well CrEX-1," Los Alamos National Laboratory document LA-UR-15-20165, Los Alamos, New Mexico. (LANL 2015, 600170)

Vesselinov, V.V., and D.R. Harp, October 2011. "Adaptive Hybrid Optimization Strategy for Calibration and Parameter Estimation of Physical Models," Los Alamos National Laboratory document LA-UR-11-11755, Los Alamos, New Mexico. (Vesselinov and Harp 2011, 227709)

Zyvoloski, G.A., B.A. Robinson, Z.V. Dash, and L.L. Trease, May 20, 1996. "Users Manual for the FEHMN Application," Rev. 1, Los Alamos National Laboratory document LA-UR-94-3788, Los Alamos, New Mexico. (Zyvoloski et al. 1996, 054421)

Zyvoloski, G.A., B.A. Robinson, Z.V. Dash, and L.L. Trease, July 1997. "Summary of the Models and Methods for the FEHM Application — A Finite-Element Heat- and Mass-Transfer Code," Los Alamos National Laboratory report LA-13307-MS, Los Alamos, New Mexico. (Zyvoloski et al. 1997, 070147)

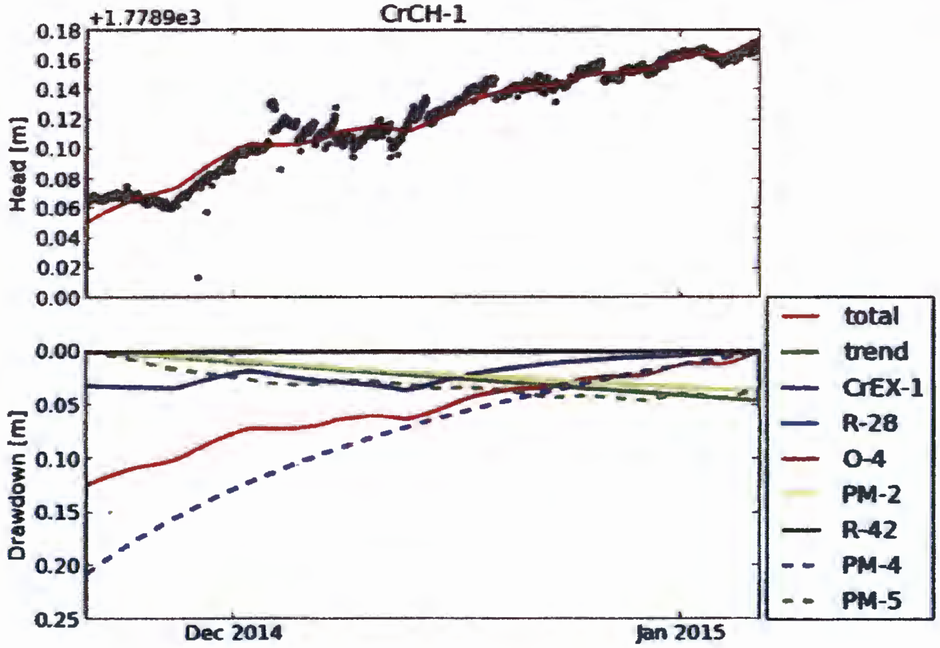

Figure A-4.0-1 **Observed (black dots in the upper figure) and simulated (red line in the upper figure) heads are depicted in the upper figure, and the simulated drawdowns are depicted in the lower figure for CrCH-1**

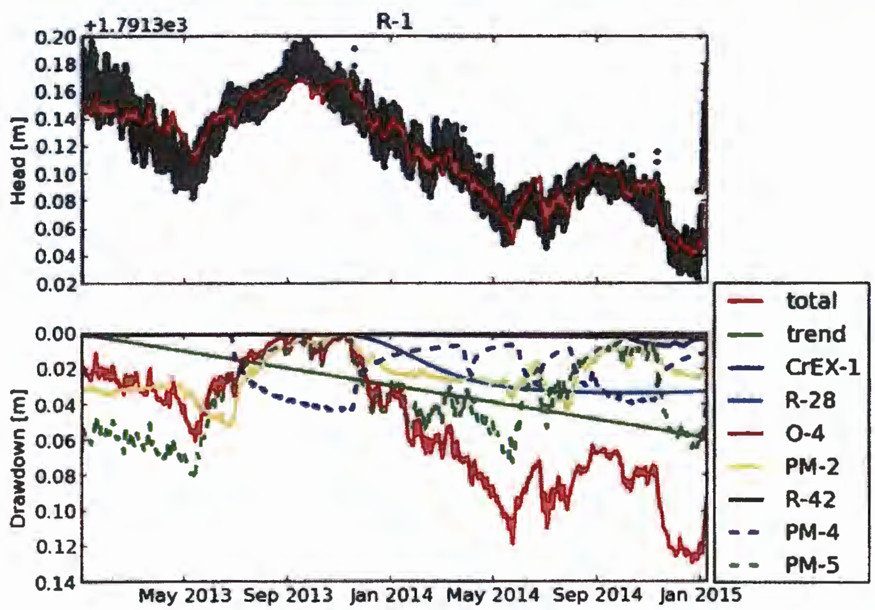

Figure A-4.0-2 **Observed (black dots in the upper figure) and simulated (red line in the upper figure) heads are depicted in the upper figure, and the simulated drawdowns are depicted in the lower figure for R-1**

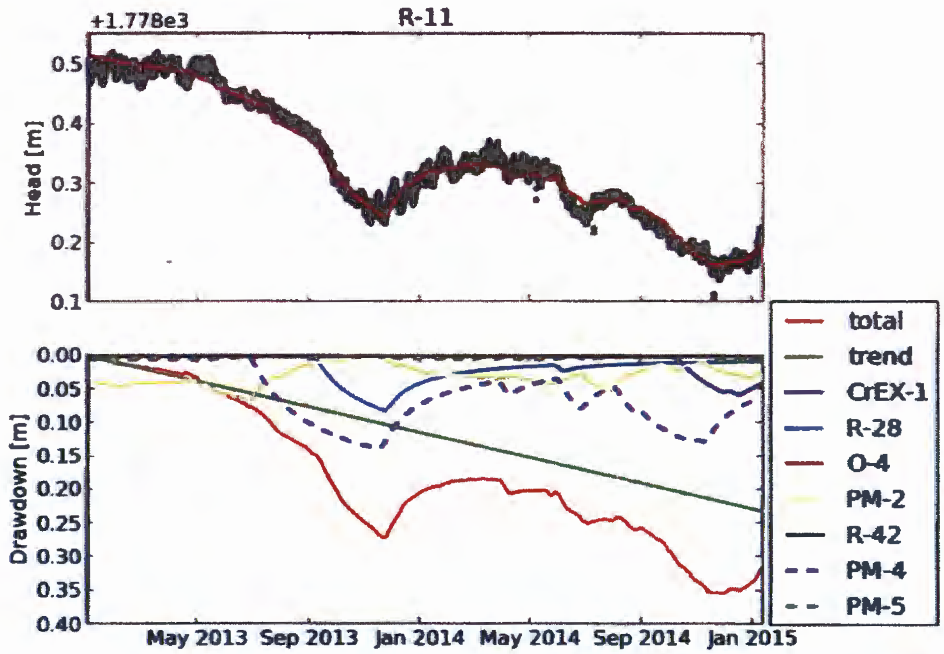

Figure A-4.0-3 **Observed (black dots in the upper figure) and simulated (red line in the upper figure) heads are depicted in the upper figure, and the simulated drawdowns are depicted in the lower figure for R-11**

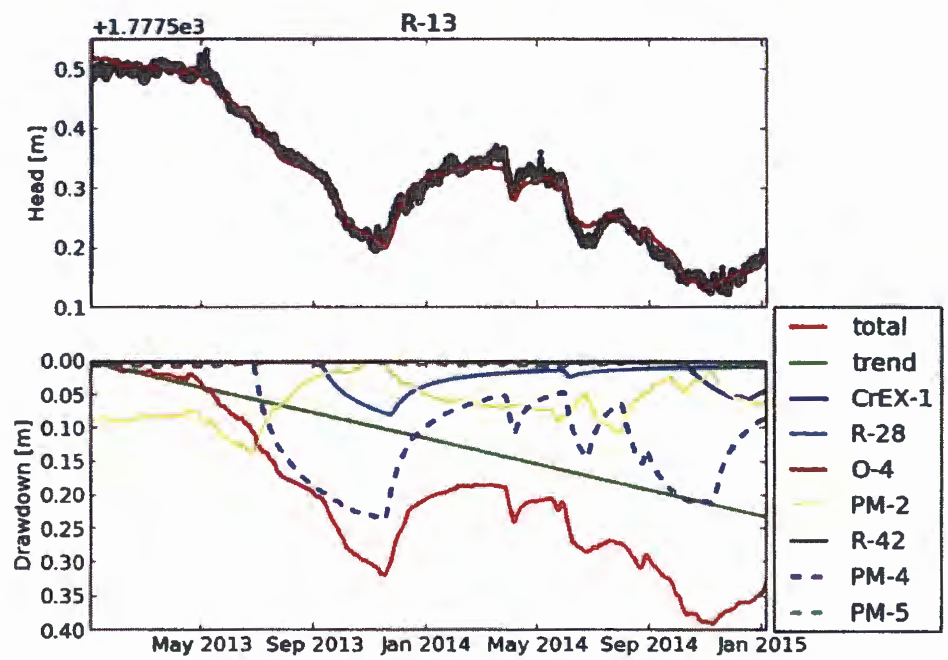

Figure A-4.0-4 **Observed (black dots in the upper figure) and simulated (red line in the upper figure) heads are depicted in the upper figure, and the simulated drawdowns are depicted in the lower figure for R-13**

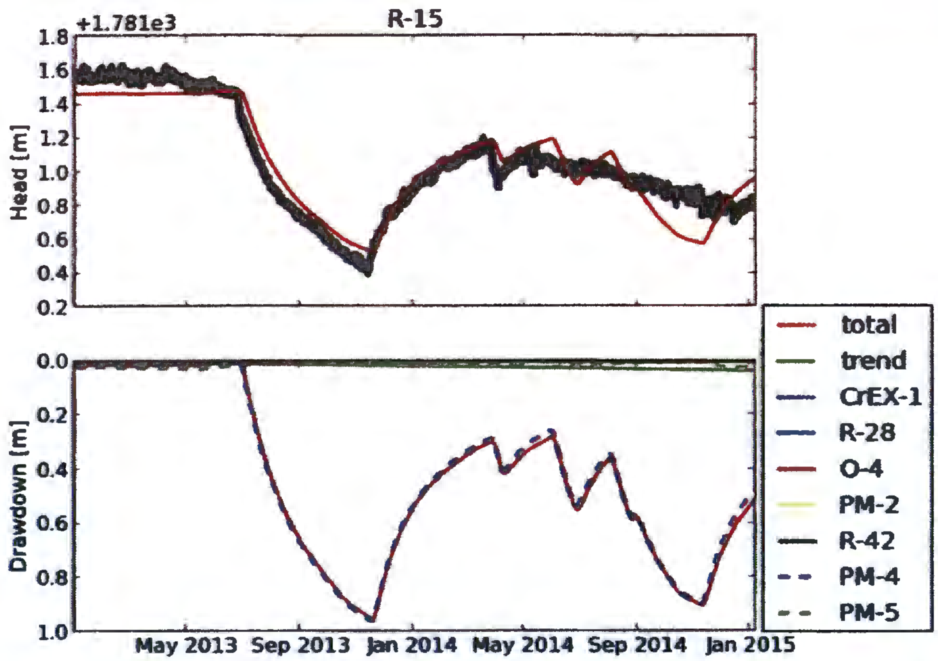

Figure A-4.0-5 **Observed (black dots in the upper figure) and simulated (red line in the upper figure) heads are depicted in the upper figure, and the simulated drawdowns are depicted in the lower figure for R-15**

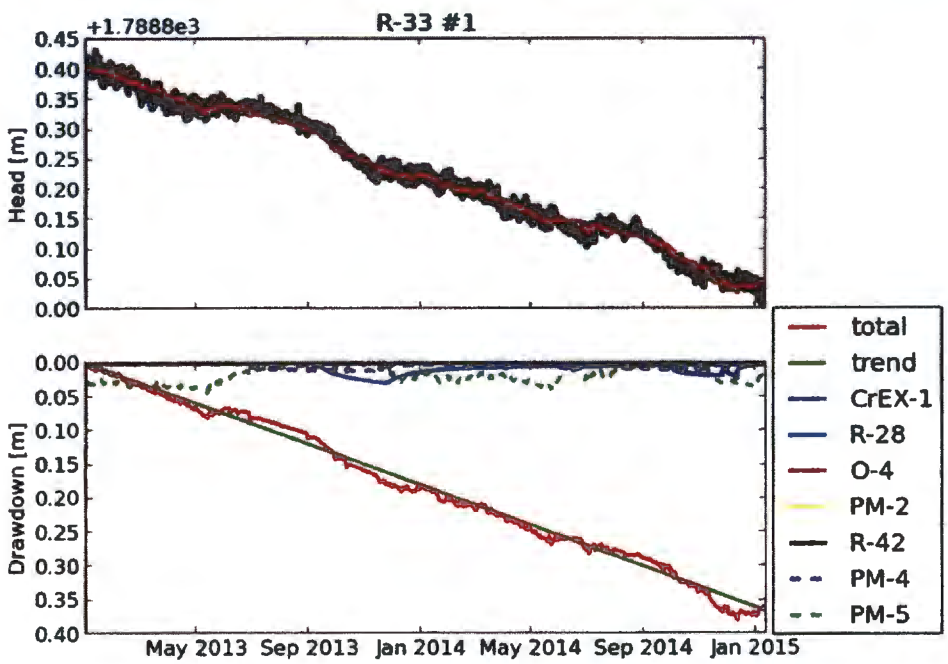

Figure A-4.0-6 **Observed (black dots in the upper figure) and simulated (red line in the upper figure) heads are depicted in the upper figure, and the simulated drawdowns are depicted in the lower figure for R-33 screen 1**

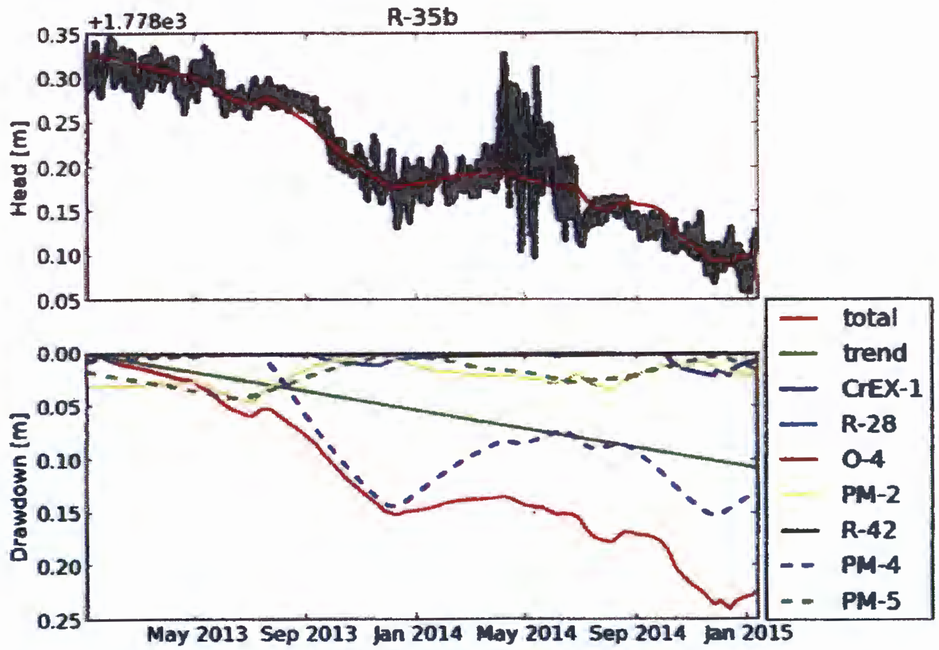

Figure A-4.0-7 **Observed (black dots in the upper figure) and simulated (red line in the upper figure) heads are depicted in the upper figure, and the simulated drawdowns are depicted in the lower figure for R-35b**

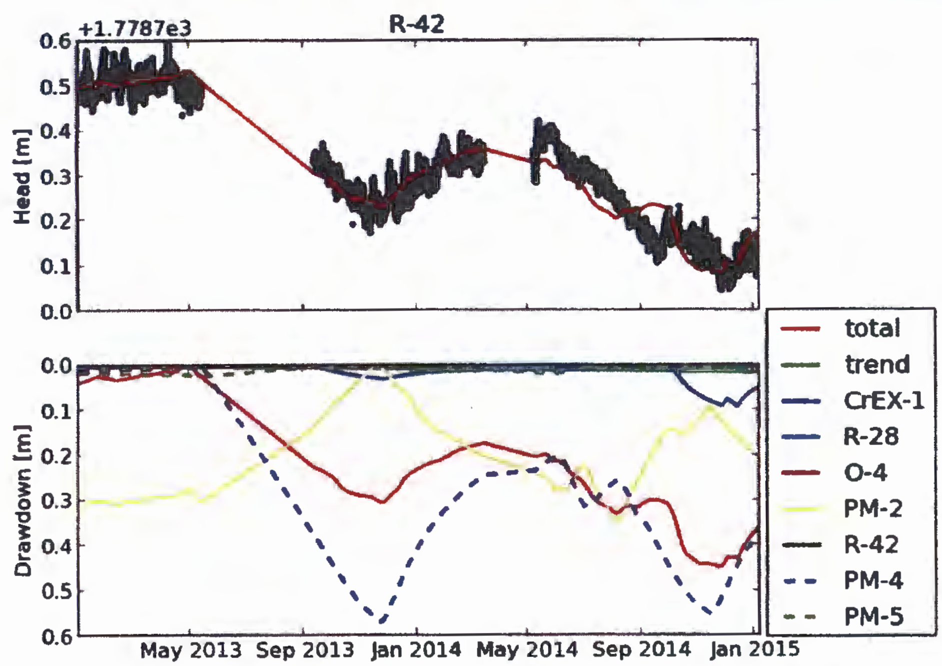

Figure A-4.0-8 **Observed (black dots in the upper figure) and simulated (red line in the upper figure) heads are depicted in the upper figure, and the simulated drawdowns are depicted in the lower figure for R-42**

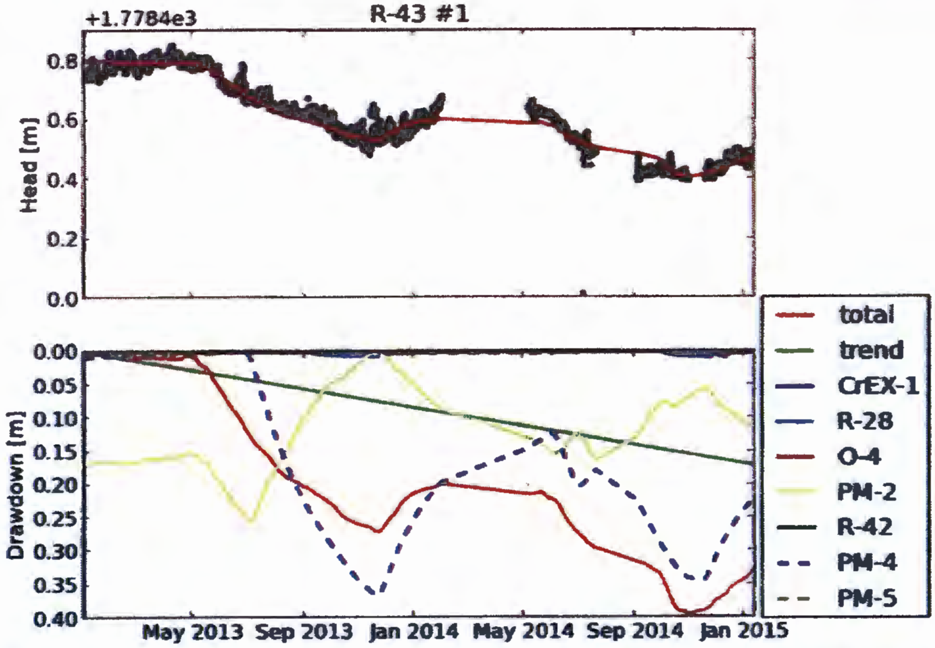

Figure A-4.0-9 **Observed (black dots in the upper figure) and simulated (red line in the upper figure) heads are depicted in the upper figure, and the simulated drawdowns are depicted in the lower figure for R-43 screen 1**

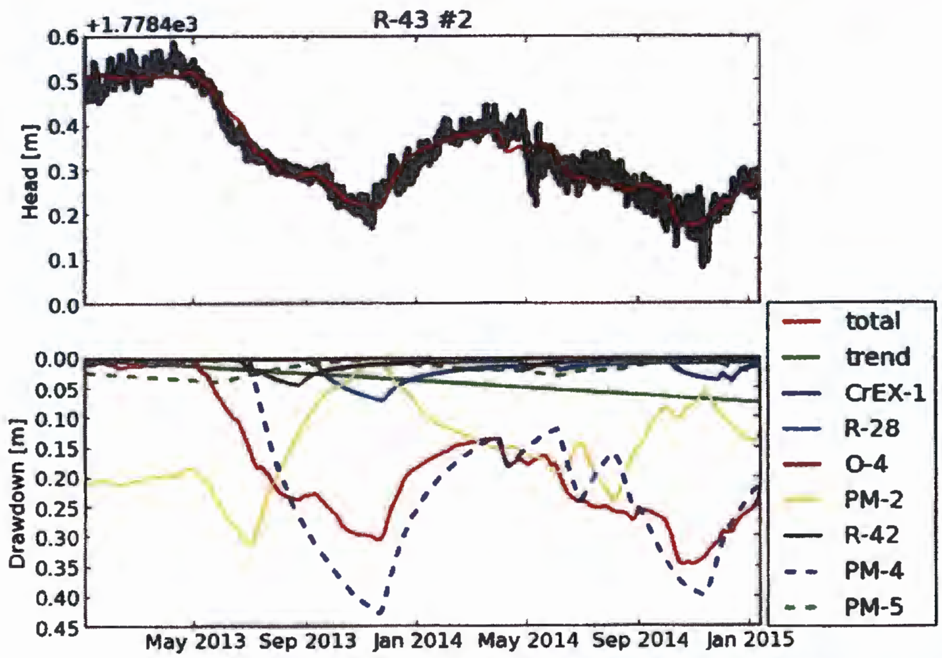

Figure A-4.0-10 **Observed (black dots in the upper figure) and simulated (red line in the upper figure) heads are depicted in the upper figure, and the simulated drawdowns are depicted in the lower figure for R-43 screen 2**

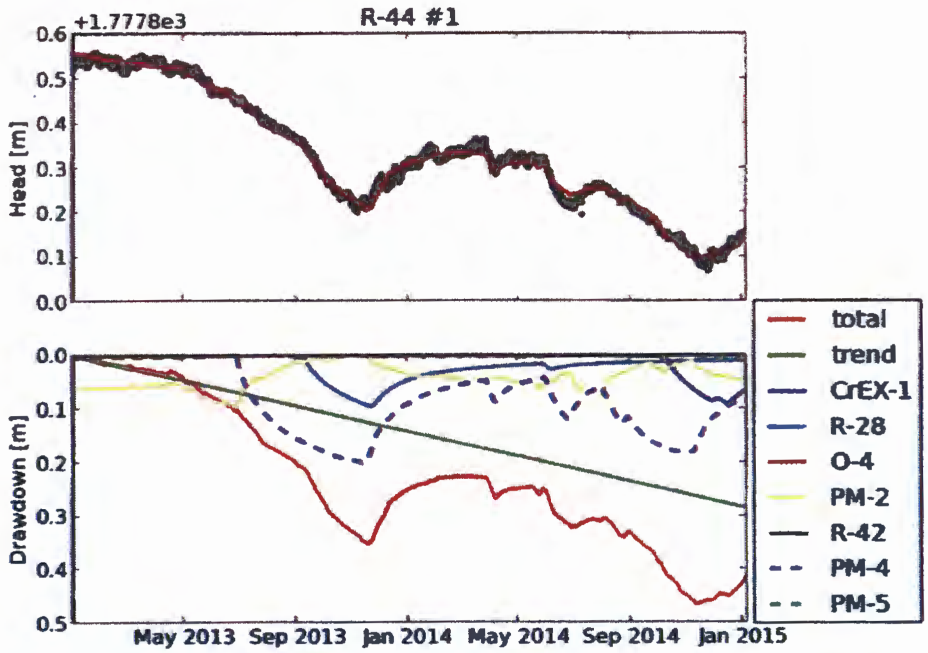

Figure A-4.0-11 **Observed (black dots in the upper figure) and simulated (red line in the upper figure) heads are depicted in the upper figure, and the simulated drawdowns are depicted in the lower figure for R-44 screen 1**

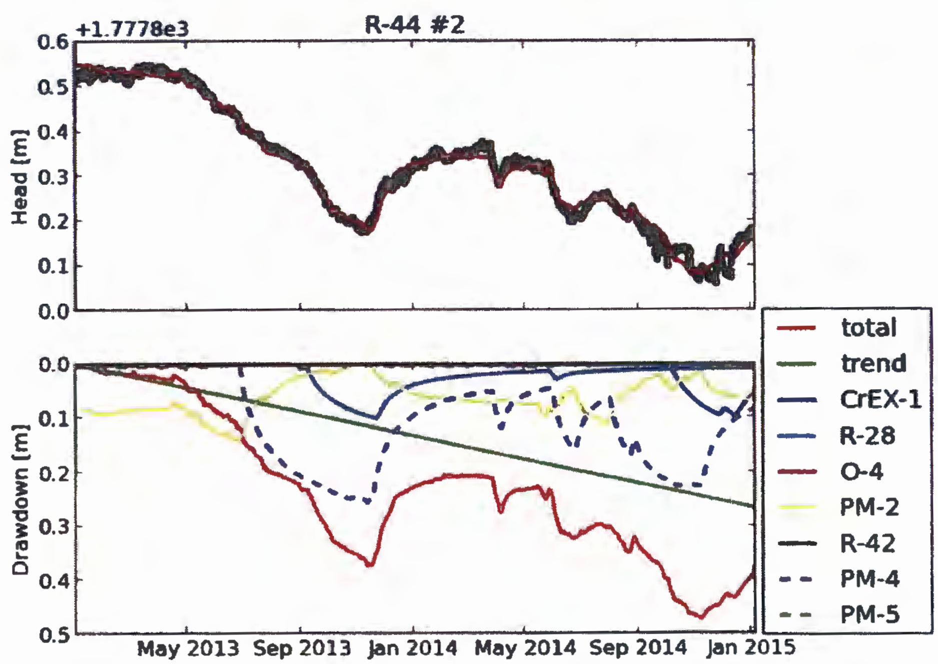

Figure A-4.0-12 **Observed (black dots in the upper figure) and simulated (red line in the upper figure) heads are depicted in the upper figure, and the simulated drawdowns are depicted in the lower figure for R-44 screen 2**

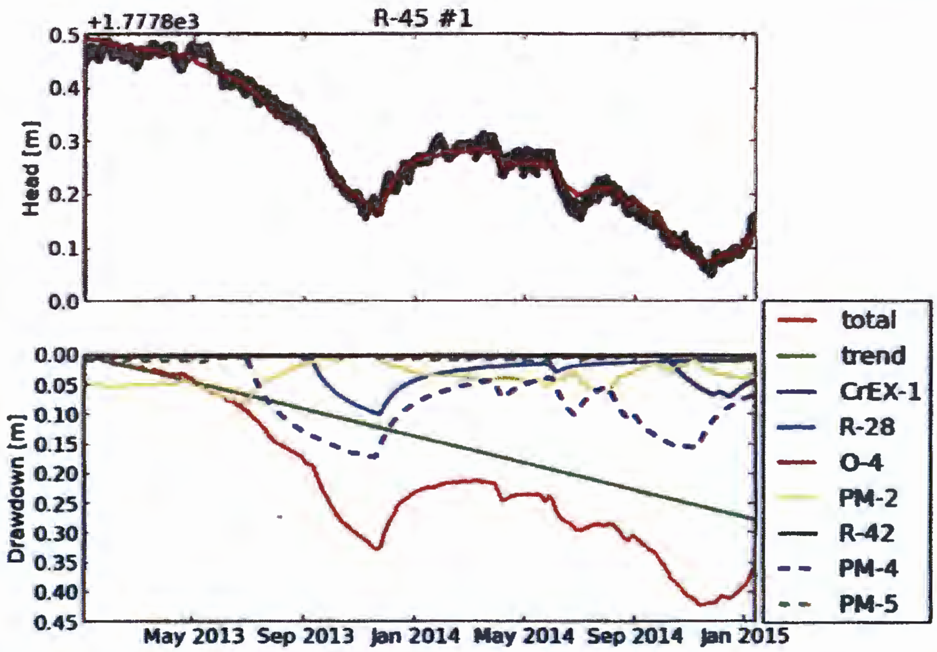

Figure A-4.0-13 **Observed (black dots in the upper figure) and simulated (red line in the upper figure) heads are depicted in the upper figure, and the simulated drawdowns are depicted in the lower figure for R-45 screen 1**

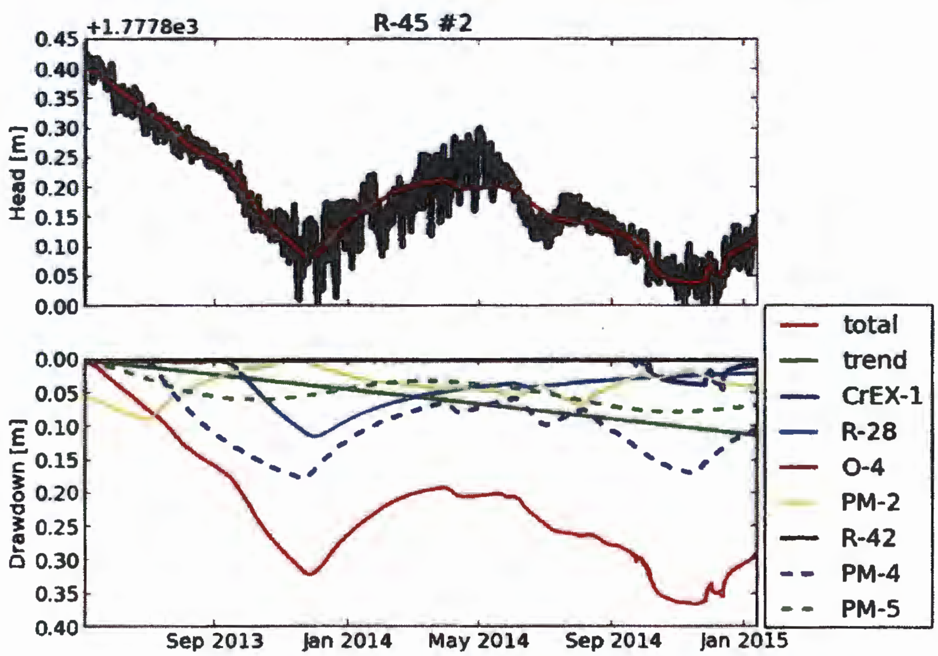

Figure A-4.0-14 **Observed (black dots in the upper figure) and simulated (red line in the upper figure) heads are depicted in the upper figure, and the simulated drawdowns are depicted in the lower figure for R-45 screen 2**

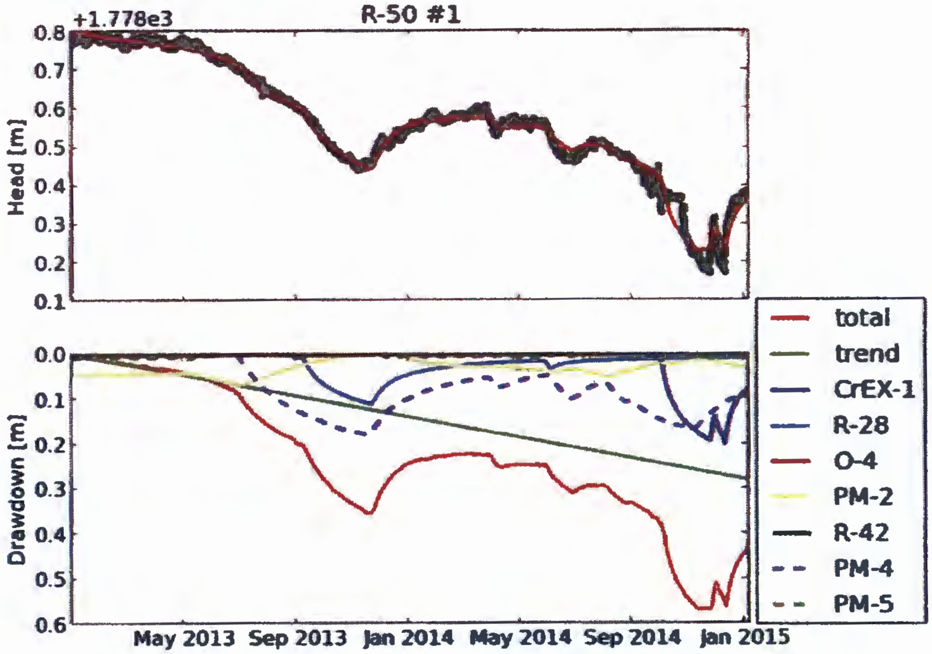

Figure A-4.0-15 **Observed (black dots in the upper figure) and simulated (red line in the upper figure) heads are depicted in the upper figure, and the simulated drawdowns are depicted in the lower figure for R-50 screen 1**

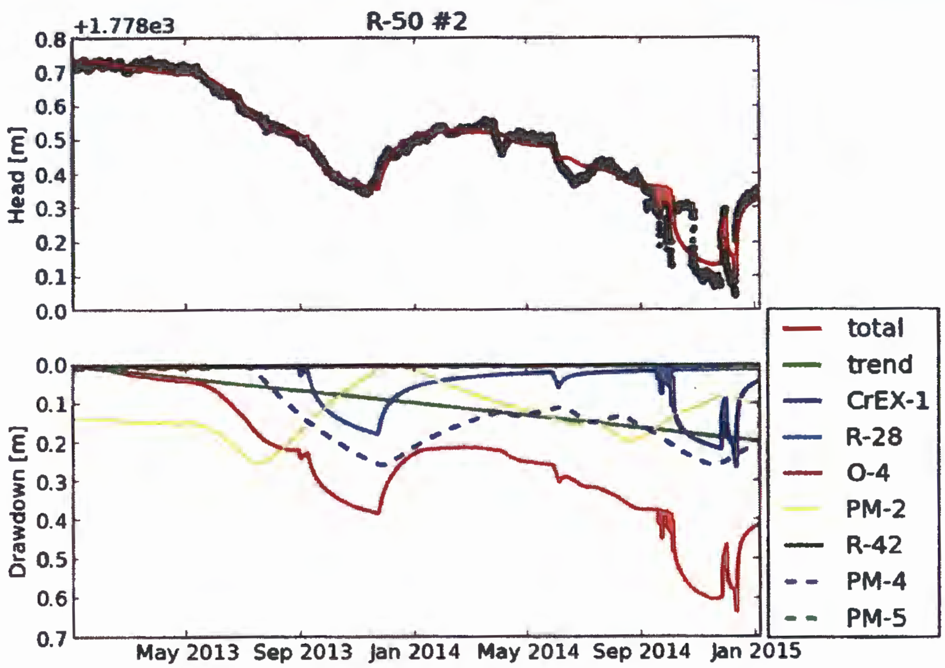

Figure A-4.0-16 **Observed (black dots in the upper figure) and simulated (red line in the upper figure) heads are depicted in the upper figure, and the simulated drawdowns are depicted in the lower figure for R-50 screen 2**

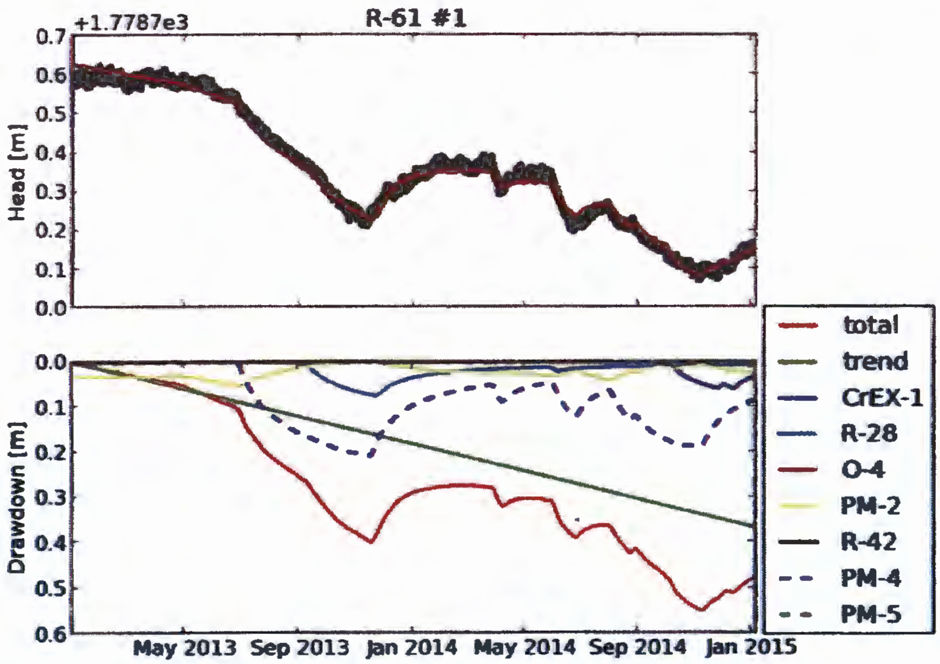

Figure A-4.0-17 Observed (black dots in the upper figure) and simulated (red line in the upper figure) heads are depicted in the upper figure, and the simulated drawdowns are depicted in the lower figure for R-61 screen 1

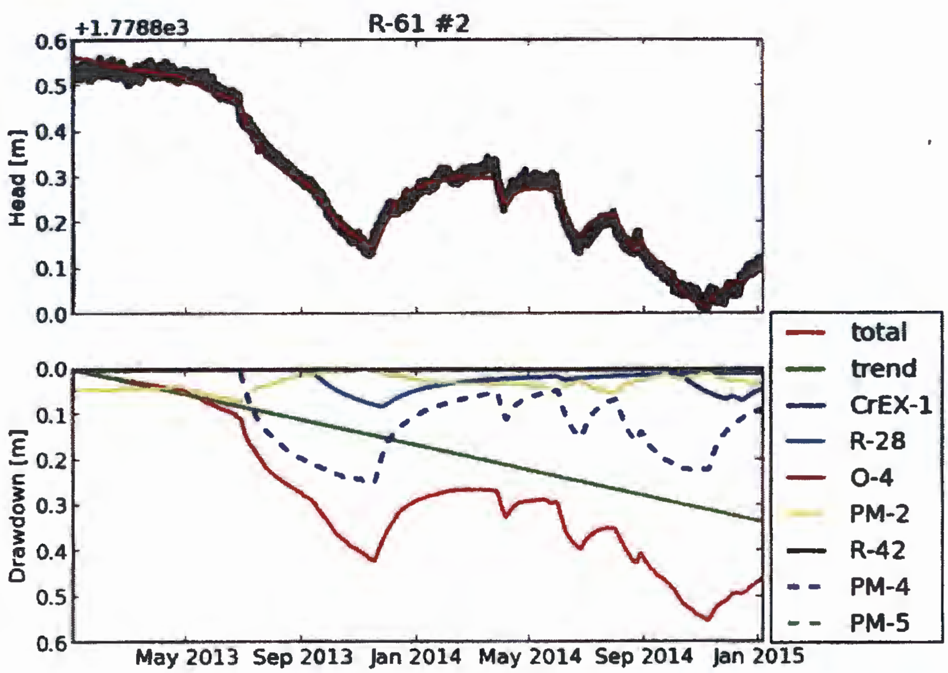

Figure A-4.0-18 Observed (black dots in the upper figure) and simulated (red line in the upper figure) heads are depicted in the upper figure, and the simulated drawdowns are depicted in the lower figure for R-61 screen 2

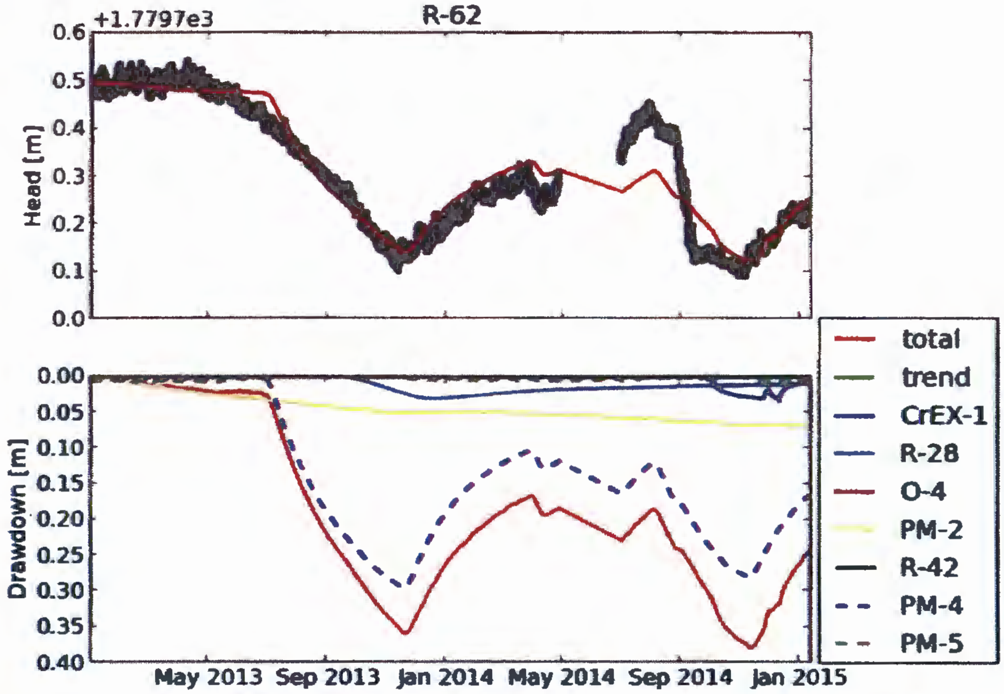

Figure A-4.0-19 **Observed (black dots in the upper figure) and simulated (red line in the upper figure) heads are depicted in the upper figure, and the simulated drawdowns are depicted in the lower figure for R-62**

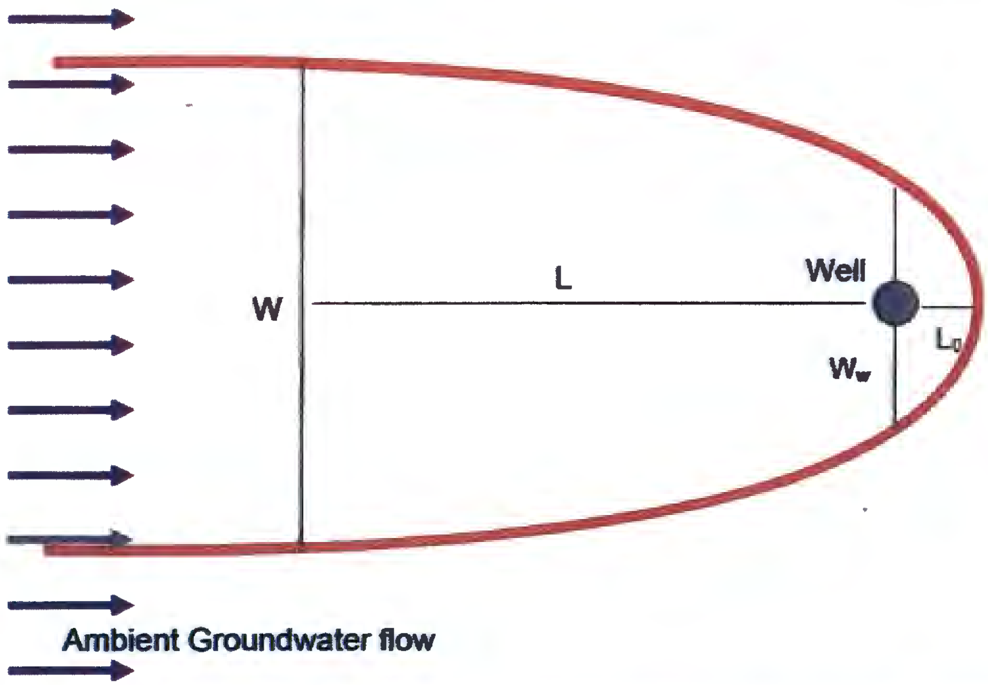

Figure A-5.0-1 Schematic representation of CZ of CrEX-1 assuming only advective steady-state groundwater flow through the regional aquifer

Notes: The computational grid is structured with local grid refinements near the existing wells. Vertically, the grid has higher resolution close to the top of the model and grid spacing increases with depth. The lateral spacing is ~50 × 50 m (~160 × 160 ft). The vertical spacing varies from about 1 m to 15 m. The grid includes about 540,000 nodes and about 3,053,000 elements. The coloring represents the different geologic units. The top of the model is constrained by the regional water table.

Figure A-6.0-1 The model domain and the computational grid

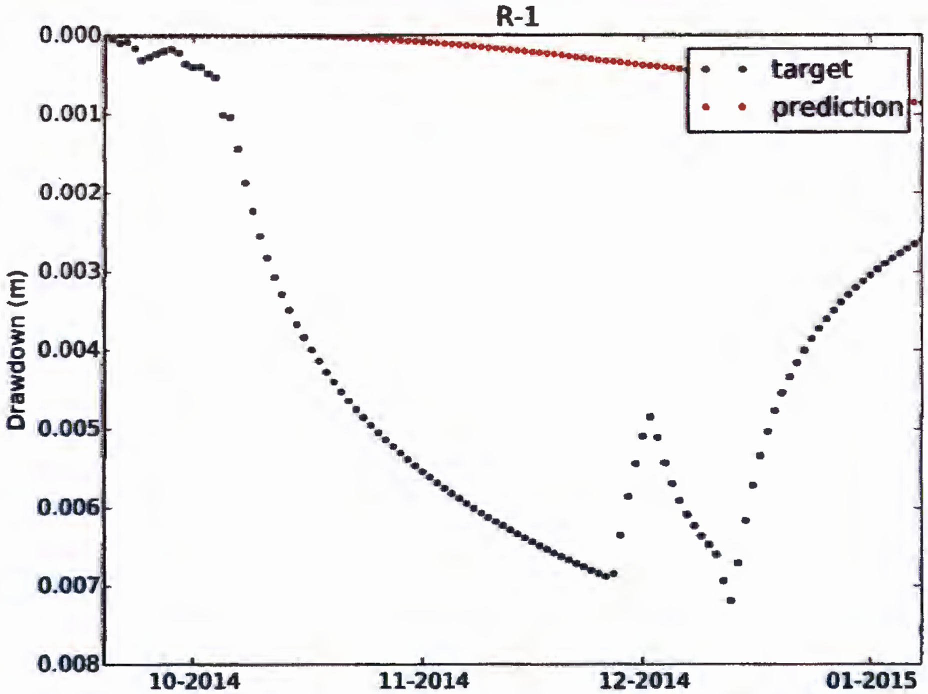

Figure A-6.0-2 Model calibration targets (black dots) and predictions (red dots) for the drawdown at R-1 to pumping at CrEX-1

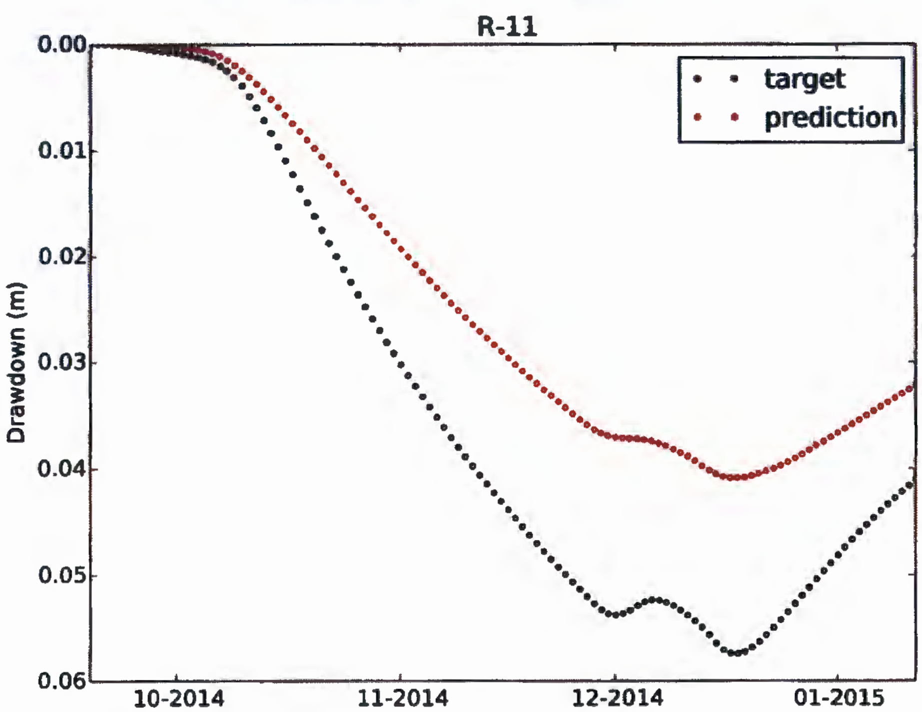

Figure A-6.0-3 Model calibration targets (black dots) and predictions (red dots) for the drawdown at R-11 to pumping at CrEX-1

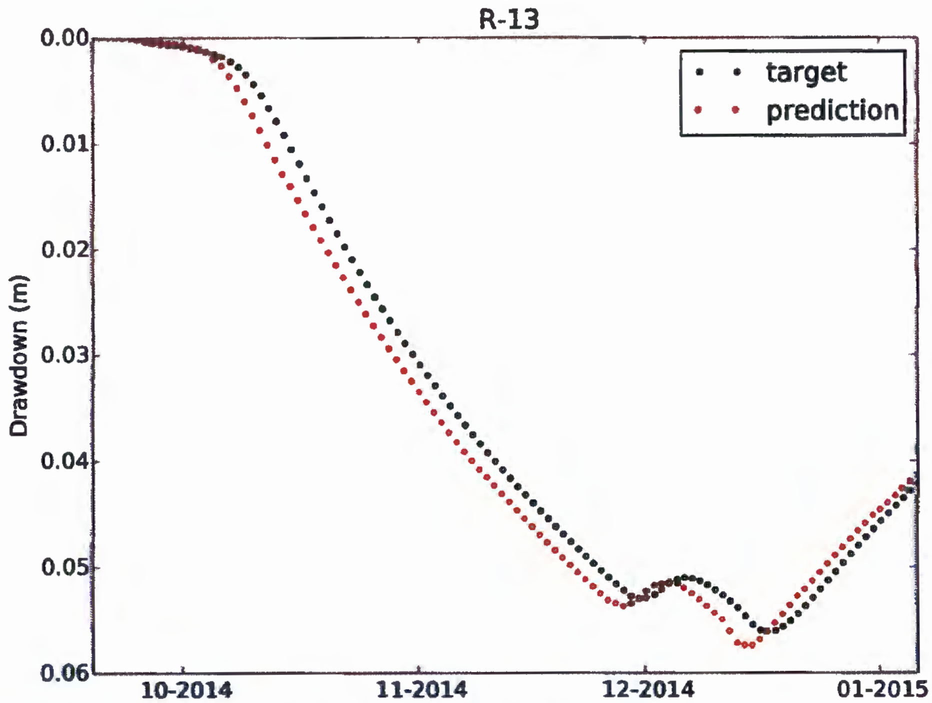

Figure A-6.0-4 Model calibration targets (black dots) and predictions (red dots) for the drawdown at R-13 to pumping at CrEX-1

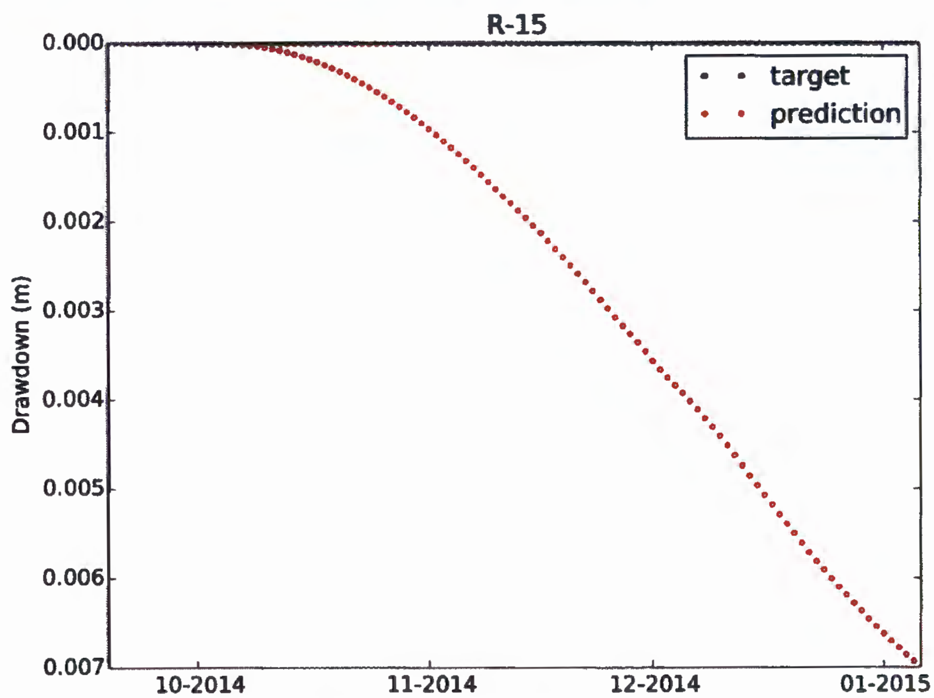

Figure A-6.0-5 Model calibration targets (black dots) and predictions (red dots) for the drawdown at R-15 to pumping at CrEX-1

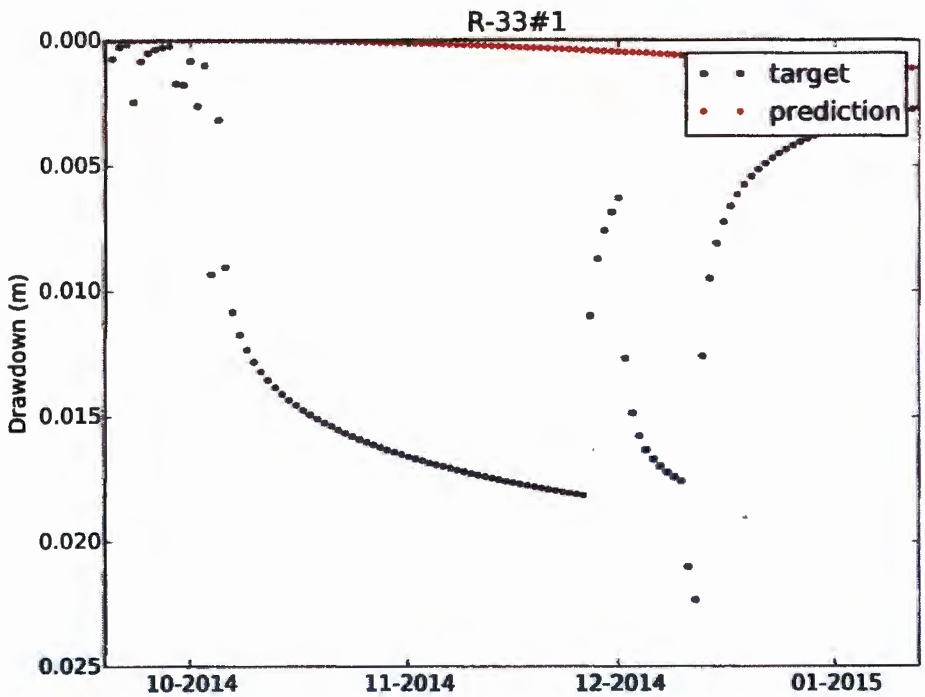

Figure A-6.0-6 Model calibration targets (black dots) and predictions (red dots) for the drawdown at R-33 #1 to pumping at CrEX-1

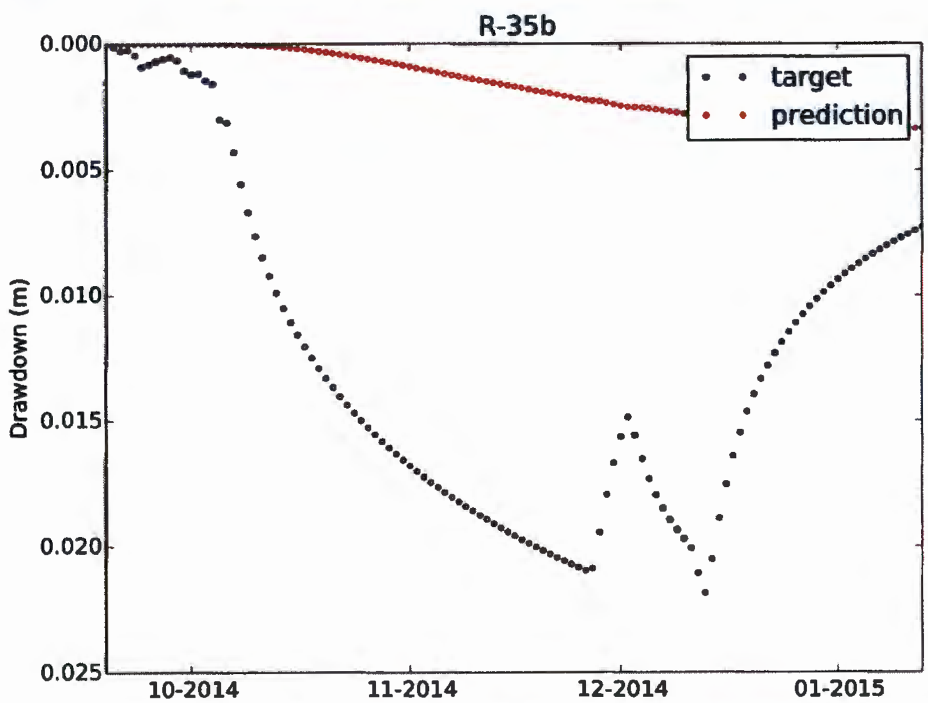

Figure A-6.0-7 Model calibration targets (black dots) and predictions (red dots) for the drawdown at R-35b to pumping at CrEX-1

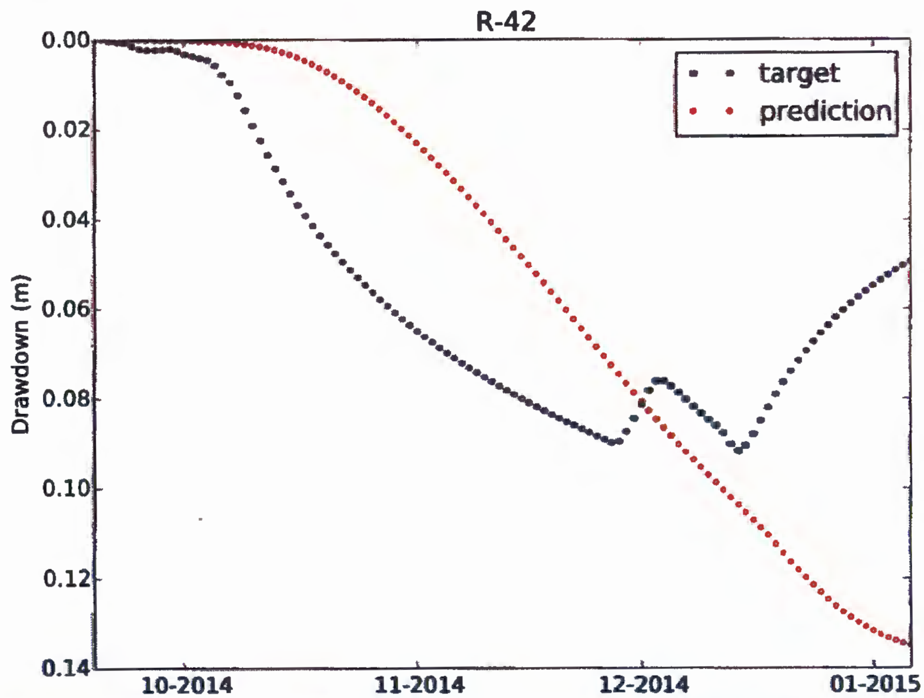

Figure A-6.0-8 Model calibration targets (black dots) and predictions (red dots) for the drawdown at R-42 to pumping at CrEX-1

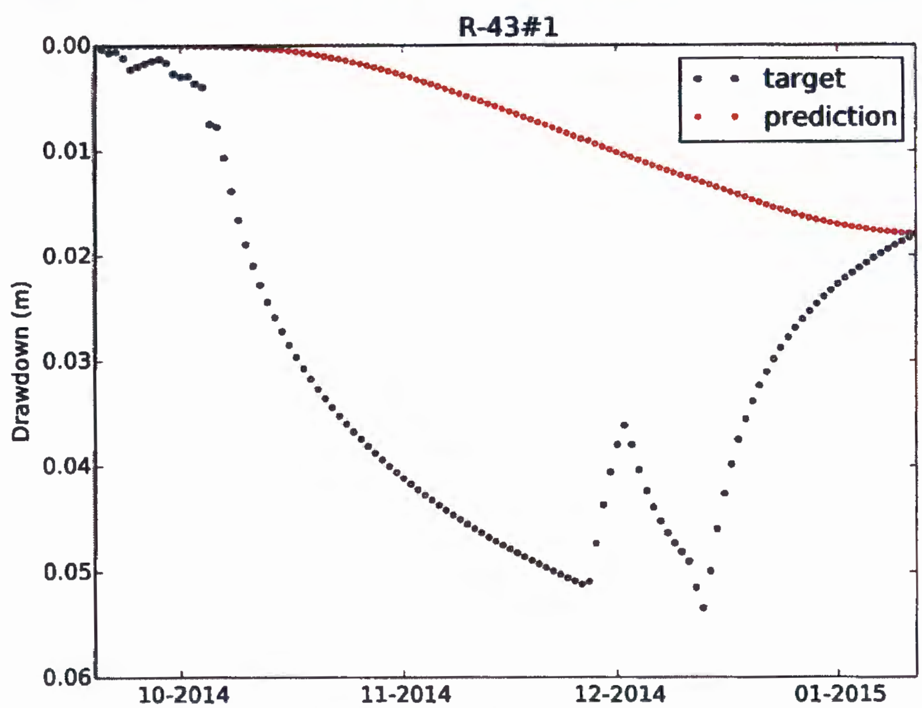

Figure A-6.0-9 Model calibration targets (black dots) and predictions (red dots) for the drawdown at R-43 screen 1 to pumping at CrEX-1

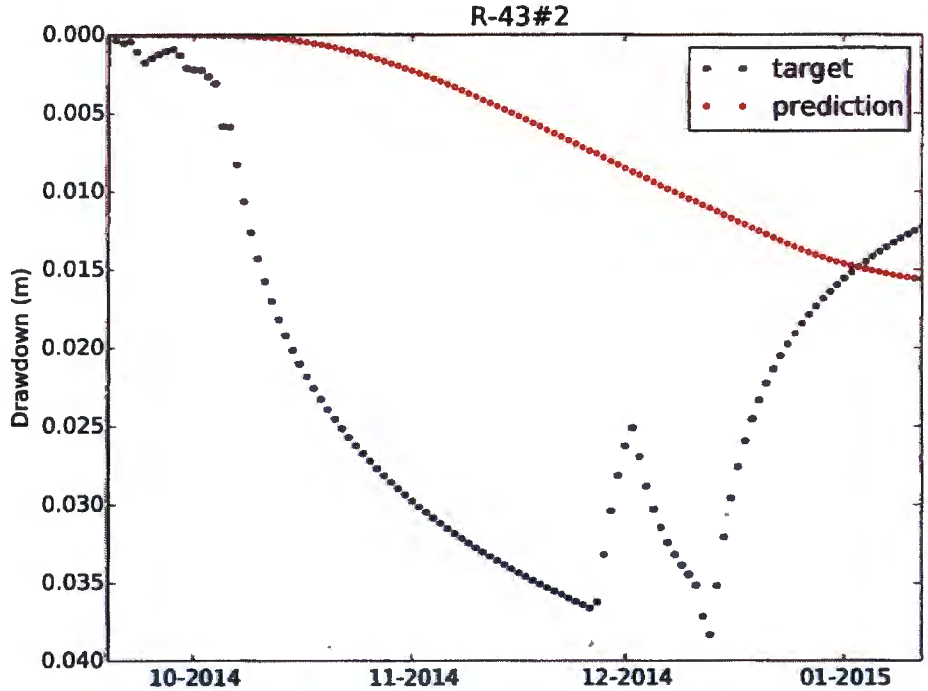

Figure A-6.0-10 Model calibration targets (black dots) and predictions (red dots) for the drawdown at R-43 screen 2 to pumping at CrEX-1

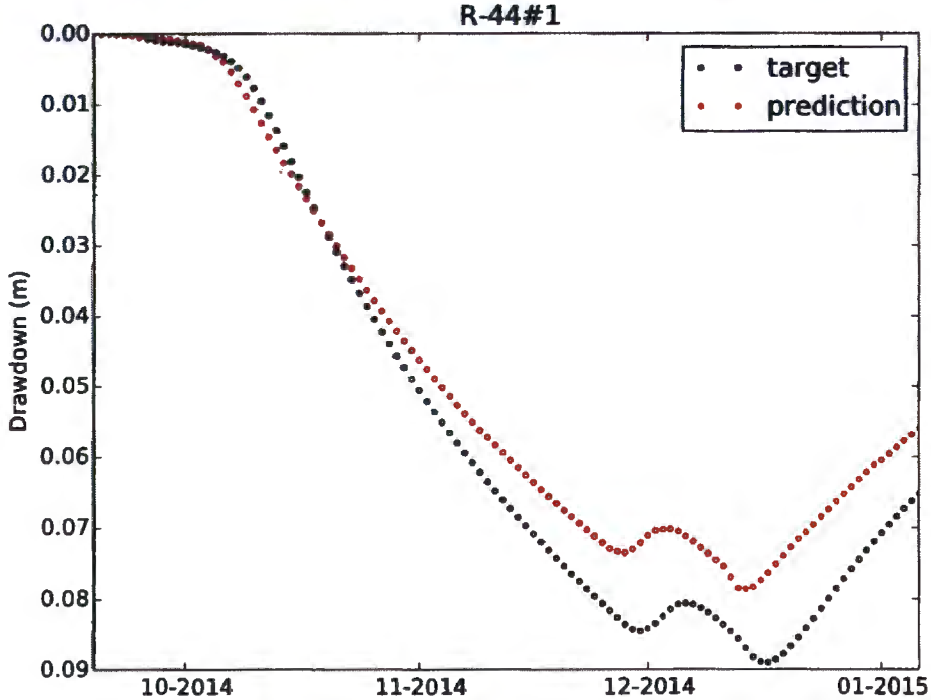

Figure A-6.0-11 Model calibration targets (black dots) and predictions (red dots) for the drawdown at R-44 screen 1 to pumping at CrEX-1

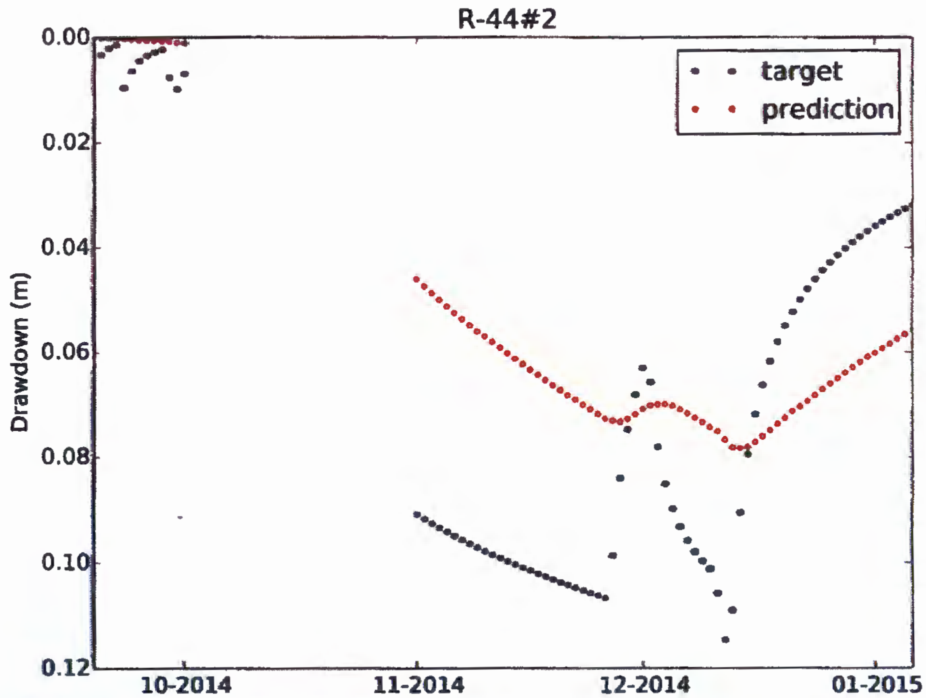

Figure A-6.0-12 Model calibration targets (black dots) and predictions (red dots) for the drawdown at R-44 screen 2 to pumping at CrEX-1

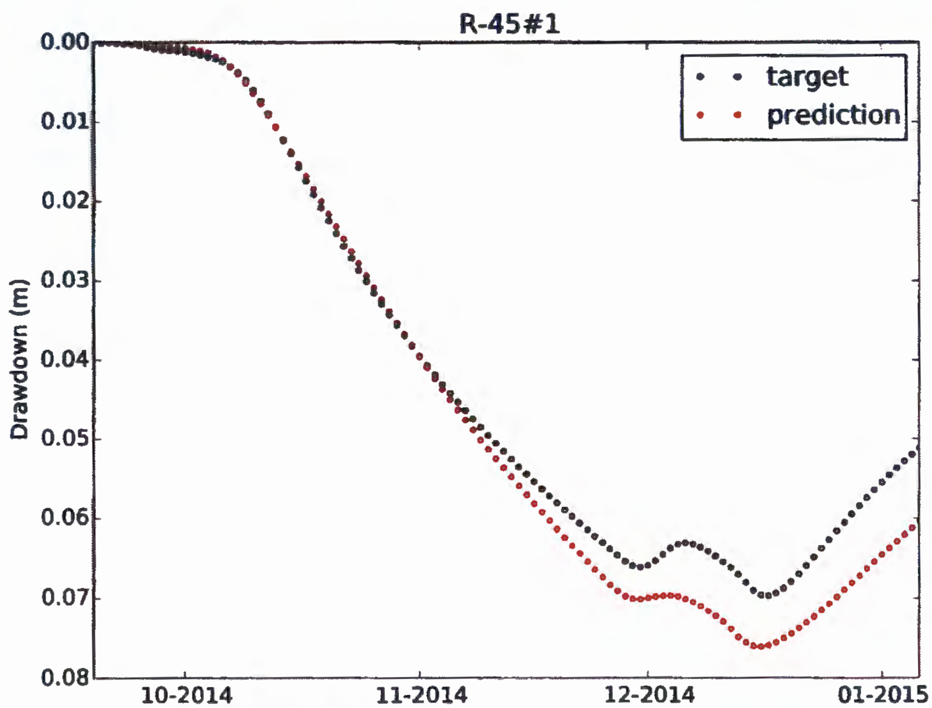

Figure A-6.0-13 Model calibration targets (black dots) and predictions (red dots) for the drawdown at R-45 screen 1 to pumping at CrEX-1

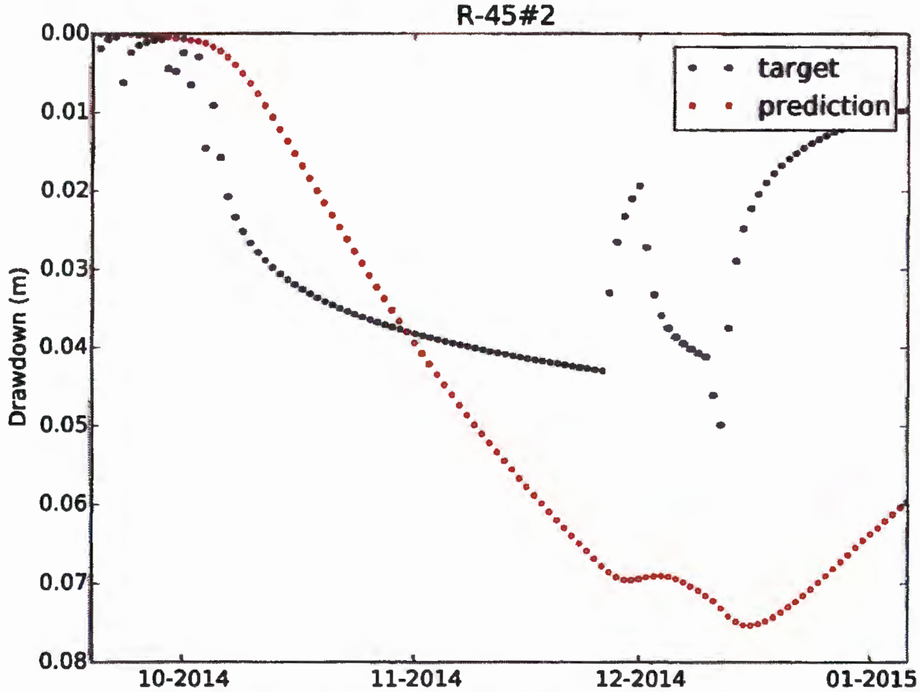

Figure A-6.0-14 Model calibration targets (black dots) and predictions (red dots) for the drawdown at R-45 screen 2 to pumping at CrEX-1

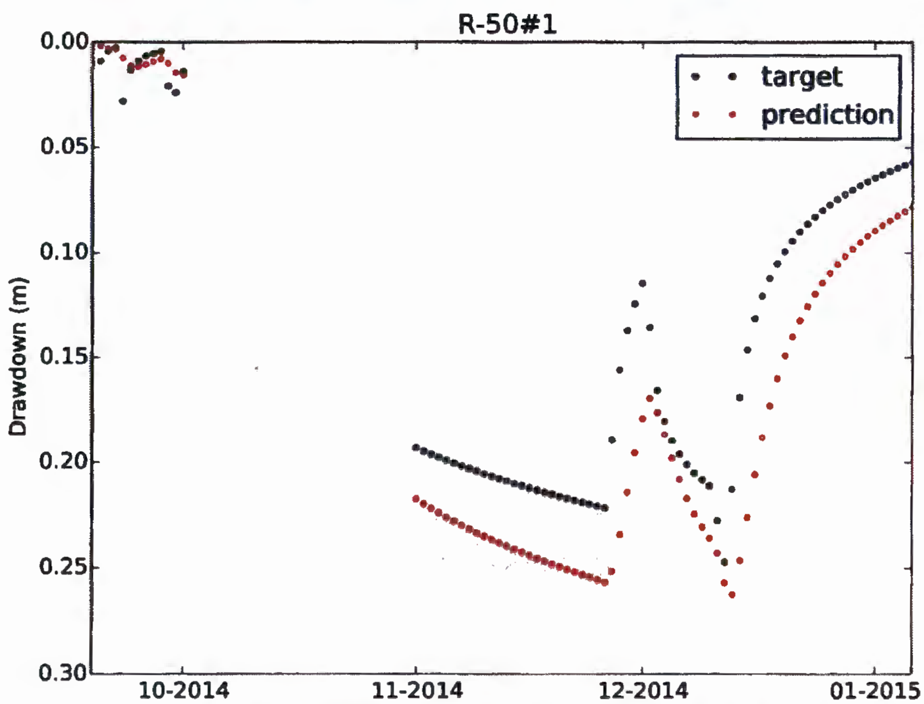

Figure A-6.0-15 Model calibration targets (black dots) and predictions (red dots) for the drawdown at R-50 screen 1 to pumping at CrEX-1

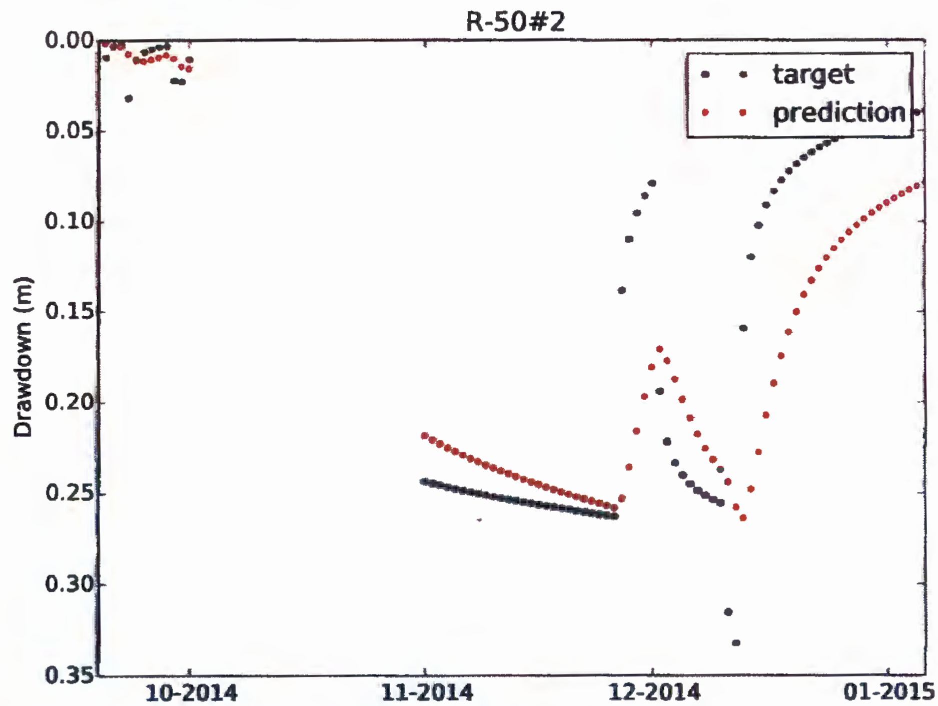

Figure A-6.0-16 Model calibration targets (black dots) and predictions (red dots) for the drawdown at R-50 screen 2 to pumping at CrEX-1

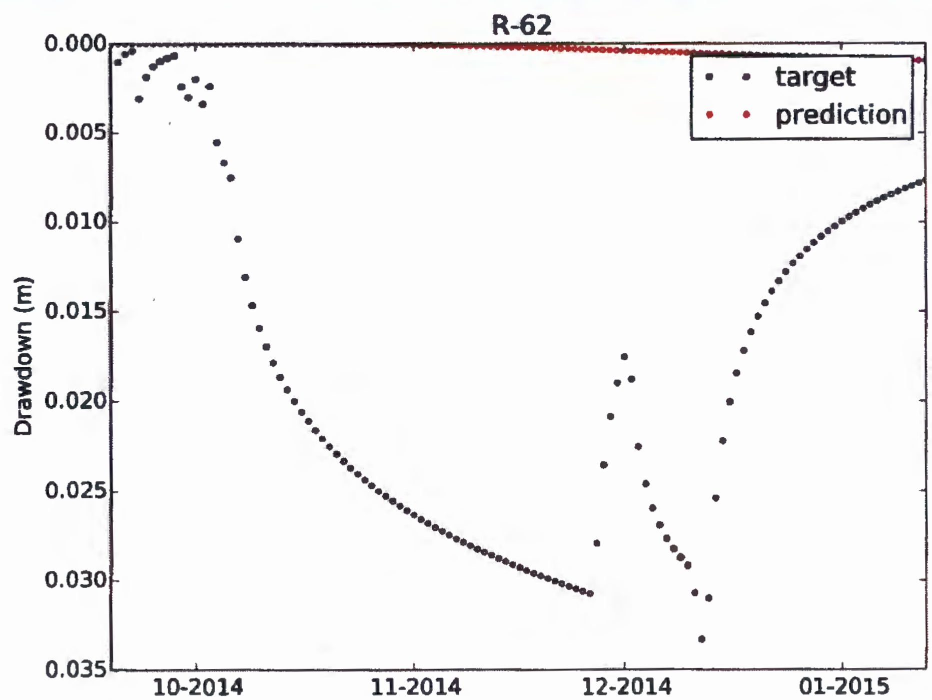

Figure A-6.0-17 Model calibration targets (black dots) and predictions (red dots) for the drawdown at R-62 to pumping at CrEX-1

(a) Lateral permeability

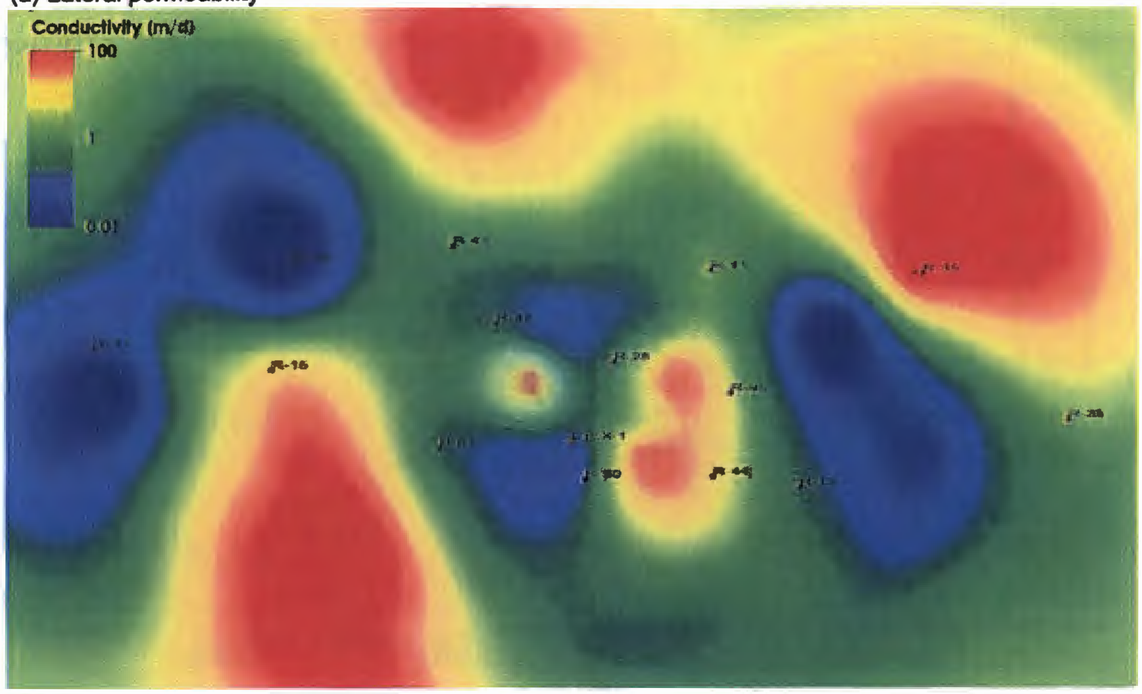

(b) Vertical permeability

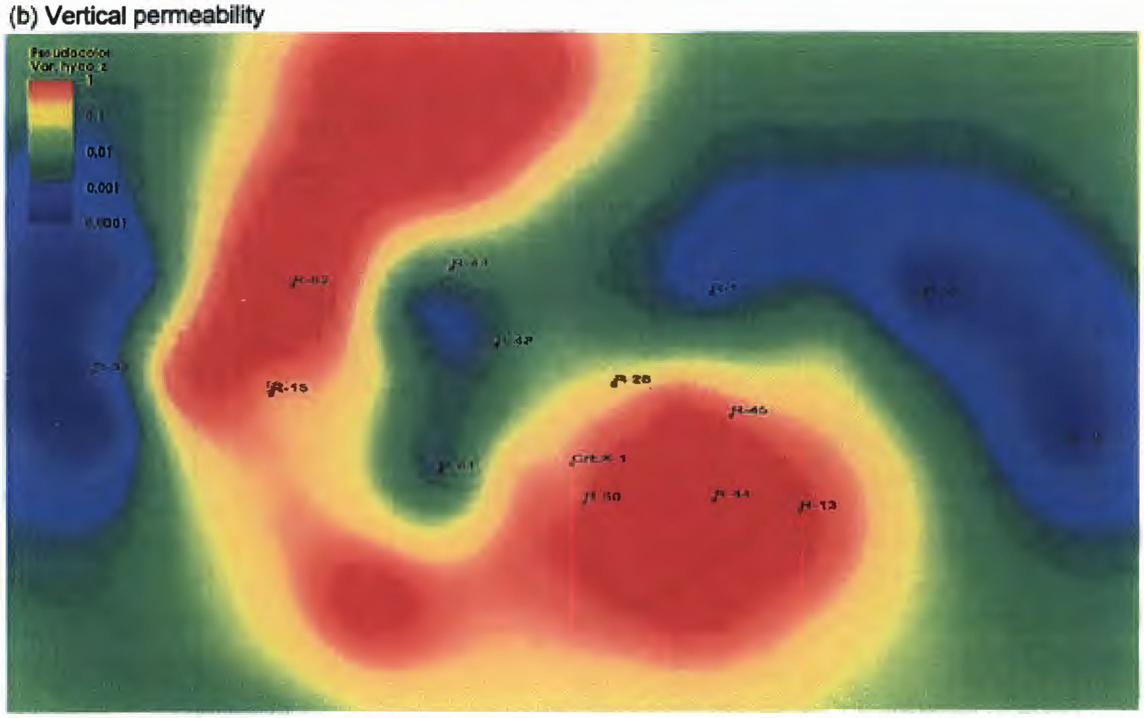

Notes: The inverse model analysis also takes into account the pressure changes observed from municipal water-supply pumping in the nearby groundwater production wells.

Figure A-6.0-18 Model estimated hydraulic conductivity (lateral and vertical) based on R-28 and CrEX-1 pumping tests

(a) 1 yr of pumping

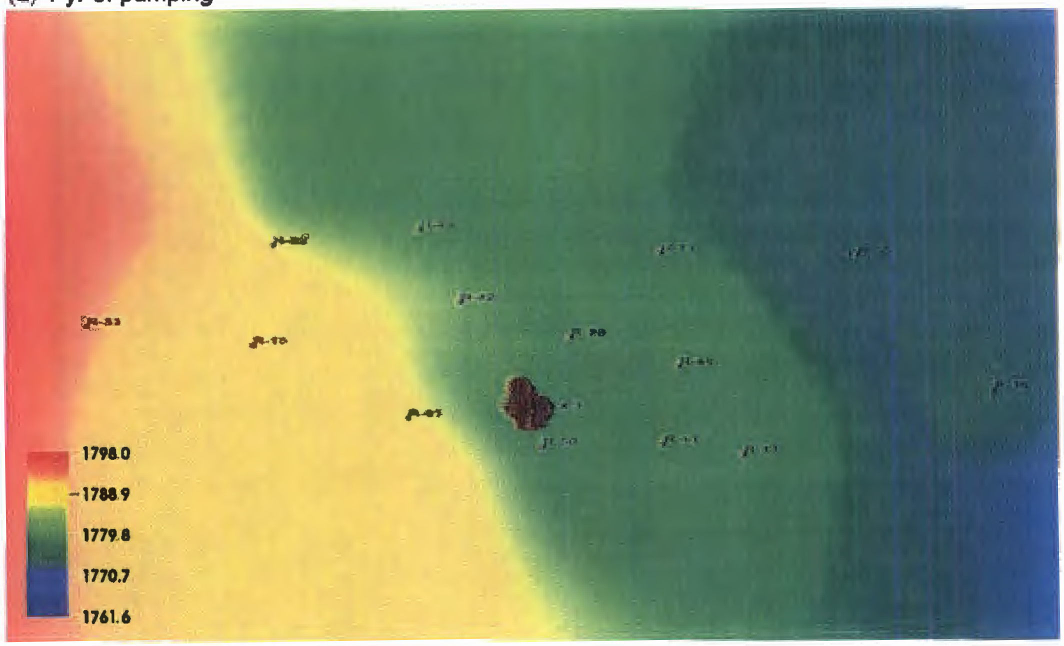

(b) 3 yr of pumping

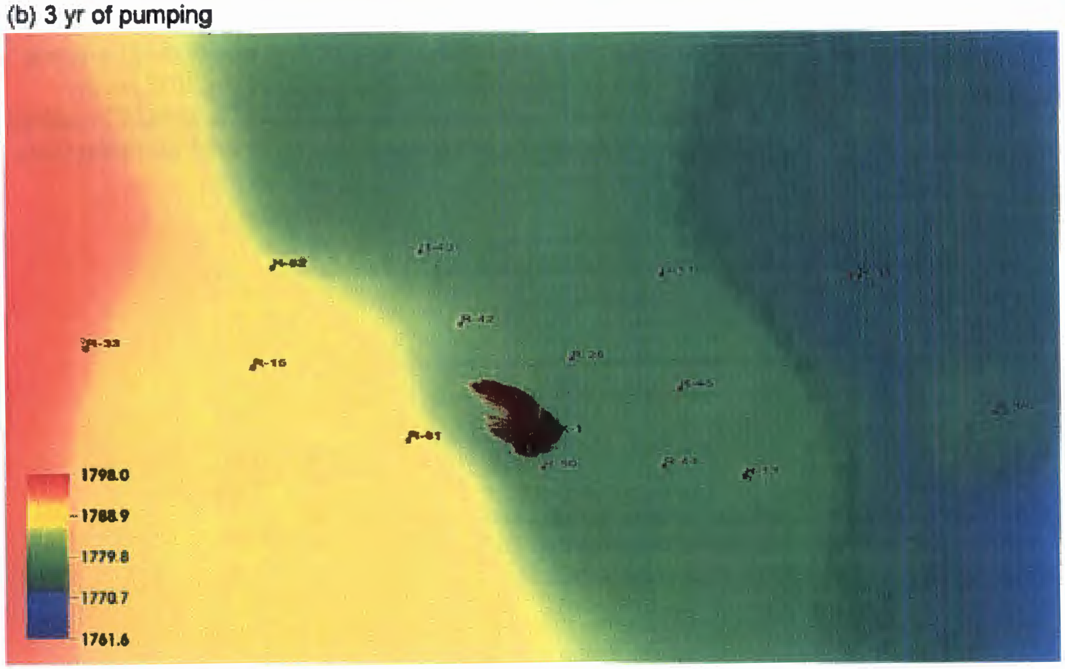

Notes: The CZ accounts only for advective groundwater flow; it does not account for diffusion, dispersion and dual-porosity effects. Results are preliminary and will be updated with new data from pumping.

Figure A-7.0-1 Model predictions of the CrEX-1 CZ after 1, 3 and 5 yr of pumping model predictions using 2014 model update of the 2012 model (Phase II Sandia Investigation Report [LANL 2012, 228624]) accounting for aquifer heterogeneity based on R-28 and CrEX-1 pumping tests

(c) 5 yr of pumping

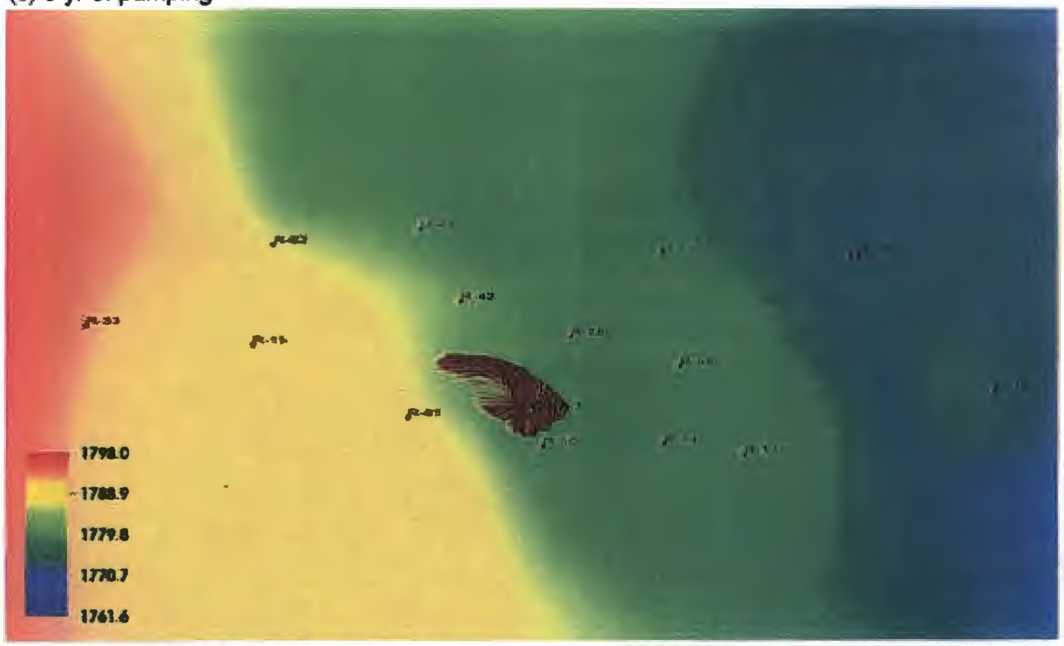

Notes: The CZ accounts for only advective groundwater flow; it does not account for diffusion, dispersion, and dual-porosity effects. Results are preliminary and will be updated with new data from pumping.

Figure A-7.0-1 (continued) Model predictions of the CrEX-1 CZ after 1, 3, and 5 yr of pumping model predictions using 2014 model update of the 2012 model (Phase II Sandia Investigation Report [LANL 2012, 228624]) accounting for aquifer heterogeneity based on R-28 and CrEX-1 pumping tests

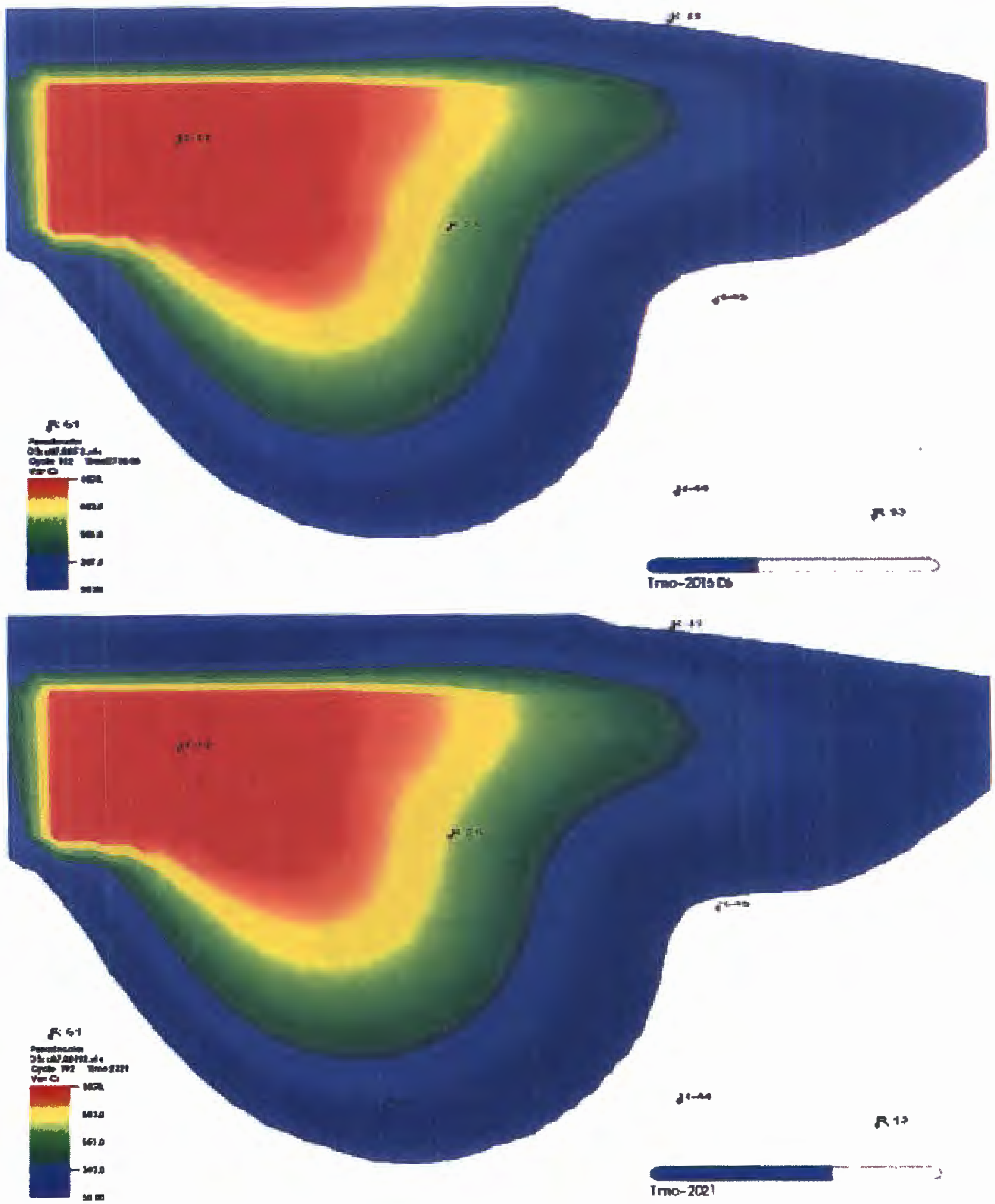

Notes: The model predictions are based on the 2012 model (Phase II Sandia Investigation Report [LANL 2012, 228624]). The results are preliminary and still a work in progress.

Figure A-8.0-1 Model predictions of the chromium concentrations at 2016 and 2021 without active pumping and injection

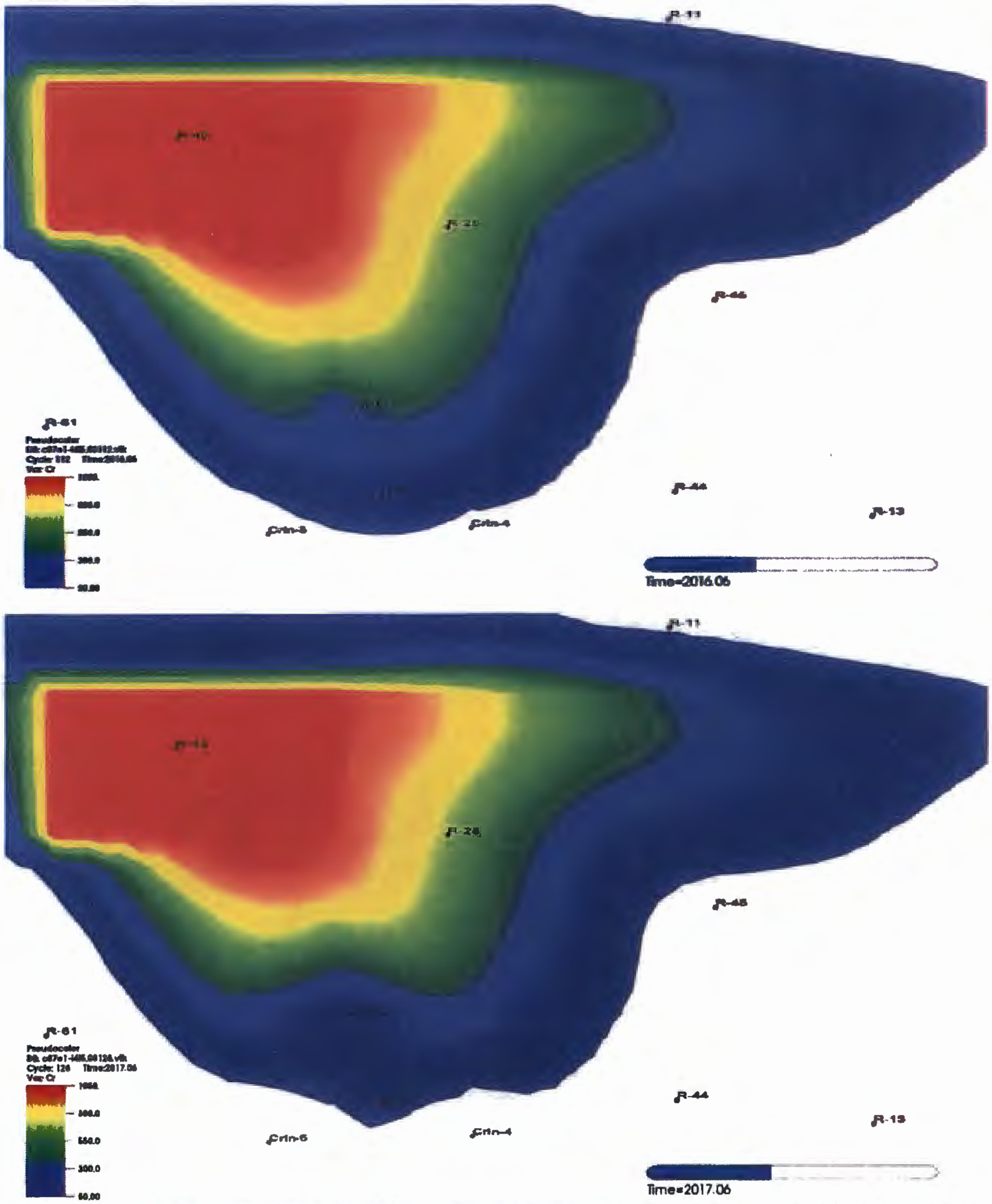

Notes: The model predictions are based on the 2012 model (Phase II Sandia Investigation Report [LANL 2012, 228624]). The plots show model predictions for 2016, 2017, 2019, and 2021 (after 0, 1, 3, and 5 yr of pumping/injection, respectively). The results are preliminary. Here CrEX-1 is pumping at 80 gpm for 5 yr (2016–2021), and CrIN-4 and CrIN-5 are injecting for 5 yr at 40 gpm each (2016–2021).

Figure A-8.0-2 Model predictions of the impact of pumping and injection scenarios on the chromium concentrations

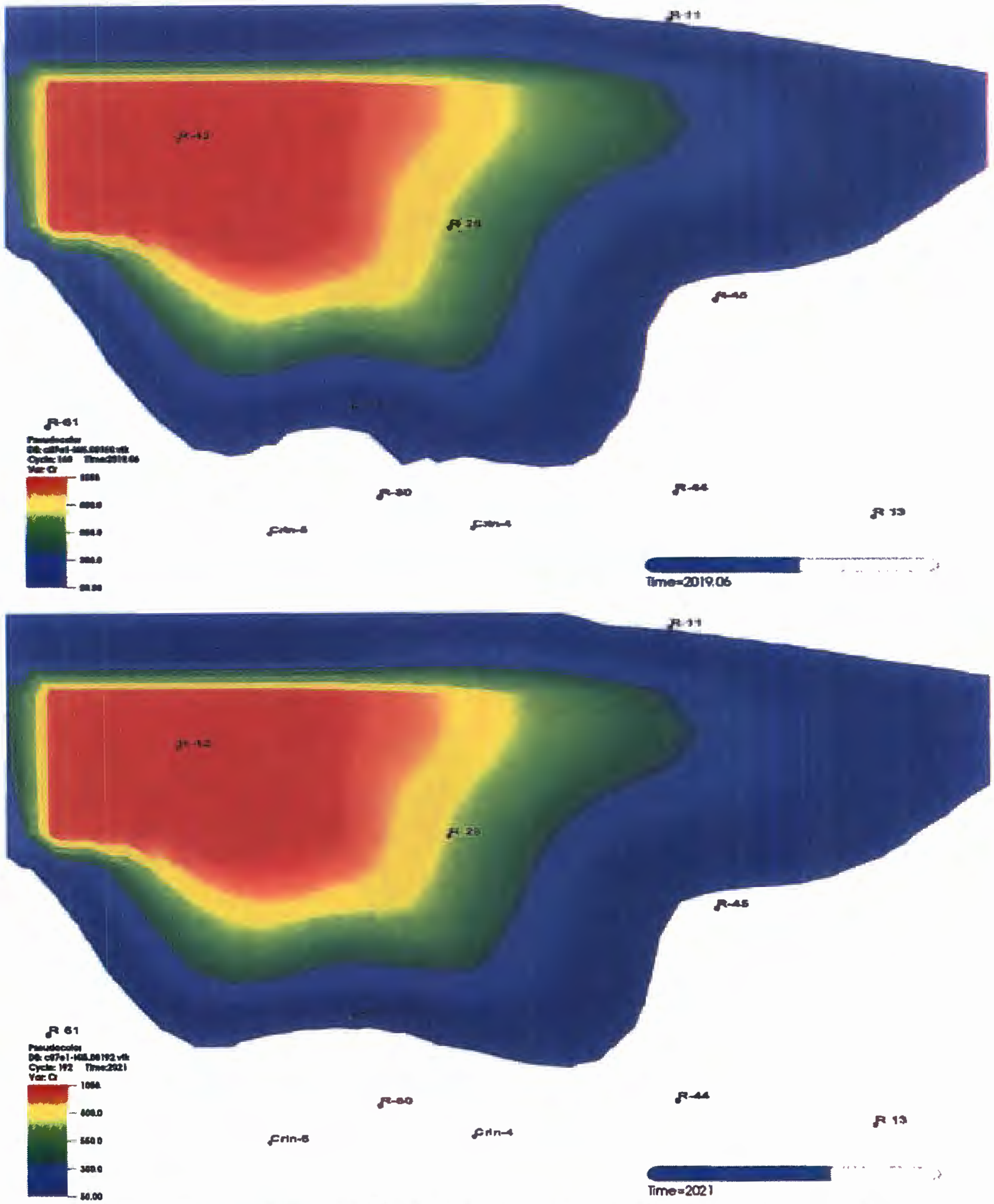

Notes: The model predictions are based on the 2012 model (Phase II Sandia Investigation Report [LANL 2012, 228624]). The plots are showing model predictions for 2016, 2017, 2019, and 2021 (after 0, 1, 3, and 5 yr of pumping/injection, respectively). The results are preliminary. Here CrEX-1 is pumping at 80 gpm for 5 yr (2016–2021), and CrIN-4 and CrIN-5 are injecting for 5 yr at 40 gpm each (2016–2021).

Figure A-8.0-2 (continued) Model predictions of the impact of pumping and injection scenarios on the chromium concentrations

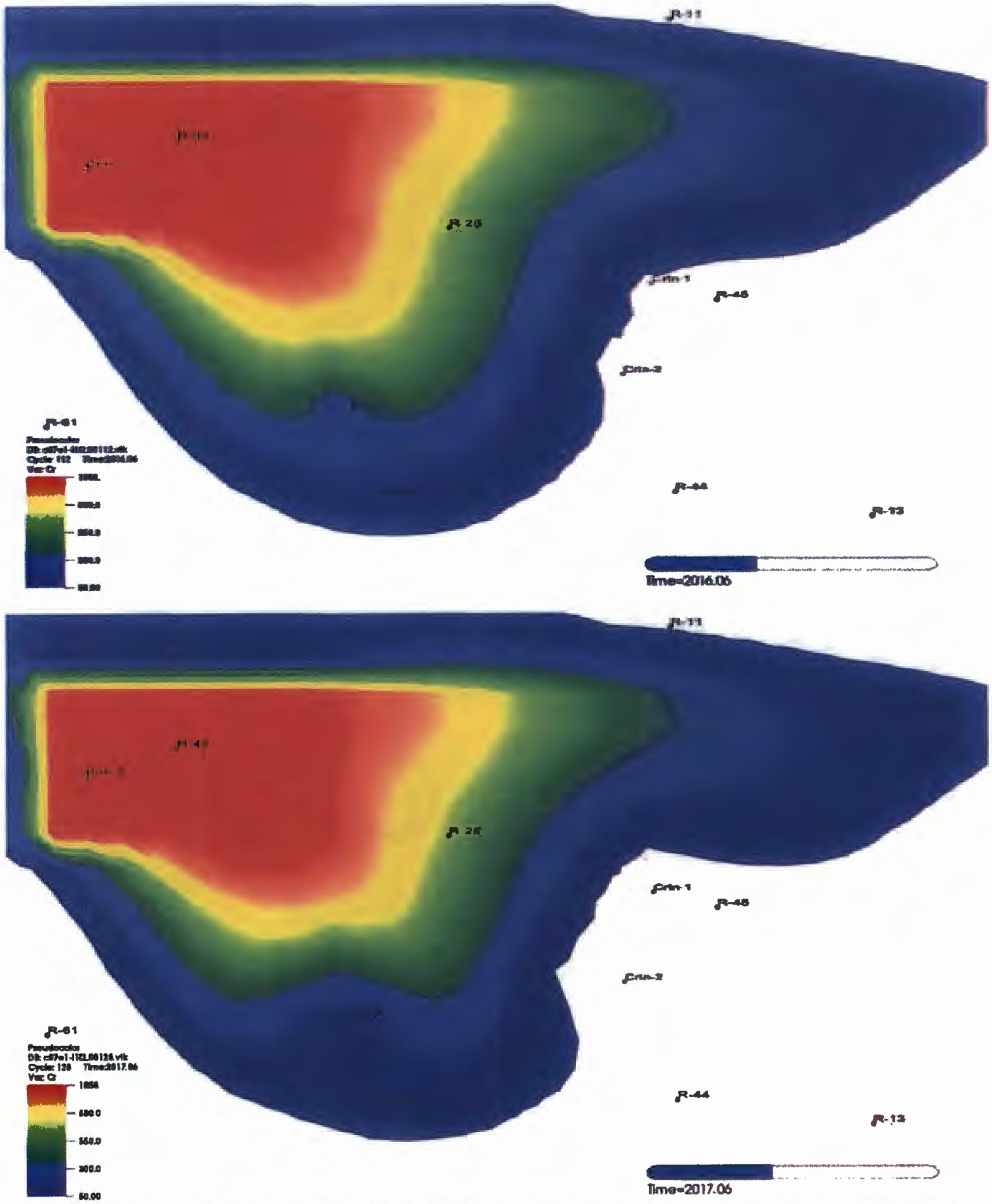

Notes: The model predictions are based on the 2012 model (Phase II Sandia Investigation Report [LANL 2012, 228624]). The plots are showing model predictions at 2016, 2017, 2019, and 2021 (after 0, 1, 3, and 5 yr of pumping/injection, respectively). The results are preliminary. Here CrEX-1 is pumping at 80 gpm for 5 yr (2016–2021), and CrIN-1 and CrIN-2 are injecting for 5 yr at 40 gpm each (2016–2021).

Figure A-8.0-3 Model predictions of the impact of pumping and injection scenarios on the chromium concentrations

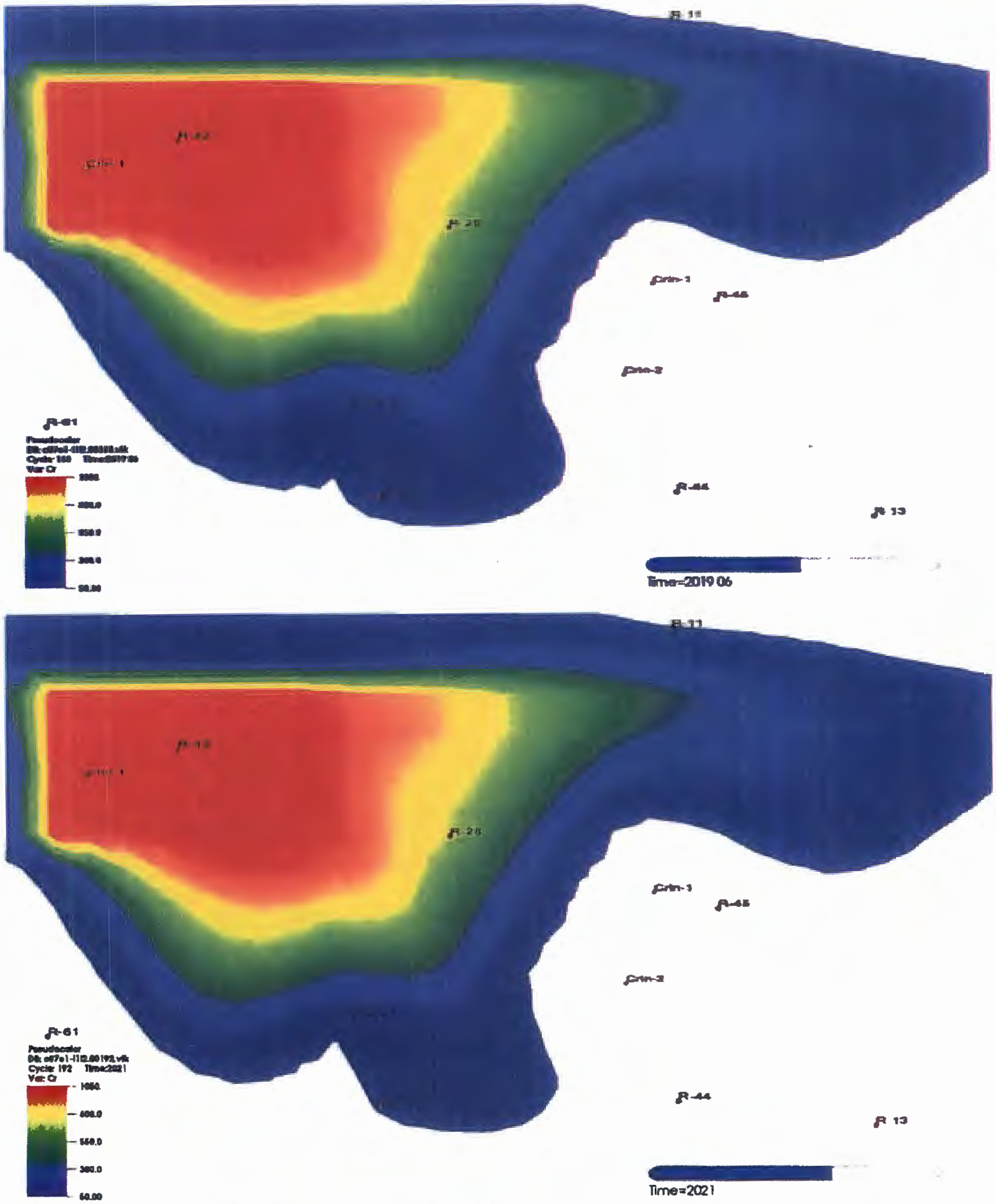

Notes: The model predictions are based on the 2012 model (Phase II Sandia Investigation Report [LANL 2012, 228624]). The plots are showing model predictions at 2016, 2017, 2019, and 2021 (after 0, 1, 3, and 5 yr of pumping/injection, respectively). The results are preliminary. Here CrEX-1 is pumping at 80 gpm for 5 yr (2016–2021), and CrIN-1 and CrIN-2 are injecting for 5 yr at 40 gpm each (2016–2021).

Figure A-8.0-3 (continued) Model predictions of the impact of pumping and injection scenarios on the chromium concentrations

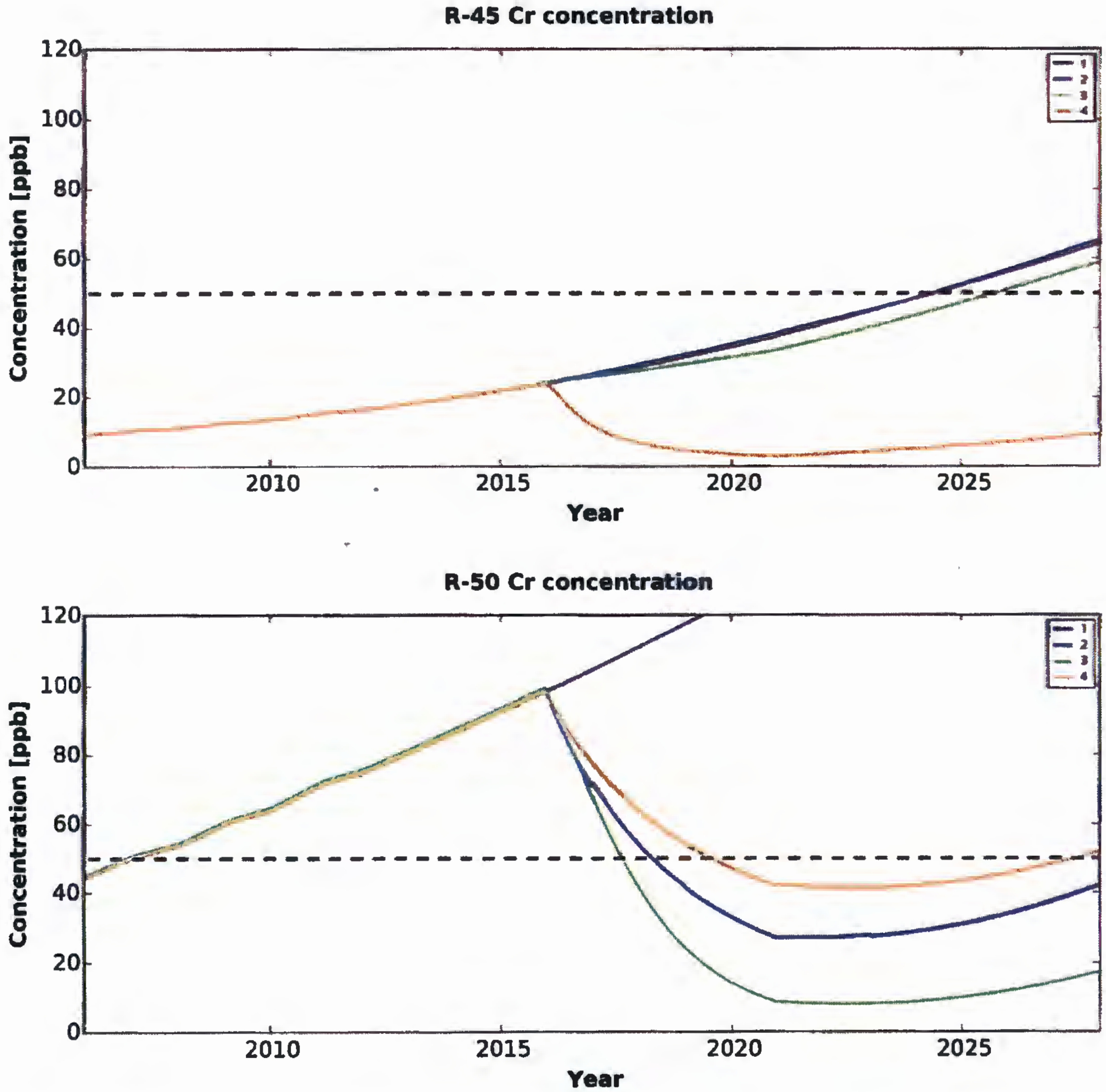

Notes: The dashed line represents 50 ppb chromium concentration. R-45 concentrations are substantially impacted only by the CrIN-3/CrIN-4 injection (see section A-8.0, scenario 4). R-50 concentrations are impacted in all pumping/injection scenarios but the highest impact is when CrIN-1 and CrIN-2 are injecting (scenario 4).

Figure A-8.0-4 Model predicted chromium concentration curves for R-45 screen 1 and R-50 screen 1 under different scenarios: (1) no action; (2) CrEX-1 pumping only; (3) CrEX-1 pumping and CrIN-4/CrIN-5 injecting; and (4) CrEX-1 pumping and CrIN-1/CrIN-2 injecting

Table A-4.0-1
Summary of the Estimated Effective Aquifer Properties between the Pumping (CrEX-1) and Observation Wells during 2014 CrEX-1 Pumping Test

Screen	Transmissivity (m^2/day)	Storativity (–)	Max drawdown (m)	Comment
CrCH-1	1700	0.06	0.06	Very limited pressure record
R-1	na*	na	>0.01	Difficult to analyze; small drawdown (?)
R-11	750	0.07	0.057	None
R-13	820	0.06	0.056	None
R-15	na	na	na	Potential transducer problems
R-28	na	na	na	Data gaps; difficult to analyze
R-33 #1	na	na	0.023	Difficult to analyze; small drawdown (?)
R-33 #2	na	na	na	Difficult to analyze small drawdown (?)
R-35a	na	na	na	Difficult to analyze; small drawdown (?)
R-35b	na	na	0.022	Difficult to analyze small drawdown (?)
R-36	na	na	na	Difficult to analyze; no drawdown (?)
R-42	820	0.06	0.092	Data gaps; difficult to analyze
R-43 #1	na	na	>0.01	Difficult to analyze; small drawdown (?)
R-43 #2	3100	0.03	0.039	None
R-44 #1	540	0.1	0.089	None
R-44 #2	680	0.06	0.097	None
R-45 #1	780	0.09	0.069	None
R-45 #2	5200	0.007	0.045	None
R-50 #1	540	0.2	0.2	None
R-50 #2	1000	0.01	0.26	None
R-61 #1	1200	0.1	0.06	None
R-61 #2	850	0.1	0.069	None
R-62	4900	0.007	0.034	Data gaps; difficult to analyze

*na = Not available.

ENCLOSURE 3

Injection Wells Hydrology Fact Sheet and Figure

EPC-DO-16-118

LA-UR-16-22806

Date: MAY 1 2 2016

Discharge Permit Application DP-1835
Injection Wells Hydrology Fact Sheet

1) What is an environmental injection well?
An environmental injection well is a groundwater well used to return treated groundwater to an aquifer.

2) What role will injection wells play in the Chromium Project at LANL?
The Laboratory is taking a projective action for the Chromium Project that involves pumping contaminated groundwater to hydraulically control chromium migration in the aquifer and to test feasibility of large-scale pumping to permanently remove chromium from the plume. Contaminated groundwater that is pumped to the surface with extraction wells is treated using ion exchange. Treated water will be conveyed to the injection wells in pipes and returned to the regional aquifer. Two key benefits of using injection wells for the chromium project are: 1) they return high-quality groundwater to the aquifer to preserve the groundwater resource, and 2) injected water will locally affect the groundwater gradient in a manner that helps meet the objective of hydraulically controlling the plume. Groundwater modeling has shown that use of injection wells along the downgradient portion of the chromium plume will provide faster and more effective hydraulic control of the plume in these areas.

3) How will the Chromium Project injection wells operate?
Figure 1 shows a conceptualization of how the injection wells will work. The flow of the water into the well will be controlled and monitored by a computerized operating system. The control system will collect and save monitoring parameters such as flow rate, pressure, and depth to water level in each well. This control system will be programmed to notify an operator or shut down the system if parameters fall outside the ranges selected for safe operation. The injection wells will also be equipped with a submersible pump to allow maintenance on the well if a well screen becomes clogged. Operation of the injection wells will require a permit with NMED.

4) Do injection wells pose a water-quality risk to the groundwater?
No. All groundwater pumped from the extraction wells will be treated to remove all contaminants (including chromium) to levels at or below levels established under a discharge permit with the NMED. Testing will be conducted at a frequency that will also be set by the permit. In addition, the treated groundwater will be injected into locations within the regional aquifer close to where it was extracted, thereby reducing any potential impacts that can sometimes occur when waters with significantly different chemistry are mixed.

5) Will the Chromium Project injection wells cause seismicity?
It is highly unlikely. Much work is being conducted on a national scale on seismicity induced by injection of hydraulic fracturing fluids into deep geologic formations. Data and modeling indicate that induced seismicity typically occurs when pressurized fluids enter a fault, thus reducing its resistance to sliding.

For the Chromium Project, treated groundwater will be injected into the upper portion of a highly porous, unconfined (i.e., unpressurized) sand and gravel aquifer. The treated groundwater will not be injected into the aquifer under pressure as is the case with hydraulic fracturing in the oil industry, but rather via a method more similar to natural infiltration. The infiltration is not expected to deform or rearrange aquifer materials in a manner that would induce seismicity.

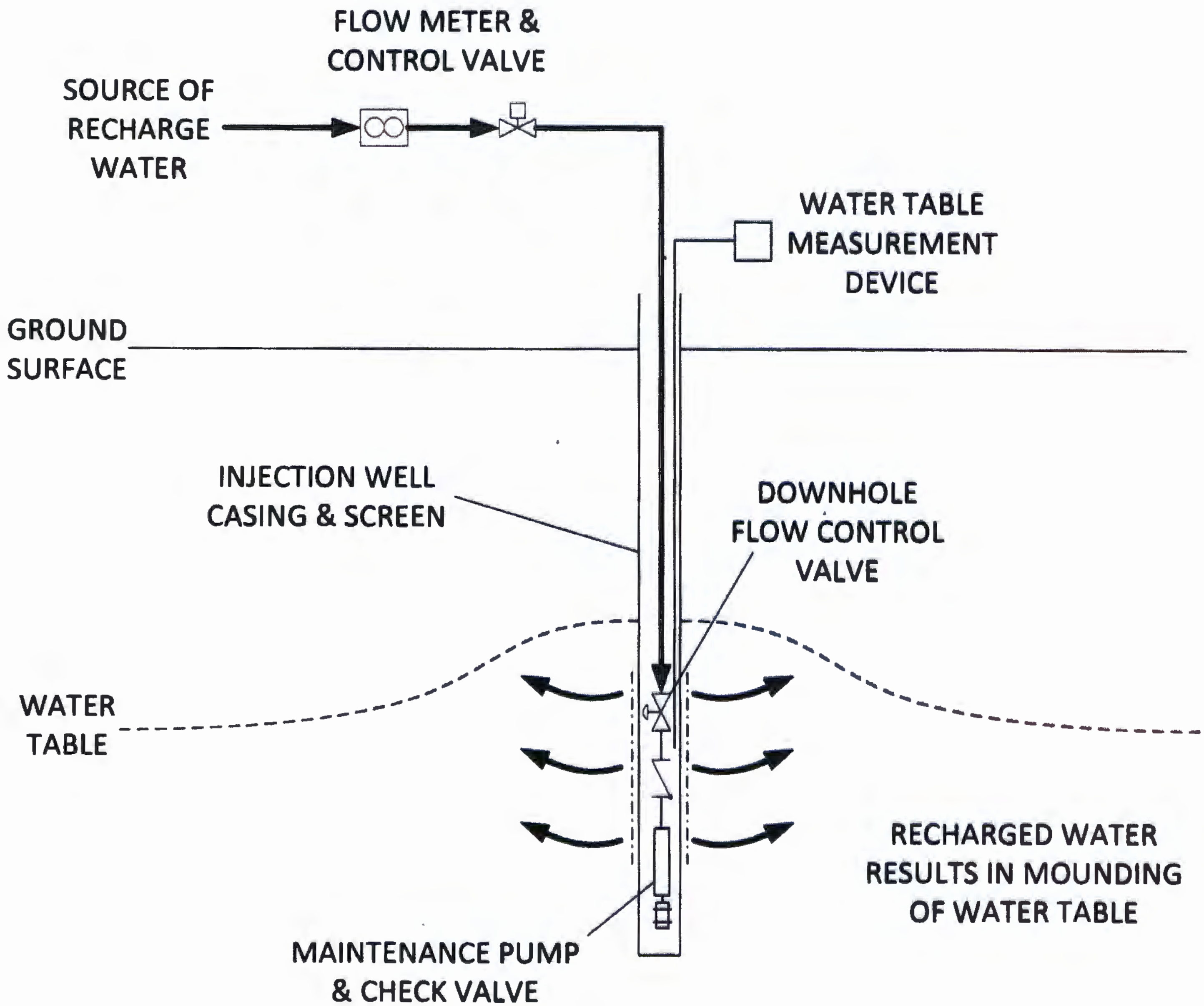
FLOW METER &
CONTROL VALVE
SOURCE OF
RECHARGE
WATER
WATER TABLE
MEASUREMENT
DEVICE
GROUND
SURFACE
INJECTION WELL
CASING & SCREEN
DOWNHOLE
FLOW CONTROL
VALVE
WATER
TABLE
RECHARGED WATER
RESULTS IN MOUNDING
OF WATER TABLE
MAINTENANCE PUMP
& CHECK VALVE